

# **The regulation of meiosis in mouse oocytes**

**Petros Marangos**

**Department of Physiology  
University College London**

**A thesis submitted for the degree of Doctor of Philosophy**

**May 2004**



ProQuest Number: 10014850

All rights reserved

INFORMATION TO ALL USERS

The quality of this reproduction is dependent upon the quality of the copy submitted.

In the unlikely event that the author did not send a complete manuscript and there are missing pages, these will be noted. Also, if material had to be removed, a note will indicate the deletion.



ProQuest 10014850

Published by ProQuest LLC(2016). Copyright of the Dissertation is held by the Author.

All rights reserved.

This work is protected against unauthorized copying under Title 17, United States Code.  
Microform Edition © ProQuest LLC.

ProQuest LLC  
789 East Eisenhower Parkway  
P.O. Box 1346  
Ann Arbor, MI 48106-1346

# Abstract

The overall aim of the experiments presented in this thesis is to investigate the regulation of meiosis in mammalian oocytes.

To investigate the role of cyclin B during progression through meiosis I to II we have made use of a cyclin B1-GFP fusion protein. Injection of cyclin B1-GFP accelerates GVBD and overrides cAMP-mediated arrest at the GV stage. Excess cyclin B can accelerate or inhibit the extrusion of Pb1 in a dose-dependent manner. The distribution of cyclin B1-GFP was found to be controlled through the regulation of nuclear import and export. Within 15 minutes of GVBD, cyclin B1-GFP accumulates in the GV, presumably due to a rise in import and a decrease in export.

Cyclin B1-GFP is also a tool for examining cyclin degradation that is necessary for exit from M-phase. In MI we find cyclin B destruction is necessary for progression through MI. Cyclin B destruction at MII is stimulated by an increase in  $Ca^{2+}$  at fertilisation. This destruction results in an increase in the rate of cyclin B degradation. Producing  $Ca^{2+}$  transients during MI does not induce cyclin B degradation showing cyclin B destruction becomes sensitive to  $Ca^{2+}$  late in meiosis.

Furthermore, we examined the role of Em1 in meiosis. Em1 is present in both MI and MII. By microinjecting Em1 protein we found that Em1 blocks polar body extrusion. By injecting morpholinos aimed against the endogenous Em1 mRNA, we managed to block the maturation of oocytes at prometaphase which implies a role for Em1 in MI. Em1 depletion also

caused the release of MII eggs from metaphase arrest. This showed that this protein may be, as MAPK, a component of the cytostatic factor, which is responsible for the arrest at MII.

Finally, we examined the relationship of  $\text{Ca}^{2+}$  oscillations and cell cycle resumption at fertilisation.  $\text{Ca}^{2+}$  oscillations do not depend on normal levels of CDK1-cyclin B since they continue after CDK1 activity has declined. Moreover, they are not sensitive to the MAPK inhibitor, UO126. The data demonstrate a strong correlation between  $\text{Ca}^{2+}$  oscillations and Pn formation. In this thesis we present a model whereby  $\text{Ca}^{2+}$  oscillations at fertilisation and mitosis are controlled by the nuclear sequestration of a sperm-derived  $\text{Ca}^{2+}$ -releasing factor, such as PLC $\zeta$ .

## **Publications containing work from this thesis**

Ca<sup>2+</sup> oscillations at fertilization in mammals are regulated by the formation of pronuclei.

Marangos P., FitzHarris G. and Carroll J. *Development*. 2003 Apr 1; 130(7):1461-1472.

Sperm-triggered [Ca<sup>2+</sup>] oscillations and Ca<sup>2+</sup> homeostasis in the mouse egg have an absolute requirement for mitochondrial ATP production. Dumollard R, Marangos P, Swann K, Duchen M and Carroll J. Accepted in *Development*.

Ca<sup>2+</sup> accelerates the rate of cyclin destruction specifically during meiosis II in mouse oocytes. Marangos P, Carroll J. Accepted *Developmental Biology*.

The dynamics of cyclin B1 distribution during meiosis I in mouse oocytes. Marangos P, Carroll J. Accepted in *Reproduction*.

Ca<sup>2+</sup> oscillations at fertilization in mammals. Halet G, Marangos P, FitzHarris G, Carroll J. *Biochem Soc Trans*. 2003 Oct; 31(Pt 5):907-11.

# Table of contents

<b>List of figures</b>	10
<b>List of tables</b>	12
<b>Abbreviations</b>	13
<b>1. General Introduction</b>	17
1.1 A morphological description of early mammalian development	17
1.1.1 Oogenesis	17
1.1.2 Oocyte maturation	19
1.1.3 Fertilisation	20
1.1.4 Preimplantation embryonic development	21
1.2 Control of the cell cycle	22
1.2.1 MPF history and discovery	23
1.2.2 Activation of CDK1-cyclin B	28
1.2.2a Temporal activation of CDK1-cyclin B	28
1.2.2b Spatial control of M-phase entry	30
1.2.3 Inactivation of CDK1-cyclin B	33
1.2.4 Metaphase-anaphase transition	34
1.3 Meiotic cell cycle	36
1.3.1 CDK1-cyclin B regulation in meiosis	37
1.3.1a Resumption of meiosis I	37
1.3.1b Metaphase I to Metaphase II	38
1.3.2 The Mos/MAPK pathway during oocyte maturation	39
1.4 Cytostatic Factor	42
1.4.1 Discovery of CSF	42
1.4.2 Mos/ MAPK pathway-dependent CSF arrest	43
1.4.3 CSF arrest is mediated by inhibition of the APC/C	46
1.4.4 Mos/MAPK-independent pathways involved in APC inhibition during CSF arrest	47
1.5 Ca <sup>2+</sup> signalling	48

1.5.1 Ca <sup>2+</sup> as a second messenger	48
1.5.2 Spatiotemporal organisation of Ca <sup>2+</sup> signals	50
1.5.3 Ca <sup>2+</sup> signalling at fertilisation	51
1.5.4 Sperm-egg fusion triggers Ca <sup>2+</sup> oscillations	52
1.5.5 Ca <sup>2+</sup> oscillations cause inactivation of CSF and CDK1-cyclin B	53
1.6 Synopsis	55
<b>2. Materials and methods</b>	56
2.1 Oocyte and embryo collection	56
2.2 In vitro fertilisation (IVF) and parthenogenetic activation	57
2.3 Microinjection	58
2.4 H1 and MBP Kinase Assays	58
2.5 Expression and purification of Cyclin B1-GFP	60
2.6 Depletion of Emi1 using Morpholino oligonucleotides	61
2.7 Immunolocalisation of Emi1	63
2.8 Fluorophores	63
2.8.1 Fluorescence imaging of DNA	63
2.8.2 Imaging of the spindle	64
2.8.3 Measurement of intracellular [Ca <sup>2+</sup> ] and photorelease of ‘caged-InsP <sub>3</sub> ’	64
2.8.4 Cyclin B1-GFP fusion protein	66
2.9 Confocal microscopy	67
2.10 Statistical analysis	69
<b>3. The dynamics of cyclin B1 distribution during meiosis I in mouse oocytes.</b>	72
3.1 Introduction	72
3.2 Results	74

3.2.1 Exogenous Cyclin B1-GFP induces premature GVBD	74
3.2.2 Cyclin B1-GFP has a concentration-dependent effect on extrusion of the 1st polar body	76
3.2.3 Cyclin B1 overrides cAMP-mediated arrest in germinal vesicle stage mouse oocytes	77
3.2.4 GVBD is associated with nuclear localisation of cyclin-GFP	79
3.2.5 Cyclin B1 is actively exported from the germinal vesicle	81
3.2.6 Inhibition of nuclear export accelerates accumulation of nuclear cyclin-GFP	83
3.3 Discussion	85
3.3.1 Effects of cyclin abundance on GVBD	85
3.3.2 Effects of cyclin abundance on first polar body extrusion	87
3.3.3 Localisation of cyclin-B1 GFP in GVBD	87
3.3.4 Cyclin transport	89
<b>4. Ca<sup>2+</sup> oscillations at fertilisation of mouse oocytes maintain a persistent rate of cyclin B degradation that is exclusive to exit from meiosis II.</b>	91
4.1 Introduction	91
4.2 Results	95
4.2.1 Cyclin destruction in MI is not associated with a detectable Ca <sup>2+</sup> transient	95
4.2.2 Ca <sup>2+</sup> dependent cyclin destruction only occurs in MII arrested oocytes	97
4.2.3 Cyclin B destruction at fertilisation	99
4.2.4 Sr <sup>2+</sup> containing medium also induces incremental fluorescence changes and oscillations in autofluorescence	102
4.2.5 The proteasome is necessary for the increased rate of cyclin B destruction but not the incremental steps	102
4.2.6 Fertilisation induces Ca <sup>2+</sup> -dependent oscillations in autofluorescence	105
4.3 Discussion	107
4.3.1 Autofluorescence oscillations at fertilisation of mouse eggs	107
4.3.2 Cyclin B degradation at fertilisation	108
4.3.3 Ca <sup>2+</sup> has no effect on cyclin B degradation at MI	110
<b>5. The role of Emi1 in mouse oocytes</b>	111



5.1 Introduction	111
5.2 Results	115
5.2.1 Localisation of Emi1 during meiosis of mouse oocytes	115
5.2.2 Emi1 depletion causes spindle formation inhibition and arrest at MI	117
5.2.3 Excess Emi1 blocks Pbl extrusion	120
5.2.4 Emi1 depletion causes spontaneous activation of MII arrested eggs	121
5.2.5 Excess Emi1 delays fertilisation	125
5.2.6 Excess Emi1 delays egg activation caused by UO126	125
5.3 Discussion	128
5.3.1 Emi1 persists during MI in mouse oocytes	128
5.3.1a Emi1 localisation during meiotic maturation	128
5.3.1b Emi1 and cyclin A in meiosis and mitosis	129
5.3.2 Emi1 is necessary for progression through oocyte maturation	130
5.3.3 Excess Emi1 causes arrest at MI	132
5.3.4 Emi1 is involved in CSF activity	132
<b>6. Ca<sup>2+</sup> oscillations at fertilisation in mammals are regulated by the formation of pronuclei</b>	<b>135</b>
6.1 Introduction	135
6.2 Results	139
6.2.1 The relationship between Ca <sup>2+</sup> transients, pronucleus formation and CDK1-cyclin B and MAP kinase at fertilisation	139
6.2.2 Inhibition of MAPK activity has no effect on Ca <sup>2+</sup> oscillations	142
6.2.3 Injection of cyclin B1-GFP can lead to persistent Ca <sup>2+</sup> oscillations	144
6.2.4 Low cycling levels of CDK1-cyclin B can not explain the maintenance of Ca <sup>2+</sup> transients	147
6.2.5 Inhibition of pronucleus formation leads to persistent Ca <sup>2+</sup> oscillations	149
6.2.6 Inhibition of importin $\beta$ -mediated nuclear transport leads to prolonged generation of Ca <sup>2+</sup> transients	152
6.3 Discussion	154
<b>7. Conclusions</b>	<b>158</b>

7.1 Using cyclin B1-GFP to monitor cyclin B levels in oocytes and eggs.	158
7.2 Spatial regulation of meiosis	160
7.2.1 Spatial control of M-phase entry	160
7.2.2 Spatial control of protein degradation during exit from M-phase	162
7.3 Differential regulation of MI and MII	164
7.3.1 Regulation of MII arrest	164
7.3.2 Differential sensitivity to Ca <sup>2+</sup>	165
7.4 The nuclear sequestration of a PLC may regulate Ca <sup>2+</sup> release in mouse eggs and embryos	167
<b>Reference list</b>	171
<b>Acknowledgements</b>	193

## List of figures

Figure 3.1 Cyclin B1-GFP accelerates GVBD	75
Figure 3.2 Cyclin B1-GFP overrides cAMP-mediated meiotic arrest	78
Figure 3.3 Cyclin B1-GFP enters the GV just prior to GVBD	80
Figure 3.4 Cyclin B1-GFP is actively exported from the germinal vesicle	82
Figure 3.5 Inhibition of nuclear export leads to nuclear accumulation of cyclin B1-GFP	84
Figure 4.1 Destruction of cyclin B1 and progression through MI is independent of Ca <sup>2+</sup>	96
Figure 4.2 Ca <sup>2+</sup> -stimulated cyclin destruction is specific to oocytes arrested in an MII-like state	98
Figure 4.3 The dynamics of Ca <sup>2+</sup> -induced cyclin B1-GFP degradation at fertilisation	101
Figure 4.4 Sr <sup>2+</sup> -containing medium causes fluorescence decreases similar to fertilisation in cyclin B1-GFP injected eggs	103
Figure 4.5 Inhibition of the proteasome inhibits the gradual decrease in cyclin B1-GFP fluorescence but not the oscillations	104
Figure 4.6 Fertilisation stimulates oscillations in autofluorescence that are Ca <sup>2+</sup> -dependent	106
Figure 5.1 Emi1 localisation during oocyte maturation	116
Figure 5.2 Emi1 localisation at fertilisation	118
Figure 5.3 Emi1 depletion causes abnormal spindle formation leading to inhibition of Pb1 extrusion at MI	119
Figure 5.4 Excess of Emi1 blocks Pb1 extrusion	122

Figure 5.5 Emi1 depletion causes spontaneous activation of MII eggs	124
Figure 5.6 Excess Emi1 delays fertilisation and egg activation	127
Figure 6.1 The correlation between Ca <sup>2+</sup> transients, CDK1-cyclin B and MAPK activities and pronucleus (Pn) formation	140
Figure 6.2 Inhibition of MAPK activity does not inhibit Ca <sup>2+</sup> oscillations	143
Figure 6.3 Injection of excess cyclin B1-GFP leads to long-lasting Ca <sup>2+</sup> oscillations	146
Figure 6.4 Low levels of CDK1-cyclin B activity do not explain persistent Ca <sup>2+</sup> oscillations after extrusion of the second polar body	148
Figure 6.5 Inhibition of Pn formation leads to persistent Ca <sup>2+</sup> oscillations after inactivation of CDK1-cyclin B and MAPK	150
Figure 6.6 Inhibition of importin $\beta$ -mediated nuclear transport inhibits pronucleus formation and prolongs Ca <sup>2+</sup> oscillations	153
Figure 7.1 Model depicting the nuclear localisation and release of sperm-derived Ca <sup>2+</sup> -releasing activity	170

## List of tables

Table 2.1	10% SDS-PAGE gel	60
Table 2.2	Spectra of fluorophores used	69
Table 2.3	Final concentrations of microinjected agents inside the oocyte	70
Table 2.4	Reagents and indicators used in treatments	71
Table 6.1	The relationship between pronucleus formation and the time when sperm induced Ca <sup>2+</sup> oscillations stop	145

## Abbreviations

AM (Fura-2 AM)	acetoxymethyl ester form
APC/C	Anaphase Promoting Complex/ Cyclosome
ATP	Adenosine Triphosphate
BAPTA	1,2-bis(2-aminophenoxy)ethane-N,N,N',N'-tetraacetic acid
BP	Band Pass
BSA	Bovine Serum Albumin
Bub1	Budding uninhibited by benzimidazole 1
BubR1	Bub Related 1
$[Ca^{2+}]_i$	Intracellular calcium concentration
CaM	Calmodulin
CaMKII	Calmodulin-dependent Kinase II
cAMP	cyclic Adenosine Monophosphate
Cdc	Cell division cycle
CDK	Cyclin Dependent Kinase
CHX	Cycloheximide
CRM1	Chromosomal Region Maintenance 1
CRS	Cytoplasmic Retention Sequence
CSF	Cytostatic Factor
DAG	Diacylglycerol
dbcAMP	dibutyryl cAMP

DM	Dichroic Mirror
dsRNA	double-stranded RNA
Emi1	Early mitotic inhibitor 1
ER	Endoplasmic Reticulum
Erk	Extracellular regulated kinase
FAD	Flavin Adenine Dinucleotide
FITC	Fluorescein Isothiocyanate
FSH	Follicle Stimulating Hormone
G1	Gap 1
G2	Gap 2
GFP	Green Fluorescent Protein
GV	Germinal Vesicle
GVBD	Germinal Vesicle Breakdown
H1	Histone 1
hCG	human Chorionic Gonadotrophin
IBMX	3-isobutyl-1-methylxanthine
ICSI	Intra-Cytoplasmic Sperm Injection,
IP <sub>3</sub>	Inositol (1,4,5)-triphosphate
IP <sub>3</sub> R	IP <sub>3</sub> Receptor
IU	International Units
IVF	<i>In Vitro</i> Fertilisation
LH	Luteinising Hormone
LMB	Leptomycin B

LP	Long Pass
MI	Meiosis I
MII	Meiosis II
M/A	Metaphase-Anaphase transition
Mad1	Mitotic arrest defective 1
MAPK	Mitogen Activated Protein Kinase
MBP	Myelin Basic Protein
MEK	MAP/Erk Kinase
Mos	Moloney murine sarcoma
MPF	Maturation Promoting Factor
MTOC	Microtubule Organising Centre
Myt1	Membrane-associated, tyrosine- and threonine-specific
NEBD	Nuclear Envelope Breakdown
NES	Nuclear Export Signal
NLS	Nuclear Localisation Signal
Pb	Polar body
PBS	Phosphate Buffered Saline
Pds1	Precocious disassociation of sister chromatids 1
PIP <sub>2</sub>	Phosphatidyl Inositol (4,5) biphosphate
PKA	Protein Kinase A
PLC	Phospholipase C
Plk1	Polo-like kinase 1
PMSG	Pregnant Male Serum Gonadotrophin



Pn	Pronucleus
PVA	Polyvinyl Alcohol
Rca1	Regulator of cyclin A 1
Rec8	Recombination 8
RNAi	RNA interference
Rsk	Ribosomal protein S6 kinase
RT	Room Temperature
RyR	Ryanodine Receptors
SAC	Spindle Assembly Checkpoint
SCF	Skp1/Cullin/F-box protein
Sgo1	Shugoshin 1
Thr	Threonine
Tyr	Tyrosine
Wee1	wee= small in scotish wee= small in scotish
WGA	Wheat Germ Agglutinin
YFP	Yellow Fluorescent Protein
ZP	Zona Pellucida

# 1. General Introduction

In most organisms, the meiotic cell cycle is driven by two major kinases, CDK1-cyclin B and MAPK. CDK1-cyclin B is a heterodimer of CDK1 and cyclin B and is responsible for nuclear envelope breakdown, chromatin condensation and spindle formation. Cyclin needs to be destroyed for CDK1-cyclin B inactivation so that anaphase and polar body extrusion will occur. The MAPK activity is regulated by Mos and is necessary for metaphase II arrest, for stabilising the second meiotic spindle and for spindle migration during MI. The experiments presented in this thesis have been designed to investigate the murine meiotic cell cycle and the dynamics of the two M-phase kinases during mouse oocyte maturation and fertilisation. This introduction will therefore introduce topics relevant to the experiments presented. Following a brief overview of oogenesis and preimplantation development, the mechanisms of CDK1-cyclin B and MAPK-dependent cell cycle regulation are considered. Finally, the role of  $\text{Ca}^{2+}$  at mammalian fertilisation and the relationship between the cell cycle and  $\text{Ca}^{2+}$  release are discussed.

## 1.1 A morphological description of early mammalian development

### 1.1.1 Oogenesis

Patterns of reproduction vary among species. In some species, such as sea urchins and frogs, the female routinely produces hundreds or thousands of eggs at a time, whereas in other species, such as mice, humans and most mammals, only a few thousands of eggs are

produced during the lifetime of an individual. During gestation, in mammals, primordial germ cells migrate from extragonadal sites to the primitive ovary. At this stage they are called oogonia. Oogonia will continue to proliferate mitotically to reach a population of millions, but eventually will enter meiosis, before the end of the gestation period (O W and Baker, 1976), and become oocytes (primary oocytes). The oocytes stop proliferating and meiosis progresses through leptotene, zygotene and pachytene stages and arrests at the diplotene stage (dictyate state) of the first prophase of meiosis. From then on, their number begins to decrease. During the reproductive (menstrual) cycle, a small proportion of these oocytes will start resuming meiosis from the onset of puberty and until the end of the reproductive life of the animal (Yding Andersen and Byskov, 1996).

At around the time the oocytes reach the diplotene stage (dictyate state) of the first meiotic prophase, they become surrounded by a single layer of epithelial cells (pregranulosa cells) to form primordial follicles. By a mechanism, still not understood, a group of primordial follicles is recruited to undergo further development. Upon the initiation of follicular development, the oocytes undergo a period of growth in which they enlarge from 15-20  $\mu\text{m}$  in diameter to more than 100  $\mu\text{m}$  in some species. In the mouse, the oocyte increases in size from 15 (0.9 pl in vol) in a primordial follicle to 80  $\mu\text{m}$  (270pl) in a fully developed follicle. An accompanying nuclear growth ensues, such that fully grown oocytes contain a characteristically large nucleus termed the germinal vesicle (GV; Chouinard, 1975). Concomitant with oocyte growth is an increase in the number of follicular granulosa cells which develop layers around the oocyte to form a primary follicle. Throughout follicular development, the granulosa cells communicate with the oocyte via gap junctions (Anderson and Albertini, 1976; Kidder and Mhawi, 2002). These channels enable the transport of

molecules responsible for processes essential for oocyte growth (Herlands and Schultz, 1984). Besides the increase in size, another important change in the structure of the growing oocyte is the formation of the zona pellucida, the extracellular coat of the oocyte. This glycoprotein coat functions during fertilisation to mediate sperm binding, induce the acrosome reaction, promote sperm penetration and provide the primary block to polyspermy (Green, 1997; Wassarman *et al.*, 2001c).

At any given time, a small group of follicles is maturing in the ovary. To survive, the follicle must be exposed to gonadotropic hormones. During the reproductive cycle, the pituitary secretes follicle stimulating hormone (FSH) which supports further growth of the follicles that have reached the early antral stage of development. In a normal mouse reproductive cycle, 6-15 follicles respond to FSH causing follicular cells to secrete fluid within the follicle to form a Graafian, or antral follicle. Ovulation is triggered by a surge in circulating levels of luteinising hormone (LH) which causes the rupture of several follicles in the mouse, and the liberation of their contents. A normal mouse ovulation results in the release of 8-12 eggs over the course of two or three hours, each surrounded by a mass of cumulus cells. Administration of gonadotropins can be used to induce superovulation, allowing the collection of an increased number of eggs or embryos (see Chapter 2). As the cells are released from the ovary, they are gathered in by the ciliated epithelium of the open end of the oviduct and swept along the oviduct towards the uterus (Hogan *et al.*, 1994).

### **1.1.2 Oocyte maturation**

Oocytes remain arrested at the dictyate stage of meiosis throughout oocyte growth. Mouse oocytes typically become competent to resume meiosis once they reach a diameter of 60µm.

(Wassarman and Albertini, 1994; Sorensen and Wassarman, 1976). The resumption of meiosis, marked by germinal vesicle breakdown (GVBD), takes place 2-3 hours after the LH surge.

A barrel-shaped metaphase I (MI) spindle is first distinguishable after about 5-6h after meiotic resumption, and is fully formed by 9-10 hours (Wassarman and Albertini, 1994). Around the time the spindle is fully formed, it migrates towards the plasma membrane (oolema), to the nearest part of the oocyte cortex (Verlhac *et al.*, 2000), providing the earliest known indication of the animal-vegetal axis (Zernicka-Goetz, 2002). Anaphase I separates the homologous chromosomes and not the individual chromatids, directing each chromosome to opposite spindle poles. Telophase I leads to cell division and extrusion of the first polar body (Pb1) 10-12 hours after the initial LH surge (Wassarman and Albertini, 1994). Following Pb1 extrusion, the oocyte re-enters meiosis II, bypassing interphase, and forms a second meiotic spindle in the oocyte cortex. The cell cycle then becomes arrested at metaphase of the second meiotic division (MII). Release from MII arrest does not take place until fertilization. This MII-arrested oocyte can be referred to as an egg.

In vitro, given appropriate culture conditions, GV-stage mouse oocytes removed from antral follicles will mature spontaneously, fertilise, and undergo normal preimplantation development in the absence of hormonal stimulation (also see Chapter 2; Schroeder and Eppig, 1984).

### **1.1.3 Fertilisation**

After the sperm are released in the female reproductive tract, they undergo a process of competence for fertilisation which lasts until they reach the ovulated egg and is known as

capacitation (Aitken, 1996). Several hundred spermatozoa eventually reach and penetrate the cumulus cell mass surrounding the MII-arrested egg and bind to the zona pellucida protein ZP3 (Wassarman *et al.*, 2001b). This binding triggers the acrosome reaction, a process in which the acrosome (a secretory vacuole in the sperm head) fuses with the sperm plasma membrane releasing hydrolytic enzymes which allow zona-penetration (Wassarman *et al.*, 2001a). Fertilisation is initiated after the fusion of the sperm to the egg plasma membrane. This event triggers the exocytosis of cortical granules, which results in the release of hydrolytic enzymes from the egg in the sub-zonal (perivitelline) space. This leads to alterations of the zona glycoprotein structures (zona reaction) causing a block of further sperm penetration and fusion (block to polyspermy).

Fertilisation stimulates the release from the MII arrest with the segregation of the sister chromatids, leading to the extrusion of a second polar body (Pb2). As in meiosis I, most of the cytoplasm is retained by the mature egg, and the Pb2 receives little more than a haploid nucleus. Thus, oogenic meiosis conserves the volume of the oocyte cytoplasm in a single cell rather than splitting it equally among four progeny, as is the case in meiosis in the male germ line.

The series of events starting from sperm-egg fusion leading to Pb2 extrusion are collectively termed oocyte activation. In the mouse, extrusion of Pb2 occurs approximately 90 minutes after sperm-egg fusion.

#### **1.1.4 Preimplantation embryonic development**

Individual nuclear membranes first become visible around the maternal and paternal chromosomes around four hours after sperm-egg fusion forming separate haploid pronuclei.

This marks the transition from meiotic to mitotic cell divisions. At this stage, the embryo is called a zygote. In the mouse, the paternally derived pronucleus is significantly larger than the maternally derived one. Formation of the pronuclei is followed by their coordinated repositioning towards the centre of the cell (termed pronuclear syngamy) such that the two pronuclei become closely apposed, but remain separate.

The first embryonic cell division occurs after the disassembly of the two pronuclei, 17-20 hours post activation (Howlett and Bolton, 1985; Yanagimachi, 1994). The second embryonic cell division in the mouse occurs 46-54 hours after fertilisation, and the embryo typically reaches the 8-cell stage by around 60 hours. The activation of intercellular adhesion at the 8-cell stage causes the embryonic cells (blastomeres) to become tightly packed, forming a compacted morula (Fleming *et al.*, 2000). Three to four days after fertilisation the embryo becomes differentiated into an outer cell layer, the trophoectoderm, enclosing an accumulation of cells at one pole termed the inner cell mass. This embryo is called a blastocyst. During these processes, the embryo is transported through the oviduct and into the uterus. The blastocyst-stage embryo will eventually hatch from the zona pellucida and implant in the uterine wall, some four to five days after fertilisation (timings from Hogan *et al.*, 1994).

## **1.2 Control of the cell cycle**

The meiotic cell cycle events are regulated by two major activities, Maturation Promoting Factor (MPF) and the Cytostatic Factor (CSF). MPF releases the oocytes from the GV arrest at prophase and coordinates the first meiotic cell cycle. At the metaphase-anaphase transition

MPF is inactivated to allow the extrusion of the first polar body and is then immediately upregulated leading directly to metaphase of the second meiotic division. CSF will keep the mature eggs arrested at MII. Inactivation of MPF at fertilisation releases the eggs from the arrest and allows the completion of meiosis. In the following chapter I will describe the way these activities were discovered and discuss the hypotheses and experimental proof regarding their characterisation, action and regulation during meiosis.

### **1.2.1 MPF history and discovery**

Discovery of MPF was made in the oocyte of the frog *Rana Pipiens* (Masui and Markert, 1971). Masui showed that cytoplasm transferred from mature (progesterone treated) MII frog eggs causes recipient immature oocytes to undergo maturation. A similar result was not observed after transfer of cytoplasm from untreated oocytes. This implied that there is a factor in the cytoplasm that causes oocyte maturation. Thus, the factor was named Maturation Promoting Factor. Masui measured the activity of MPF indirectly by expressing it as the percentage of recipient oocytes undergoing maturation after injection with a constant volume of cytoplasm (Masui and Markert, 1971). It wasn't until the late 80's when MPF was found to be a kinase able to phosphorylate Histone 1 (H1), that a H1 kinase assay was developed for measuring MPF activity (Lohka *et al.*, 1988; Labbe *et al.*, 1988).

Measuring the relative activity of MPF immediately showed that this activity is not constantly stable during meiosis. In the frog, it appears six hours after progesterone treatment and three hours before GVBD and remains at high levels during the MII arrest before declining at fertilisation (Masui and Markert, 1971; Masui, 2001). The universal role of this factor was later shown by its presence in *Xenopus*, starfish and mouse oocytes (Drury and



Schorderet-Slatkine, 1975;Doree *et al.*, 1983;Hashimoto and Kishimoto, 1986). In 1978 the periodic appearance of MPF was demonstrated for the first time. MPF was found in cleaving amphibian embryos and the role of MPF was extended to mitosis (Wasserman and Smith, 1978). It was later shown that the periodicity of MPF activity also extends to meiosis. In *Xenopus* oocytes, MPF disappears rapidly at the end of MI reappearing before the second metaphase (Gerhart *et al.*, 1984).

Although MPF remained a mysterious activity in the 70s, the first genes to control the cell cycle were identified from temperature sensitive cell division cycle (*cdc*) mutants in the fission yeast (Nurse, 1975;Nurse *et al.*, 1976). The phenotype of *cdc2* mutants that are blocked at the onset of M-phase, is fully rescued by their transformation with the *cdc2* gene and the transformed yeast cells divide as wild type yeasts (Beach *et al.*, 1982). Similarly to MPF, *cdc2* had a conserved cell cycle action since the human gene is capable of rescuing fission yeast *cdc2* mutants (Lee and Nurse, 1987). Cdc2 is a 34 kDa phosphoprotein with protein kinase activity whose protein levels remain unchanged during the cell cycle (Simanis and Nurse, 1986). By measuring, however, the phosphorylation state of the protein it was demonstrated that, like MPF, the activity of Cdc2 varies considerably during the cell cycle, peaking at the onset of mitosis, but being lost at G1 (Simanis and Nurse, 1986;Moreno *et al.*, 1989).

The oscillations of MPF activity are also accompanied by protein synthesis and degradation (Picard *et al.*, 1985). Proteolysis at the end of M-phase was first observed by Tim Hunt's group in the sea urchin embryo and involved the degradation of a novel protein: cyclin (Evans *et al.*, 1983). These proteins were found to be synthesised and degraded in each cell cycle and their destruction correlates with the time of the metaphase/ anaphase

transition (Evans *et al.*, 1983; Swenson *et al.*, 1986). Swenson and co-workers were the first to indicate that the rise in cyclin levels plays a direct role in driving cells into M-phase. They demonstrated that microinjecting clam cyclin A mRNA induced maturation in *Xenopus* oocytes (Evans *et al.*, 1983; Swenson *et al.*, 1986). All these results implied for the first time a connection between MPF, cyclins and the cdc2 protein kinase.

MPF was purified from *Xenopus* eggs seventeen years after the activity was first described (Lohka *et al.*, 1988). The purified preparation displayed protein kinase activity and contained two major proteins of 32 kDa and 45 kDa. The 32 kDa protein was thought to be the *Xenopus* homologue of cdc2. That view was greatly strengthened by the fact that MPF activity is inhibited by antibodies against Cdc2, and that MPF co-immunoprecipitates with Cdc2 (Gautier *et al.*, 1988). In addition, purified Cdc2 kinase releases oocytes from the GV arrest in a number of species (Doree and Hunt, 2002). These experiments showed that Cdc2 is the catalytic subunit of MPF. Identification of the 45 kDa protein was made a year later in the starfish oocyte (Labbe *et al.*, 1989). Direct microsequencing showed this protein to be cyclin B. Labbe and co-workers also observed a 1:1 stoichiometry of Cdc2 and cyclin B in the M-phase kinase. These results demonstrated that MPF, the kinase activity controlling M-phase, is a heterodimer comprised of one molecule of Cdc2 and one of cyclin B.

In 1989, an experimental system was developed for the investigation of the properties of cyclin and MPF (Murray and Kirschner, 1989). For this assay, called “cyclin extract assay”, interphase extracts are prepared *in vitro* after parthenogenetic activation of MII arrested *Xenopus* eggs, followed by centrifugal crushing of the eggs one hour later. Such extracts can perform a few complete cell cycles mimicking the early cell cycle transitions of an intact embryo. By using this cell-free system, Murray and Kirschner demonstrated that

cyclin B and MPF levels both cycle. MPF and cyclin B are suppressed when protein synthesis is inhibited. The same effect was observed when mRNA-depleted extracts were used (Murray and Kirschner, 1989). Inhibition of the RNase used to deplete the mRNA and addition of cyclin B mRNA can restore the cell cycle. Moreover, translation in these extracts of indestructible cyclin B blocks the cell cycle with high MPF activity and cyclin B levels (Murray *et al.*, 1989; Murray and Kirschner, 1989). These results proved that progression through cell cycle events requires only synthesis and degradation of cyclin B to cause a rise and fall of MPF activity, identifying cyclin B as the regulatory subunit of MPF.

Two different isoforms of B-type cyclins have been identified that bind Cdc2 forming an active MPF protein kinase (Gautier *et al.*, 1990). Their different localisation mirrors their different properties. In interphase of mammalian cells, cyclin B1 is found in the cytoplasm colocalising with microtubules, while cyclin B2 colocalises with the Golgi apparatus (Gallant and Nigg, 1994; Jackman *et al.*, 1995). Responsible for the differential localisation of B-type cyclins is their NH<sub>2</sub> terminus (Pines and Hunter, 1994). A cyclin B1 with a cyclin B2 NH<sub>2</sub> terminus only localises to the Golgi (Draviam *et al.*, 2001).

Information about the necessity of the different isoforms was provided by knockout experiments. Nullizygous cyclin B1 mice died very early *in utero*, whereas cyclin B2 knockout mice were viable and fertile (Brandeis *et al.*, 1998). This indicates that Cdc2-cyclin B2 is dispensable for M-phase progression or that Cdc2-cyclin B1 is capable of compensating for the loss of Cdc2-cyclin B2. However, the mice lacking cyclin B2 are smaller in size and have reduced litters, indicating that cyclin B2 confers a growth advantage.

In prophase, cyclin B1, translocates from the cytoplasm to the nucleus when the cells enter mitosis or meiosis (Pines and Hunter, 1991;Ookata *et al.*, 1992). This translocation is probably connected with the role of CDK1-cyclin B as the nuclear lamin kinase that causes nuclear envelope breakdown at the end of prophase (Peter *et al.*, 1990). Cyclin B2, however, can not translocate to the nucleus (Jackman *et al.*, 1995). This accounts for its inability to compensate for the absence of Cdc2-cyclin B1 in the cyclin B1 knockout. Cyclin B2 acquires M-phase initiating properties, only when its NH<sub>2</sub> region is replaced by that of cyclin B1 (Draviam *et al.*, 2001). A potential reason for cyclin B2 to specifically target the Golgi apparatus may be the fact that Cdc2 is necessary for M-phase fragmentation of the Golgi by phosphorylating Golgi matrix proteins (Lowe *et al.*, 1998).

Recently, a human cyclin B3 cDNA was cloned. When cyclin B3 expression is enforced in HeLa cells, the protein localises in the nucleus. Cyclin B3 shows meiosis specific expression since it is only expressed in leptotene and zygotene spermatocytes (Nguyen *et al.*, 2002). This expression pattern suggests that the mammalian cyclin B3 may be important for events occurring early in the first meiotic prophase.

Besides cyclin B, however, experiments in the clam showed that Cdc2 forms complexes with type A cyclins (Draetta *et al.*, 1989). Furthermore, it was shown that, unlike the yeasts where only one cdc kinase exists, different cdc kinases are present in other organisms (Pines and Hunter, 1990). These cdc kinases interact with different types of cyclins. Cyclin B binds Cdc2, while cyclin A can bind to cdc2 but predominantly to the cdc2-related kinase p33 (Pines and Hunter, 1990;Pines and Hunter, 1992). The fact that all Cdc2 homologues were found to bind to cyclins led to a new convention for naming these kinases: kinases associated with cyclins would be called Cyclin-Dependent Kinases (CDKs)

and Cdc2 became CDK1. Because of this, MPF activity is preferentially called CDK1-cyclin B.

### **1.2.2 Activation of CDK1-cyclin B**

One characteristic of the *cdc2* gene product is that phosphorylation keeps the protein inactive before mitosis (Gould and Nurse, 1989). Protein phosphorylation, associated with increased protein kinase activities was also found to be coupled with meiotic maturation and cycling changes in MPF activity levels in starfish oocytes, indicating the importance of phosphorylation/dephosphorylation events for cell division (Guerrier *et al.*, 1977; Doree *et al.*, 1983). Thus, in order to enter M-phase, eukaryotic cells need to activate MPF, the CDK1-cyclin B protein kinase. Activation of CDK1-cyclin B occurs in prophase and leads to NEBD, chromosome condensation and spindle formation. The complex is regulated both temporally and spatially. Thus, CDK1-cyclin B is activated both by phosphorylation/dephosphorylation of its components and by its translocation into the nucleus.

#### *1.2.2a Temporal activation of CDK1-cyclin B*

CDK1 protein levels do not change substantially during the cell cycle and the kinase remains inactive as a monomer requiring cyclin B synthesis and binding to be activated. This binding is facilitated by CDK1 phosphorylation on Threonine 161 (Ducommun *et al.*, 1991). Cyclin binding changes the conformation of the ATP binding segment of a CDK kinase by realigning active site amino acid residues and revealing the catalytic domains of the kinase (Jeffrey *et al.*, 1995).

The complex remains inactive, as pre-MPF, in G<sub>2</sub>, even after cyclin binding, because of inactivation by phosphorylation by kinases like wee1. wee1 was discovered in the fission yeast, one year before cdc2 was found (Nurse, 1975). wee1 mutants undergo mitosis faster than normal leading to reduced yeast size. It became apparent from these experiments that wee1 and cdc2 act together in a regulatory network controlling the onset of M-phase. Wee1 phosphorylates CDK1 on Tyrosine 15 which is located near the ATP binding site of the protein kinase (Gould and Nurse, 1989). This implies that inhibitory phosphorylation of CDK1 may interfere with the transfer of phosphate from the kinase to its substrates. Mutation of Tyr15 in yeasts leads to a block of CDK1 phosphorylation and mitotic entry even in the presence of unreplicated DNA (Gould and Nurse, 1989). In higher eukaryotes, inhibitory phosphorylation of CDK1 is catalysed by two kinases, Wee1 and Myt1, which both phosphorylate CDK1 on Tyr15 and Thr14 (Liu *et al.*, 1997).

Activation of CDK1-cyclin B requires the dephosphorylation of Tyr15 and Thr14 by the Cdc25 phosphatase. Two Cdc25 isoforms are required for entry into M-phase: Cdc25B and Cdc25C. Experiments in the fission yeast showed that increased expression of cdc25 causes a phenotype very similar to that of wee1 thermo-sensitive mutants where mitosis initiates early resulting in a reduced cell size when the cells are cultured at the restrictive temperature (Nurse, 1975; Russell and Nurse, 1986). The work on Cdc25 and Wee1 led to the conclusion that the level of CDK1 phosphorylation is regulated by the balance of activities between the Wee1 protein kinase M-phase inhibitor and the Cdc25 M-phase activator. Thus, entry in M-phase drives the balance towards an active Cdc25 phosphatase.

Cdc25C is also directly phosphorylated and activated by CDK1-cyclin B itself (Hoffmann *et al.*, 1993). This positive feedback loop is also enhanced by the ability of

CDK1-cyclin B to hyperphosphorylate and inactivate Wee1 (Mueller *et al.*, 1995; Watanabe *et al.*, 1995). There is also evidence that CDK1-cyclin B stimulates xPlk1 activation in *Xenopus* extracts enhancing indirectly its own activation (Abrieu *et al.*, 1998). These results form the basis of the “MPF amplification” process (Masui and Markert, 1971) which consists of a positive feedback loop of post-translational events by which the initial small amount of activated CDK1-cyclin B acts as a primer, leading to the production of more CDK1-cyclin B. A model was proposed recently stating that activation of CDK1 behaves as a bi-stable switch (Pomerening *et al.*, 2003). In this model relatively small changes in cyclin B levels and CDK1 activity can lead to a switch-like activation of CDK1-cyclin B from an interphase to M-phase state of activation.

#### *1.2.2b Spatial control of M-phase entry*

Besides the temporal control however, CDK1-cyclin B activation is also regulated spatially. In most organisms, the M-phase regulators have distinct subcellular localisations that alter according to the cell cycle phase.

In interphase, CDK1-cyclin B1 is retained in the cytoplasm. This localisation is attributed to a sequence of its NH<sub>2</sub> amino-terminal called the cytoplasmic retention sequence (CRS) (Pines and Hunter, 1994). Deletion of this sequence causes cyclin to enter and remain in the nucleus. The construction, in Jon Pines' laboratory, of a chimeric protein comprising of one molecule of cyclin B1 and one of green fluorescent protein (cyclin B1-GFP) allowed the study of cyclin in real time in living cells and brought new insight into the dynamic behaviour of the protein (Hagting *et al.*, 1998). When the fusion protein is injected into

interphase HeLa cell nuclei, it is rapidly exported from the nucleus suggesting that cyclin has a nuclear export signal (NES). This leucine-rich NES is located in the CRS and when mutated, cyclin B1 export is inhibited. When the mutant is injected in the cytoplasm, the protein enters and remains in the nucleus. The same effect is obtained by treating interphase cells with leptomycin, an inhibitor of the export factor CRM1, indicating that cyclin B1 export is mediated by the CRM1 pathway (Hagting *et al.*, 1998; Yang *et al.*, 1998). The fact that the block of export results in nuclear localisation, although cyclin B1 is cytoplasmic in interphase, shows that, during this stage of the cell cycle, the protein shuttles into and out of the nucleus and that the rate of export exceeds that of import, resulting in cytoplasmic localisation. Thus, the localisation of cyclin B1 is determined by the relative rates of nuclear import and export.

However, both cyclin B1 and CDK1 lack an obvious nuclear localisation signal (NLS). Because of this, the complex can not bind to the alpha subunit of the importin- $\alpha/\beta$  heterodimer in order to enter the nucleus. Instead, cyclin B1 binds directly to a sequence at the NH<sub>2</sub> terminal of the importin- $\beta$  transporter (Moore *et al.*, 1999). In the nucleus, cyclin B1 dissociates from importin- $\beta$  and binds to exportin CRM1 (Hagting *et al.*, 1998).

A combination of site-directed mutagenesis and phosphopeptide-mapping in *Xenopus* oocytes indicated that cyclin B1 is being phosphorylated on a cluster of five serine residues in the NES region, prior to M-phase (Li *et al.*, 1995). Phosphorylation of cyclin B1 is not required for CDK1 kinase activity or for binding to CDK1 protein, but it plays a significant role in cyclin B1 nuclear accumulation (Li *et al.*, 1995; Hagting *et al.*, 1999). This phosphorylation process can be partly attributed to CDK1-cyclin B's auto-catalytic kinase activity and partly to Plk (Borgne *et al.*, 1999; Toyoshima-Morimoto *et al.*, 2001). Hagting



and co-workers developed forms of cyclin B1 where the five serine residues of the NES were mutated either into threonine (T) to simulate phosphorylation or into alanine (A) to disable cyclin B1 phosphorylation. The mutants were linked to yellow fluorescent protein (YFP) and their kinetics were observed in interphase HeLa cells. The T-mutants accumulate in the nucleus faster than the wild type protein whereas the A-mutants remain in the cytoplasm even during NEBD (Hagting *et al.*, 1999). This work shows that, at the time of M-phase entry, cyclin B1 needs to be phosphorylated so that CDK1-cyclin B1 accumulates in the nucleus by acceleration of import and inhibition of export. Export is blocked because the hyper-phosphorylation of cyclin B1 disables the NES and the protein is unable to bind to CRM1 (Yang *et al.*, 2001). Furthermore, importin- $\beta$  is unable to stimulate the import of these mutants suggesting that phosphorylation causes the formation of a nuclear import signal in the CRS of cyclin B1 capable of accelerating import in M-phase through an importin-independent pathway (Hagting *et al.*, 1999).

Differential localisation, however, is not restricted to cyclins. Most of the important regulators of M-phase entry also show evidence of spatial organisation. Cdc25C has been shown to be a nuclear protein, whereas Cdc25B is cytoplasmic in interphase accumulating in the nucleus prior to NEBD (Karlsson *et al.*, 1999). In addition, Wee1 is a nuclear protein, but Myt1 is associated with the endoplasmic reticulum and the Golgi apparatus in the cytoplasm (Liu *et al.*, 1997).

It is well established by now that CDK1-cyclin B1 is activated in the cytoplasm in many cell systems (Peter *et al.*, 2002b; Jackman *et al.*, 2003). CDK1-cyclin B1 is activated initially by Cdc25B in the cytoplasm. The translocation to the nucleus can then raise the intra-nuclear concentration of CDK1-cyclin B1 to saturate Wee1 and activate Cdc25C

through its positive feedback action leading to a 'switch-like' activation of CDK1-cyclin B1 that will induce NEBD (Ferrell, Jr., 1998).

### **1.2.3 Inactivation of CDK1-cyclin B**

While entry into M-phase is driven by CDK1-cyclin B activation, exit from M-phase only occurs after CDK1-cyclin B downregulation. Inactivation of the protein kinase is driven by the proteolytic degradation of its cyclin partner.

The importance of cyclin B destruction and subsequent CDK1-cyclin B inactivation was first demonstrated by truncated forms of sea urchin cyclin that render cyclin indestructible and cause M-phase arrest associated with high levels of CDK activity (Murray *et al.*, 1989). The degradation of cyclin is dependent on a conserved 9-residue motif in the N-terminal region termed the destruction box (Glotzer *et al.*, 1991). This element, targets cyclin to the ubiquitin ligase Anaphase Promoting Complex/ Cyclosome (APC/C) for multiple ubiquitination steps (King *et al.*, 1995; Fang *et al.*, 1998a). The APC/C holoenzyme is an 11-subunit complex which catalyses the transfer of ubiquitin and the subsequent formation of poly-ubiquitin chains onto the target proteins. The poly-ubiquitinated proteins are then recognised and degraded by a large cytosolic protease complex, the 26S proteasome (Hershko, 1997). Although proteasomal degradation of cyclin B is not regulated during the cell cycle, the APC/C can differentially regulate the timing of its ubiquitination. The APC/C is inactive in metaphase and requires activation prior to anaphase. APC/C activation is obtained by its association with a WD40-containing co-activator protein, cdc20/fizzy (Lorca *et al.*, 1998; Kramer *et al.*, 1998). Cdc20 is also inactive in metaphase and when activated prior to anaphase, it binds directly to the proteins targeted for proteolysis and recruits them to

the APC/C complex (Fang *et al.*, 1998a;Pfleger *et al.*, 2001). It is important to note that in *Xenopus* cycling extracts, CDK1-cyclin B regulates its own inactivation by being the initial trigger for APC activation (Felix *et al.*, 1990).

In *Drosophila*, proteolytic degradation of cyclin B initiates at the centrosomes and spreads along the spindle towards the equator. Cytoplasmic cyclin B is destroyed slightly later. Thus, cyclin is degraded in two waves, first from the spindles and then from the cytoplasm (Raff *et al.*, 2002). Real time GFP fluorescence studies have also shown spatial and temporal regulation of cyclin B proteolysis in *Drosophila* and human mitotic cells (Huang and Raff, 1999;Clute and Pines, 1999). As soon as the last chromosome aligns on the metaphase plate, cyclin is rapidly eliminated from the chromosomes, then the rest of the spindle and eventually the cytoplasm. It is proposed that spindle-associated proteolysis of cyclin B in M-phase is regulated via a Cdc20-dependent ubiquitination pathway, whereas the subsequent cytoplasmic degradation is controlled by Cdh1, a Cdc20 related protein that also activates the APC/C (Raff *et al.*, 2002). Cyclin B degradation eventually leads to the termination of M-phase and entry into interphase.

#### **1.2.4 Metaphase-anaphase transition**

Onset of anaphase requires the proteolytic destruction of cyclin B and subsequent inactivation of CDK1-cyclin B. Prior to this, however, the absolute necessity for anaphase to occur is the alignment of all the chromosomes at the metaphase plate. Before the complete formation of the metaphase plate, APC/C activation, cyclin B degradation and onset of anaphase are inhibited by the spindle assembly checkpoint.

During the formation of the spindle, one kinetochore of a duplicated chromosome or homologous chromosome pair becomes attached to a single microtubule. The mono-oriented chromosome acquires additional microtubules and then oscillates within the spindle area. The unattached kinetochore of a microtubule from the opposite pole will then capture the chromosome, or chromosome pair, leading it to the spindle equator. The spindle assembly checkpoint acts to block entry into anaphase until the kinetochores of every chromosome have attached correctly to spindle microtubules at the metaphase plate. The importance of the spindle assembly checkpoint as a “wait anaphase” signal was demonstrated by a number of experiments. Detachment of a chromosome from a spindle by manipulation with a microneedle delays anaphase indefinitely (Li and Nicklas, 1995), while laser ablation of the last kinetochore produces immediate anaphase onset (Li and Nicklas, 1995; Rieder *et al.*, 1995).

A number of spindle assembly checkpoint proteins have been originally identified in budding yeast mutants that were unable to arrest in metaphase after the addition of microtubule poisons (Hoyt *et al.*, 1991). Since then, several of these proteins were shown to be conserved in many organisms, from yeasts to mammals. Unattached kinetochores bind to a variety of these proteins like Bub1 (budding uninhibited by benzimidazole), BubR1, Mad1 (mitotic arrest defective), Mad2 and others (Cleveland *et al.*, 2003). While binding to unattached microtubules, spindle assembly checkpoint proteins like Mad2, BubR1 or Pds1 form complexes that sequester Cdc20 in order to keep it in an inactive state (Fang *et al.*, 1998b; Hilioti *et al.*, 2001; Fang, 2002). Following microtubule attachment of every chromosome, these complexes are destroyed and the checkpoint is inactivated releasing Cdc20 for APC/C activation. The APC/C then coordinates the degradation of cyclin B and

securin (Zur and Brandeis, 2001; Raff *et al.*, 2002; Hagting *et al.*, 2002). Securin destruction activates the separase proteins responsible for destroying the cohesins that “glue” the sister chromatids together (Zachariae and Nasmyth, 1999). Experiments in *Xenopus*, however, have shown that separase activation also relies on cyclin B destruction, since CDK1-cyclin B prevents sister chromatid separation through inhibitory phosphorylation of separase (Stemmann *et al.*, 2001). Cyclin B destruction-dependent separase activation may act independently from securin, since chromosome segregation can occur, although incomplete, in the presence of a non-degradable securin mutant (Zur and Brandeis, 2001). Thus, chromosome alignment enables APC<sup>cdc20</sup> activation which in turn coordinates the separation of chromosomes and exit from M-phase through securin destruction and through cyclin B proteolysis to reduce CDK1-cyclin B.

### **1.3 Meiotic cell cycle**

There are many aspects in which the regulation of M-phase kinase activity is similar in the mitotic and meiotic cell cycles. CDK1-cyclin B activation causes NEBD or GVBD and spindle formation, while cyclin B destruction leads to CDK1-cyclin B inactivation and onset of anaphase in both mitosis and meiosis. However, there are also very significant differences. In this section, I will discuss the special characteristics of the meiotic cell cycle.

### 1.3.1 CDK1-cyclin B regulation in meiosis

#### 1.3.1a Resumption of meiosis I

As already mentioned, oocytes within ovarian follicles are arrested at prophase of meiosis I until LH acts on the follicle to cause meiotic resumption. Maintaining the arrest in a fully grown oocyte depends on the presence of the surrounding follicle. This was demonstrated by the fact that oocytes resume meiosis spontaneously when released from the follicle into a suitable culture medium (Edwards, 1965). This follicle-mediated meiotic arrest seems to be controlled by cAMP since the use of agents that raise intracellular cAMP blocks spontaneous in vitro maturation (Cho *et al.*, 1974; Downs and Hunzicker-Dunn, 1995). The origin of cAMP in the oocyte has been under investigation for many years. One possibility is that cAMP enters the oocyte through gap-junctions with the follicle (Anderson and Albertini, 1976). Alternatively, cAMP may be generated in the oocyte with the follicle cells acting to maintain its concentration (Mehlmann *et al.*, 2002). This may occur through the maintenance of the activity of a stimulatory G protein ( $G_s$ ) which in turn maintains the activity of adenylyl cyclase necessary for the generation of cAMP. The requirement of a  $G_s$  protein for the maintenance of meiotic arrest was shown by the microinjection of a  $G_s$ -specific antibody, able to inhibit  $G_s$  function, into mouse follicles.  $G_s$  inhibition led to spontaneous resumption of meiosis (Mehlmann *et al.*, 2002).

cAMP acts through cAMP-dependent protein kinase (PKA). In vertebrates, active PKA is directly implicated with G2 arrest in meiosis (Maller and Krebs, 1977; Huchon *et al.*, 1981; Mehlmann *et al.*, 2002; Schmitt and Nebreda, 2002). In *Xenopus* oocytes, Cdc25C, which is hyperphosphorylated and activated by Polo-like kinase xPlk1 (Matten *et al.*, 1994), is negatively regulated by PKA. PKA phosphorylates Cdc25 on Ser-287 resulting in its

sequestration by 14-3-3 (Duckworth et al., 2002). In response to progesterone, the PKA pathway becomes inactive and Cdc25 is dephosphorylated just prior to CDK1 dephosphorylation and M-phase entry (Ferrell, Jr., 1999).

Following resumption of meiosis cyclin B is synthesised (Hampl and Eppig, 1995b; Winston, 1997) and CDK1-cyclin B is activated. The kinase is activated prior to GVBD and its activity rises progressively until it reaches a plateau in M-phase of meiosis I (Verlhac *et al.*, 1994; Hampl and Eppig, 1995a). In the mouse, however, cyclin B synthesis is not necessary for GVBD since activation of CDK1-cyclin B can occur in the presence of protein synthesis inhibitors (Hampl and Eppig, 1995b). This means that the initial activation of CDK1-cyclin B is due to the activation of a limited pool of pre-existing inactive (pre-MPF) complexes. Cyclin B synthesis leading to newly formed CDK1-cyclin B complexes is necessary for progression of meiosis beyond GVBD (Hampl and Eppig, 1995b).

### *1.3.1b Metaphase I to Metaphase II*

In the mouse, cyclin synthesis, and the subsequent CDK1-cyclin B activation, rises from 28% of the maximal level during GVBD to 56% during the next few hours until reaching 100% in the following hours leading to the first polar body extrusion. There is no substantial cyclin destruction during that period (Winston, 1997). For anaphase to occur CDK1-cyclin B levels need to reach a plateau of activity. In strains of mice with different rates of cyclin B synthesis it was found that faster CDK1-cyclin B activation, progression to anaphase and extrusion of the first polar body occur in the strain showing the fastest rate of cyclin B synthesis (Polanski *et al.*, 1998). Further evidence for this is the finding that polar body

extrusion is faster if oocytes are injected with cyclin B mRNA with a long polyA tail (Ledan *et al.*, 2001). These results demonstrate that the rate of cyclin B synthesis controls the length of M-phase.

Unlike mitosis, during the meiotic anaphase I, cyclin B is not completely destroyed and some protein escapes degradation during the transition from MI to MII (Hampl and Eppig, 1995a; Winston, 1997). The degradation is almost complete in the mouse (Winston, 1997), but in *Xenopus* it is only 50% (Tunquist and Maller, 2003). A remaining amount of cyclin and CDK1-cyclin B activity is probably necessary for avoiding entry into interphase after the first M-phase. The different extents of degradation in mouse and *Xenopus* also reflect the role of cyclin B proteolysis for MI/II transition in the species. In the mouse, cyclin overexpression (Ledan *et al.*, 2001) or the use of non-destructible cyclin (Herbert *et al.*, 2003) block first polar body extrusion, whereas in *Xenopus*, inhibition of cyclin B destruction does not prevent chromosome segregation and Pb1 extrusion (Taieb *et al.*, 2001; Peter *et al.*, 2001).

Following Pb1 extrusion, cyclin B is synthesised rapidly and CDK1 kinase rises to reach a maximum level at metaphase II where the egg remains arrested until fertilisation (Levasseur and McDougall, 2000; Ledan *et al.*, 2001). The stability of CDK1-cyclin B activity during the MII arrested state is mediated by an equilibrium of cyclin B synthesis and degradation (Kubiak *et al.*, 1993).

### **1.3.2 The Mos/MAPK pathway during oocyte maturation**

Another signalling pathway operating in oocyte maturation is the Mos/MEK/MAPK/ p90Rsk pathway. Mos, a 39 kD germ cell-specific protein, is the product of the proto-oncogene c-



mos and functions as a mitogen activated protein kinase (MAPK) kinase kinase (MAPKKK). Mos activates the MAPK/Erk kinase, MEK1, which then acts as the activator of MAPK (Crews and Erikson, 1992; Nebreda and Hunt, 1993; Posada *et al.*, 1993). In mouse oocytes, whilst Mos is detected at GV stage, expression is dramatically upregulated during oocyte maturation and is abundant in MII eggs (Paules *et al.*, 1989). Expression is subsequently reduced following fertilisation, such that only a residual amount of Mos is detectable in pronucleate embryos (Goldman *et al.*, 1988; Watanabe *et al.*, 1991; Weber *et al.*, 1991).

Mouse oocytes possess two forms of MAPK, p44 ERK 1 (extracellular signal-regulated kinase 1) and p42 ERK 2 (Verlhac *et al.*, 1993). In oocytes, MAPK activation is driven by newly synthesised Mos (Sagata *et al.*, 1988). When MAPK rises after GVBD, it remains at maximum levels of activity during MI, the MI/MII transition and the MII arrest only to be inactivated after the second polar body extrusion as a result of Mos degradation (Ferrell, Jr. *et al.*, 1991; Verlhac *et al.*, 1993; Verlhac *et al.*, 1994). More direct evidence for the involvement of Mos in MAPK activation is provided by the finding that MAPK fails to activate in oocytes of the Mos knockout mouse (Verlhac *et al.*, 1996).

There are species-specific differences in the timing of the onset of MAPK activity in oocytes. In the mouse, MAPK is only activated after GVBD and the initial rise of CDK1-cyclin B activity (Verlhac *et al.*, 1993). In contrast, MAPK in the *Xenopus* egg is activated before GVBD concomitantly with CDK1-cyclin B activation (Ferrell, Jr. *et al.*, 1991). Injection of mos mRNA in *Xenopus* oocytes can induce MPF activation and GVBD in the absence of progesterone treatment (Sagata *et al.*, 1989a). This effect can be explained by the fact that Mos/MAPK may contribute to the positive regulation of CDK1-cyclin B (Palmer *et*

*al.*, 1998; Peter *et al.*, 2002a). However, the converse is also true since, in oocytes, full activation of MAPK depends on CDK1 activity (Abrieu *et al.*, 2001).

MAPK does not seem to be of great significance for MI since oocytes from Mos knockout mice and *Xenopus* oocytes injected with morpholino antisense oligonucleotides against Mos, with no MAPK activity, undergo GVBD and extrude Pb1 (Verlhac *et al.*, 1996; Dupre *et al.*, 2002). MAPK inhibition, however, affects the size of polar bodies which become larger than normal (Verlhac *et al.*, 2000; Phillips *et al.*, 2002). This is a result of disruptions of the actin-microfilament network. The spindle can not migrate to the cortex and remains in the middle of the oocyte, but still elongates at anaphase forming the midbody close to the equator of the oocyte (Verlhac *et al.*, 2000).

Although blocking the Mos/MAPK pathway does not necessarily prevent entry or exit from MI, it severely disrupts MII. In *Xenopus*, Mos ablation causes oocytes to enter interphase after MI and replicate DNA, while resynthesis of cyclin B is inhibited (Furuno *et al.*, 1994). In the Mos knockout mouse, the oocytes extrude first polar bodies at the same time as the wild-type oocytes and the MI spindles have no obvious defects. After anaphase I, however, the chromatin starts to decondense and elongated microtubules begin to form leading the oocytes in an interphase state. The majority of the oocytes eventually enter MII, but instead of arresting, they spontaneously activate forming monopolar spindles (Verlhac *et al.*, 1996).

All these experiments show that although the Mos/MAPK cascade does not seem to be involved in GVBD or entry in MI, it plays a very important role in the progression from MI to MII, maintaining chromatin and microtubules in a metaphase-like state, prohibiting entry in interphase or into a spontaneous activation state after MI, driving cyclin B

resynthesis at the MI/MII transition and coordinating polar body formation. The most important role, however, of the Mos/MAPK pathway is the regulation of the cytostatic factor (CSF) activity.

## **1.4 Cytostatic Factor**

As discussed previously, oocytes entering metaphase II remain arrested at metaphase until fertilisation. MII arrest is characterised by high CDK1-cyclin B activity which is obtained by the constant synthesis and degradation of cyclin B. This arrested state of the meiotic cell cycle is sustained by an activity known as cytostatic factor (CSF).

### **1.4.1 Discovery of CSF**

As discussed earlier, Masui and Markert discovered MPF by injecting cytoplasm from unfertilised frog eggs into immature GV-arrested oocytes and showing that this was able to cause oocyte maturation (Masui and Markert, 1971). In the same paper they discovered that injection of cytoplasm from an MII arrested eggs into one blastomere of 2-cell stage embryos caused cleavage arrest of the injected blastomere, while the uninjected blastomere divided normally. They also showed that the blastomeres injected with MII cytoplasm were arrested at metaphase. Injection of cytoplasm from GV stage oocytes or early embryos into blastomeres had no effect on cell division. These experiments led them to the assumption that a specific cytoplasmic factor is responsible for this inhibition of mitosis at metaphase. The factor was named cytostatic factor (CSF). The arrest of vertebrate eggs in metaphase of meiosis II, is therefore known as a CSF arrest. The presence of CSF activity in mouse eggs

has since been demonstrated by electrofusion experiments. Fusion of MII eggs with mitotic embryos results in a persistent metaphase arrest not observed following fusion of two mitotic cells (Kubiak *et al.*, 1993). As in the case of MPF, this factor was not a single molecule or a specific protein, but an activity found in the mature egg. CSF activity must accumulate at some point during oocyte maturation being active only in the second meiotic metaphase and disappears on fertilisation or parthenogenetic activation.

#### **1.4.2 Mos/ MAPK pathway-dependent CSF arrest**

Unlike MPF which is a well defined protein complex, CSF activity appears to be derived from a number of proteins, some of which may be necessary for the initiation and others for the maintenance of CSF activity. The primary pathway identified as being required for initiation of CSF activity is the Mos/MEK1/MAPK pathway.

Sagata and colleagues in 1989 were the first to show a connection between Mos and CSF. They injected blastomeres from *Xenopus* embryos with *mos* mRNA and revealed that, after one or two cell divisions, the blastomeres arrested at metaphase with high MPF activity and condensed chromatin. In their experiments, they also used extracts from *Xenopus* MII arrested eggs that contain high CSF activity. They immunodepleted Mos protein from these CSF extracts, as they are called, and then injected them into blastomeres, showing that the extracts were not capable to cause metaphase arrest (Sagata *et al.*, 1989b).

In addition, whole egg experiments in both *Xenopus* and mouse have shown the importance of the presence of Mos for the development of CSF activity since, although blocking the Mos/MAPK pathway does not necessarily prevent entry or exit from MI, it severely disrupts MII. In *Xenopus*, Mos ablation causes oocytes to enter interphase after MI

and replicate DNA, while resynthesis of cyclin B is inhibited (Furuno *et al.*, 1994). In the Mos knockout mouse, the oocytes extrude first polar bodies at the same time as the wild-type oocytes and the MI spindles have no defects. After anaphase I, however, the chromatin starts to decondense and elongated microtubules begin to form leading the oocytes in an interphase state. The majority of the oocytes eventually enter MII, but instead of arresting, they spontaneously activate forming monopolar spindles (Verlhac *et al.*, 1996). Furthermore, microinjection of antisense Mos oligonucleotides (O'Keefe *et al.*, 1989) or double-stranded Mos mRNA (Wianny and Zernicka-Goetz, 2000) prevent the MII arrest, causing spontaneous activation. These experiments demonstrate that Mos is a possible component of CSF.

The finding that Mos is a MAPKKK implicated MAPK in CSF. This was confirmed when injection of constitutively active MAPK in blastomeres causes cleavage arrest (Haccard *et al.*, 1993). Since MAPK is downstream of Mos, this result suggests that the Mos-dependent CSF arrest is mediated by MAPK. In addition, co-injection of a MEK1 antibody and Mos recombinant protein in blastomeres of 2-cell embryos does not arrest the injected cells in metaphase (Kosako *et al.*, 1994). In the injected blastomeres MAPK is never activated. Moreover, the MEK1 inhibitor UO126 activates mouse eggs and produces parthenogenetic embryos (Phillips *et al.*, 2002). Thus, the effect of Mos in establishing CSF arrest must operate through the activation of MEK1 that leads to the MAPK-mediated MII arrest.

The next component of the Mos/MAPK pathway is thought to be p90Rsk (Ribosomal protein S6 kinase). p90Rsk is activated by MAPK in *Xenopus* and mouse oocytes (Sturgill *et al.*, 1988; Erikson and Maller, 1989; Kalab *et al.*, 1996). In oocytes from the Mos knockout

mouse, where there is no MAPK activity, p90Rsk also remains inactive throughout oocyte maturation (Verlhac *et al.*, 1996). Although, there is no direct correlation of p90Rsk with CSF in mammals, constitutively active *Xenopus* Rsk1 is able to cause cleavage arrest in blastomeres of 2-cell embryos (Gross *et al.*, 1999). Furthermore, recombinant Mos protein is unable to rescue the CSF activity of *Xenopus* extracts immunodepleted of p90Rsk. Recombinant Rsk1 or Rsk2 are able to re-establish CSF arrest in the immunodepleted egg extracts (Bhatt and Ferrell, Jr., 1999). These experiments indicate that p90Rsk, acting downstream of Mos/MAPK, is also necessary and sufficient for CSF arrest.

Thus far, the nature of the CSF activity appears to be downstream of only one protein, Mos. Mos is the sole member of the pathway that gets destroyed after fertilisation providing a mechanism to deactivate the MAPK pathway. Subsequently, the downstream elements of the pathway, MEK1, MAPK and p90Rsk, become inactive by dephosphorylation. This makes Mos the initial mediator of the MAPK pathway and of CSF arrest in MII eggs.

The level, however, of the Mos/MAPK pathway involvement in CSF arrest is species specific. As discussed earlier, in the mouse, disruption of the pathway both during oocyte maturation (Verlhac *et al.*, 1996; Wianny and Zernicka-Goetz, 2000) and after MII arrest is obtained (Phillips *et al.*, 2002), leads to the disappearance of CSF activity and parthenogenetic activation of MII eggs. In *Xenopus*, on the contrary, although Mos ablation in MI leads to an interphase state instead of MII arrest (Furuno *et al.*, 1994), Mos/MAPK inactivation in MII by the use of UO126 has no effect and the eggs remain arrested (Reimann and Jackson, 2002; Tunquist *et al.*, 2002). Thus, the Mos/MAPK pathway is

necessary only for establishing CSF in *Xenopus*, but both for establishing and maintaining the activity in the mouse.

### **1.4.3 CSF arrest is mediated by inhibition of the APC/C**

In MII eggs, although a complete spindle is formed with all the chromosomes attached to microtubules and aligned at the metaphase plate, the eggs are arrested in metaphase by a CSF-regulated mechanism. Release from the CSF arrest of MII eggs requires the activation of the APC/C<sup>Cdc20</sup> complex. The complex is not completely inactive since cyclin B is being destroyed during the arrested state (Kubiak *et al.*, 1993; Nixon *et al.*, 2002). However, total activation of the APC/C occurs after fertilisation or parthenogenetic activation and leads to the degradation of cyclin B (Kubiak *et al.*, 1993; Nixon *et al.*, 2002). Lorca and colleagues showed that *Xenopus* Cdc20 is necessary for exit from CSF arrest. Addition of antibodies against Cdc20 or immunodepletion of the protein from *Xenopus* CSF extracts prevented sister chromatid separation and cyclin B polyubiquitination and degradation after egg activation (Lorca *et al.*, 1998; Peter *et al.*, 2001). Lastly, overexpression of Cdc20 in CSF extracts caused spontaneous activation in the absence of Ca<sup>2+</sup> increase (Reimann and Jackson, 2002).

More evidence for the correlation of CSF with the APC/C comes from work on the Mos/MAPK pathway, which is responsible for CSF arrest. After the incubation of oocytes with the MEK1 inhibitor, UO126, the half-life of cyclin B is approximately 50% shorter than in control oocytes. Experiments on the activation state of the APC component, Cdc27, have also shown that MEK1 inhibition leads to APC activation (Gross *et al.*, 2000). In addition,

p90Rsk, which acts downstream of MAPK in the Mos/MAPK pathway, can also mediate the inhibition of the APC/C in *Xenopus* (Gross *et al.*, 2000; Taieb *et al.*, 2001).

APC/C inhibition during CSF arrest, despite the presence of an intact spindle, may also involve spindle assembly checkpoint proteins like Bub1. Immunodepletion of Bub1 from *Xenopus* cycling extracts prevents recombinant Mos from establishing CSF arrest on entry into the next M-phase. Arrest can be restored after wild-type Bub1 addition to the extracts (Tunquist *et al.*, 2002). There is also evidence that Bub1 may be a member of the Mos/MAPK pathway, since purified p90Rsk is able to phosphorylate and activate Bub1 *in vitro* (Schwab *et al.*, 2001).

#### **1.4.4 Mos/MAPK-independent pathways involved in APC inhibition during CSF arrest**

Recent evidence from *Xenopus* MII eggs imply that there may be other pathways besides the Mos/ MAPK pathway that take part in the block of APC/C activation that leads to cyclin B destruction and metaphase to anaphase transition. A pathway capable of contributing to CSF arrest and of inhibiting full activation of the APC/C, independently of MAPK, is that involving CDK2-cyclin E. A constitutively active form of CDK2-cyclin E is able to stabilise the levels of cyclin B and cause metaphase arrest of cycling *Xenopus* extracts in the absence of Mos protein (Tunquist *et al.*, 2002).

Another pathway capable of affecting CSF arrest is that of Emi1 (Early mitotic inhibitor 1) activation. This protein has been identified in *Xenopus* egg extracts and has been shown to bind and inhibit Cdc20 (Reimann *et al.*, 2001a). Since Cdc20 is the only known activator of the APC/C complex during the CSF-mediated arrest of MII, Emi1 is potentially able to regulate CSF arrest. Moreover, the addition of Emi1 in cycling extracts prevents exit



from mitosis by stabilising cyclin B protein levels (Reimann *et al.*, 2001b). Lastly, immunodepletion of Emi1 from CSF extracts causes premature cyclin B degradation and exit from meiosis in the absence of  $\text{Ca}^{2+}$ , although the MAPK pathway is fully active (Reimann and Jackson, 2002). Although, there is no evidence that Emi1 contributes to the establishment of CSF, these results indicate that Emi1 may act through a pathway independent of the Mos/MAPK pathway in Meiosis II and is necessary for the maintenance of CSF arrest.

## **1.5 $\text{Ca}^{2+}$ signalling**

At fertilisation, sperm-egg fusion triggers a series of  $\text{Ca}^{2+}$  oscillations inside the egg cytosol. These oscillations induce CDK1-cyclin B and CSF inactivation leading to P2 extrusion and pronucleus formation. In this section I will discuss the action of  $\text{Ca}^{2+}$  as a second messenger, the pattern of  $\text{Ca}^{2+}$  oscillations at fertilisation, their origin and their involvement in the resumption of meiosis and entry into the first embryonic interphase.

### **1.5.1 $\text{Ca}^{2+}$ as a second messenger**

Increases in cytosolic free calcium ion concentration ( $[\text{Ca}^{2+}]_i$ ) trigger a variety of processes in eukaryotic cells, like fertilisation proliferation, development, learning and memory, contraction and secretion (Berridge *et al.*, 2000). In resting cells,  $[\text{Ca}^{2+}]_i$  is maintained at around 100nM. On stimulation by an agonist  $[\text{Ca}^{2+}]_i$  is elevated to around 1 $\mu$ M. Unlike other second messengers, calcium ions cannot be degraded or metabolised and cells employ a wide range of calcium binding and transporting molecules to control  $[\text{Ca}^{2+}]_i$ .  $[\text{Ca}^{2+}]_i$  can be

modulated by accessing several different sources of  $\text{Ca}^{2+}$ . In oocytes, the endoplasmic reticulum (ER) is the major source of  $\text{Ca}^{2+}$  for intracellular release (Eisen and Reynolds, 1985; Han and Nuccitelli, 1990). The importance of the role of the ER as a  $\text{Ca}^{2+}$  store lies in that under resting conditions,  $[\text{Ca}^{2+}]_{\text{ER}}$  is in the range of a few hundred  $\mu\text{M}$ , some three to four orders of magnitude greater than cytosolic  $[\text{Ca}^{2+}]$  (Miyawaki *et al.*, 1997). After appropriate stimulation,  $\text{Ca}^{2+}$  channels in the ER membrane open, provoking the rapid diffusion of  $\text{Ca}^{2+}$  into the cytosol. The channels responsible for  $\text{Ca}^{2+}$  release from the ER fall into two families: inositol (1,4,5)-triphosphate receptors ( $\text{IP}_3\text{R}$ ) and ryanodine receptors (RyR).

The role of RyR in mammalian eggs is unclear. The main mechanism for  $\text{Ca}^{2+}$  release involves  $\text{IP}_3\text{R}$  channels. Typically, these channels are opened as a result of cell stimulation by extracellular signals such as hormones and growth factors that activate phospholipase C (PLC) enzymes. PLC hydrolyses the plasma membrane lipid phosphatidyl inositol (4,5) biphosphate ( $\text{PIP}_2$ ) to produce the intracellular second messenger  $\text{IP}_3$  and diacylglycerol (DAG). The hydrophilic nature of  $\text{IP}_3$  permits its diffusion to the ER and association with  $\text{IP}_3\text{R}$  (Berridge, 1993). The  $\text{Ca}^{2+}$  released from the ER is then collected by molecules called  $\text{Ca}^{2+}$  sensors. One such molecule is the small  $\text{Ca}^{2+}$  binding protein calmodulin (CaM). Binding of  $\text{Ca}^{2+}$  causes CaM to undergo conformational changes such that the  $\text{Ca}^{2+}$ -CaM complex binds and activates a variety of downstream effectors, such as protein kinases (Hoeflich and Ikura, 2002). One of the best characterised downstream targets of CaM is calmodulin-dependent kinase II (CaMKII), which in turn phosphorylates and activates downstream proteins with broad substrate specificity (Hudmon and Schulman,



2002). CaMKII is thought to be one of the principal effectors of  $\text{Ca}^{2+}$  changes in oocytes (Lorca *et al.*, 1993; Winston and Maro, 1995).

### 1.5.2 Spatiotemporal organisation of $\text{Ca}^{2+}$ signals

Since sustained elevations of  $[\text{Ca}^{2+}]_i$  are cytotoxic, many cell types respond to stimulation by producing repetitive  $\text{Ca}^{2+}$  transients, or  $\text{Ca}^{2+}$  oscillations. Two main models have been proposed to explain the generation of  $\text{Ca}^{2+}$  oscillations. The first is that constant  $\text{IP}_3$  levels cause  $\text{Ca}^{2+}$  oscillations by a process of feedback inhibition by  $\text{Ca}^{2+}$  upon the  $\text{Ca}^{2+}$ -binding site of the  $\text{IP}_3\text{R}$  (Hajnoczky and Thomas, 1997). The second model proposes that a negative feedback loop may arise whereby each  $\text{Ca}^{2+}$  transient suppresses the rate of  $\text{PIP}_2$  hydrolysis, causing the level of  $\text{IP}_3$  to oscillate (Berridge and Irvine, 1989; Harootunian *et al.*, 1991).

In addition to being temporally organised in the form of oscillations,  $\text{Ca}^{2+}$  transients can also have spatial organisation within a cell. This was first illustrated in the medaka fish by using a  $\text{Ca}^{2+}$ -sensitive luminescent protein, aequorin, to monitor the sperm-induced  $\text{Ca}^{2+}$  transient. Fertilisation of the medaka fish stimulates a wave of  $\text{Ca}^{2+}$  release that originates at the point of sperm entry and traverses the egg (Gilkey *et al.*, 1978). Confocal microscopy and fluorescent  $\text{Ca}^{2+}$  indicators have shown that  $\text{Ca}^{2+}$  release in the form of waves is a frequent process both in oocytes and somatic cells (Berridge *et al.*, 2000; Jaffe, 2002).  $\text{Ca}^{2+}$  waves are dependent on the sensitivity of  $\text{Ca}^{2+}$  release channels to  $\text{Ca}^{2+}$  itself.  $\text{Ca}^{2+}$  released from one receptor has the potential to activate neighbouring channels by a process of  $\text{Ca}^{2+}$ -induced  $\text{Ca}^{2+}$  release, triggering a wave capable of spreading throughout the cell (Berridge, 1997).

### 1.5.3 Ca<sup>2+</sup> signalling at fertilisation

The first evidence of Ca<sup>2+</sup> involvement in fertilisation came in the 70s. It was reported that microinjection of Ca<sup>2+</sup> was able to cause egg activation (Steinhardt *et al.*, 1974; Fulton and Whittingham, 1978). The first proof, however, of Ca<sup>2+</sup> oscillations was given in mouse eggs a few years later (Cuthbertson and Cobbold, 1985). Since then, it has become clear that the generation of repetitive Ca<sup>2+</sup> transients at fertilisation is the necessary trigger for the resumption of meiosis (Kline and Kline, 1992; Swann and Ozil, 1994).

In the mouse, the sperm induced Ca<sup>2+</sup> oscillations persist for about four hours after fertilisation, until around the time of pronucleus formation (Jones *et al.*, 1995; Deguchi *et al.*, 2000; Day *et al.*, 2000). The rising phase of the first Ca<sup>2+</sup> transient consists of two steps. Initially, a Ca<sup>2+</sup> wave originating at the site of sperm-egg fusion propagates across the cytoplasm within 4-5 seconds. Following a brief pause, maximal [Ca<sup>2+</sup>]<sub>i</sub> is achieved by a spatially homogeneous increase in [Ca<sup>2+</sup>]<sub>i</sub> throughout the cytoplasm (Deguchi *et al.*, 2000). The first Ca<sup>2+</sup> transient is prolonged, lasting 3-5 minutes, with several small spikes detectable on top of the plateau. Subsequent transients are shorter in duration and of lesser amplitude than the initial one. The frequency and amplitude of the oscillations remain relatively constant with the transients becoming infrequent and shorter only prior to pronucleus formation.

The importance of fertilisation induced Ca<sup>2+</sup> transients is illustrated by the fact that treatments that stimulate Ca<sup>2+</sup> changes in eggs are capable of triggering cortical granule exocytosis and meiotic resumption (Steinhardt *et al.*, 1974; Fulton and Whittingham, 1978; Kline and Kline, 1992). Conversely, egg activation is inhibited by treatments that block

Ca<sup>2+</sup> oscillations. Incubation of MII eggs with the membrane permeable Ca<sup>2+</sup> chelator BAPTA-AM, prior to egg activation, prevents both cortical granule exocytosis and resumption of meiosis (Kline and Kline, 1992; Xu *et al.*, 1996). The amplitude and frequency of the oscillations are also very important for the degree of cell cycle progression and the rate of developmental competence (Bos-Mikich *et al.*, 1997; Ozil and Huneau, 2001; Ducibella *et al.*, 2002). In experiments where mouse MII eggs were subjected to electric field pulses for the generation of Ca<sup>2+</sup> transients, lowering the amplitude and number of the oscillations led to the inhibition of Pn formation (Vitullo and Ozil, 1992; Lawrence *et al.*, 1998; Ducibella *et al.*, 2002). Thus, Ca<sup>2+</sup> oscillations are both necessary and sufficient for egg activation.

#### **1.5.4 Sperm-egg fusion triggers Ca<sup>2+</sup> oscillations**

There is strong controversy about the means by which the sperm triggers Ca<sup>2+</sup> release in the egg at fertilisation. There are two main theories. The first, the 'receptor theory', is that the sperm interacts with a receptor on the plasma membrane of the egg, thus acting as an extracellular ligand, triggering hydrolysis of PIP<sub>2</sub> by PLC, IP<sub>3</sub> production and subsequent Ca<sup>2+</sup> release (Schultz and Kopf, 1995). The second hypothesis is that after sperm-egg fusion, the sperm introduces a soluble factor inside the egg. This factor will then stimulate Ca<sup>2+</sup> release. In mammalian eggs, there is more solid evidence supporting the second theory. Firstly, microinjection of homogenised sperm extracts triggers Ca<sup>2+</sup> oscillations and egg activation (Swann, 1990). In addition, Ca<sup>2+</sup> oscillations are stimulated by introduction of the sperm inside the egg (intra-cytoplasmic sperm injection, ICSI) or microinjection of spermatogenic mRNA (Sato *et al.*, 1999; Parrington *et al.*, 2000).

A number of molecules were initially identified as the 'sperm factor', the protein with  $\text{Ca}^{2+}$  releasing activities, which is introduced in the egg at fertilisation (Parrington *et al.*, 1996; Sette *et al.*, 1997). The most intriguing finding, so far however, is the identification of a novel sperm-specific phospholipase C isoform, termed PLC $\zeta$  (Cox *et al.*, 2002; Saunders *et al.*, 2002). PLC $\zeta$  microinjection in mouse eggs stimulates  $\text{Ca}^{2+}$  oscillations remarkably similar to those generated at fertilisation even in levels approximately equivalent to one sperm. Furthermore, immunodepletion of PLC $\zeta$  from sperm extracts inhibits  $\text{Ca}^{2+}$  release when the extracts are injected in eggs (Saunders *et al.*, 2002) making PLC $\zeta$  the primary candidate to be the sperm factor.

### **1.5.5 $\text{Ca}^{2+}$ oscillations cause inactivation of CSF and CDK1-cyclin B**

As discussed above, the metaphase II arrest is maintained by high CDK1-cyclin B levels, while the block of cyclin destruction is regulated by MAPK. Resumption of meiosis is associated with cyclin destruction and thus inactivation of CDK1-cyclin B (Kubiak *et al.*, 1993). There is evidence to link sperm-induced  $\text{Ca}^{2+}$  release to cyclin B kinetics at fertilisation. In ascidian eggs the two series of  $\text{Ca}^{2+}$  oscillations at fertilisation are associated with high CDK1-cyclin B activity levels (McDougall and Levasseur, 1998). The sperm-triggered  $\text{Ca}^{2+}$  oscillations seem to be regulated by CDK1-cyclin B since microinjection of undestructible cyclin B in ascidian oocytes sustains the oscillations for much longer than normal (Levasseur and McDougall, 2000). This regulation of  $\text{Ca}^{2+}$  oscillations by CDK1-cyclin B is further suggested by experiments presented in this thesis.

Furthermore,  $\text{Ca}^{2+}$  oscillations at fertilisation are responsible for resumption of meiosis, cyclin B degradation and subsequent CDK1-cyclin B inactivation.  $\text{Ca}^{2+}$  is sufficient

to cause cyclin B destruction and, consequently, metaphase exit, since even single transients are able to initiate cyclin degradation (Lorca *et al.*, 1991; Winston *et al.*, 1995; Collas *et al.*, 1995). Resumption of meiosis following egg activation, however, is not possible in the absence of an intact spindle (Winston *et al.*, 1995). This can be explained by the fact that treatment of MII mouse eggs with nocodazole blocks cyclin destruction (Kubiak *et al.*, 1993), presumably by invoking a spindle assembly checkpoint. Further evidence of  $\text{Ca}^{2+}$  involvement in cyclin B destruction is provided by recent results suggesting that individual transients trigger incremental bursts of cyclin B destruction (Nixon *et al.*, 2002). In addition, the activity of the 26S proteasome responsible for ubiquitinated cyclin B proteolysis has been shown to be sensitive to  $\text{Ca}^{2+}$  (Kawahara and Yokosawa, 1994; Aizawa *et al.*, 1996).

Regulation of cyclin B degradation may be mediated by CaMKII. When a constitutively active CaMKII is added to *Xenopus* CSF extracts, cyclin B is degraded and CDK1-cyclin B is inactivated even in the absence of any  $\text{Ca}^{2+}$  release. Furthermore, inhibitors against the CaMKII inhibit cyclin destruction and meiosis resumption in the presence of  $\text{Ca}^{2+}$  (Lorca *et al.*, 1993). In the mouse,  $\text{Ca}^{2+}$  release causes CaMKII activation (Winston and Maro, 1995), while calmodulin inhibitors block egg activation (Xu *et al.*, 1996). Monotonic  $\text{Ca}^{2+}$  rises only cause transient increases in CaMKII (Winston and Maro, 1995). This might explain why single  $\text{Ca}^{2+}$  transients are not sufficient for permanent cyclin B destruction (Collas *et al.*, 1995). Thus, a series of oscillations may be necessary for continuous CaMKII-dependent activation of the APC/C. This leads to the overriding of CSF arrest in order to drive cyclin B destruction and CDK1-cyclin B inactivation.

## **1.6 Synopsis**

The experiments that follow address the mechanisms controlling the resumption of the meiotic cell cycle and progression through MI and MII. Finally, we address the question of whether  $\text{Ca}^{2+}$  oscillations that stimulate meiotic resumption of MII-arrested eggs are regulated by the meiotic cell cycle kinases.



## 2. Materials and methods

### 2.1 Oocyte and embryo collection

Immature (germinal vesicle stage) oocytes were retrieved from the ovaries of 21-24 day old female MF1 mice that had been administered a 7 IU intraperitoneal injection of pregnant male serum gonadotrophin (PMSG; Intervet) 48 hours earlier. Mice were kept in a light/dark cycle with free access to food and water. Prior to removal of the ovaries, the mice were culled by cervical dislocation. Ovaries were released into warmed HEPES-buffered KSOM medium (H-KSOM) (Summers *et al.*, 2000) containing 1mg/ml fraction V BSA (Sigma Chemicals, Poole, Dorset, UK) with 200 $\mu$ M IBMX or 200 $\mu$ M dibutyryl cAMP (dbcAMP) (Sigma UK) to prevent germinal vesicle breakdown, and maintained at 37°C. Oocytes were recovered by puncturing the surface of the ovary with a 27-gauge needle, collected using a mouth-operated pipette, and placed in drops of media under oil to prevent evaporation (Mineral oil; embryo tested, Sigma UK). Only oocytes with an intact layer of cumulus cells were recovered, and cumulus cells were subsequently removed by repeated pipetting with a narrow pipette.

To recover mature (MII) oocytes, human Chorionic Gonadotrophin (hCG; Intervet, Milton Keynes, UK) was administered 48-54 hours after PMSG. Mice were culled and oviducts removed 14-16 hours post-hCG. Cumulus masses were released into H-KSOM by tearing the oviduct using forceps. Cumulus cells were removed by addition of hyaluronidase

(300µg/ml; embryo tested grade, Sigma UK) to the media. Following recovery, oocytes were washed through at least three drops of hyaluronidase-free media under oil.

For recovery of pronucleate embryos, female mice were mated with males at the time of hCG administration. The embryos were recovered from the oviduct by the same method as for mature eggs, 27-28h after hCG and mating. Embryos at the two-cell stage were recovered 48 hours after hCG and mating.

Oocytes and embryos that were not immediately utilised were left to undergo oocyte maturation and embryo development, respectively, in KSOM at 37°C in an atmosphere of 5%CO<sub>2</sub> in air.

## **2.2 In vitro fertilisation (IVF) and parthenogenetic activation**

For zona-free IVF, sperm was released from the epididymi of an F1 (C57xCBA) male mouse of proven fertility into T6 media (Quinn *et al.*, 1982) containing 10mg/ml BSA (Fraction V, Sigma UK) which had been pre-equilibrated to pH7.6 at 37°C, 5%CO<sub>2</sub> in air. Following a 20-30 minute swim-out period, 100µl of sperm solution was added to 100µl T6 under oil, and the resulting 1 in 2 dilution was placed in the incubator for 2 hours to allow capacitation. The zona pellucida was removed from cumulus-free mature oocytes by a brief exposure to an acidified Tyrodes solution (Sigma UK) followed by repeated washing in H-KSOM. For IVF on the microscope stage, zona-free oocytes were transferred to 0.5ml BSA-free H-KSOM on the microscope stage to allow the oocytes to adhere to the coverslip. After 5-10 minutes 0.5ml of BSA-containing media was added to the chamber, followed by 10-15µl of the capacitated sperm. IVF was performed 17-18 hours after administration of hCG.

Parthenogenetic embryos were produced by exposure of cumulus-free metaphase-II arrested eggs (18 hours after hCG) in  $\text{Ca}^{2+}$ -free H-KSOM containing 10 mM  $\text{SrCl}_2$  for two hours.

### **2.3 Microinjection**

Oocytes and embryos were pressure injected using a micropipette and Narishige manipulators mounted on a Leica DM IRB inverted microscope (Leica, Wetzlar, Germany). Oocytes were placed in a drop of H-KSOM covered with mineral oil to prevent evaporation. Cells were immobilised with a holding pipette while the injection pipette was pushed through the zona pellucida until making contact with the oocyte plasma membrane. A brief over-compensation of negative capacitance caused the pipette tip to penetrate the cell. Microinjection was performed using a fixed pressure pulse through a pico-pump (WPI, Sarasota, FL). Injection volumes were estimated at 2-5% of total cell volume by cytoplasmic displacement. The oocyte volume is approximately 250 pl.

After microinjection, the oocytes were removed to the hot block in fresh drops of H-KSOM under oil and allowed to recover for a few minutes before any other manipulation.

### **2.4 H1 and MBP Kinase Assays**

CDK1-cyclin B activity and MAPK activity can be measured by their ability to phosphorylate histone H1 and myelin basic protein, respectively, in vitro (H1 and MBP kinase assay). Five eggs (unless stated otherwise) in 2  $\mu\text{l}$  of H-KSOM were transferred in 3

$\mu\text{l}$  of storing solution (10 $\mu\text{g/ml}$  leupeptin, 10  $\mu\text{g/ml}$  aprotinin, 10mM p-nitrophenyl phosphate, 20 mM  $\beta$ -glycerophosphate, 0.1 mM sodium orthovanadate, 5 mM EGTA) and immediately frozen on dry ice. After three thaw-freeze cycles, the samples were diluted twice by the addition of two times concentrated kinase buffer containing 60 $\mu\text{g/ml}$  leupeptin, 60  $\mu\text{g/ml}$  aprotinin, 24mM p-nitrophenyl phosphate, 90 mM  $\beta$ -glycerophosphate, 4.6 mM sodium orthovanadate, 24 mM EGTA, 24 mM  $\text{MgCl}_2$ , 0.2 mM EDTA, 4 mM NaF, 1.6 mM dithiothreitol, 2 mg/ml polyvinyl alcohol, 40 mM MOPS, 0.6 mM ATP, 2 mg/ml histone H1 ( HIII-S from calf thymus, Sigma), 0.5 mg/ml MBP (from guinea pig brain, Sigma) and 0.25 mCi/ml [ $^{32}\text{P}$ ] ATP. The samples were then incubated at 30°C for 30 min. The reaction was stopped by the addition of two times SDS-sample buffer (0.125M Tris-HCl, 4% SDS, 20% glycerol, 10% mercaptoethanol, 0.002% bromophenol blue) and boiled for 3-5 min. The samples were then analysed by SDS-PAGE (10% gel, running time: 18h at 7V; Table 2.1) followed by autoradiography. The autoradiographs were imaged using the Fuji Bas-1000 phosphorimager system and analysed with TINA 2.0 software.

**Table 2.1 10% SDS-PAGE gel**

Separating gel 10%		Stacking gel 4%*	
40% acrylamide:	24ml	40% acrylamide:	3ml
2% Bis-acrylamide:	13ml	2% Bis-acrylamide:	1.5ml
1.5M Tris-HCl pH 8.8:	25ml	0.5M Tris-HCl pH 6.8:	7.5ml
10% SDS:	1ml	10% SDS:	300 $\mu$ l
10% APS (1g/ml):	500 $\mu$ l	10% APS (1g/ml):	150 $\mu$ l
TEMED:	50 $\mu$ l	TEMED:	30 $\mu$ l
Water to 100ml		Water to 30ml	

\* The stacking gel is applied after the separating gel has solidified.

## 2.5 Expression and purification of Cyclin B1-GFP

A baculovirus-based expression system was used to obtain recombinant human Cyclin B1-GFP. Sf9 insect cells infected with the baculovirus encoding the His (6)- cyclin B1-GFP (provided by J. Pines) were grown in G10 medium at 27°C for 48h. The cells were harvested and then centrifuged for 10 min at 1000 x g at 4°C and were washed in ice-cold PBS. The cells were then resuspended in ice-cold lysis buffer (50 mM Tris-HCl, 300 mM NaCl, 1% Triton X-100, 0.1 mM PMSF, 0.1 Benzamidine, pH 7.0). The resultant suspension was centrifuged at 1500 x g for 10 min at 4°C and the supernatant recovered. The supernatant was then centrifuged at 16,000 x g for 30 min at 4°C to pellet the cellular debris. The clarified supernatant from this second centrifugation was mixed with 1-2 ml of pre-equilibrated, in

Wash Buffer (50 mM Sodium Phosphate, 300 mM NaCl, pH 7.0), packed TALON Co<sup>2+</sup> beads (BD Biosciences) and was gently agitated at RT for 60 min to allow the polyhistidine-tagged protein to bind the resin. The specific binding occurs because the histidines of cyclin B1-GFP will bind to the Co<sup>2+</sup> which is placed in the reactive core of the resin. The beads were then washed 2-3 times. The resin was transferred to a 10 ml gravity-flow column with an end-cap in place to allow the resin to settle out of suspension. The column was washed 1-2 times and the protein was recovered after the addition of Elution Buffer (50 mM Sodium Phosphate, 300 mM NaCl, 150 mM Imidazole, pH 7.0). The imidazole of the Elution Buffer competes with the cyclin B-GFP histidine tag for binding to the Co<sup>2+</sup> beads, leading to the recovery of the protein in the buffer. This solution was then concentrated by filtration by the use of Microsep 10K microconcentrators (Gelman Laboratories). Centrifugation at 10,000 x g for 60 min provides the driving force for filtration. The solution was concentrated to 30-40  $\mu$ l. 3.5 ml of injection buffer (150 mM KCl, 20 Mm HEPES, pH 7.4) were added and the sample was centrifuged under the same conditions. This final step was repeated two times to ensure the purification and desalting of the sample. The concentrated sample was measured to be approximately 2 mg/ml.

## **2.6 Depletion of Emi1 using Morpholino oligonucleotides**

In order to study the action of proteins it is often desirable to deplete the specific protein. The most common way to study the action of a specific protein in mouse oocytes is by specific mRNA degradation mediated by double-stranded RNA (dsRNA), which is termed RNA interference (RNAi) (Svoboda *et al.*, 2000; Wianny and Zernicka-Goetz, 2000). In our

experiments we used Morpholino antisense oligos (Gene Tools, USA) which have been shown to be both effective and non-toxic for mouse oocytes (Lefebvre *et al.*, 2002). An antisense oligo is designed to bind to a complementary sequence in the selected mRNA. This binding prevents the translation of that specific mRNA and, as a consequence, the protein product coded by that particular mRNA is not made. Morpholinos are very stable, specific, non-toxic, water soluble and have long-term activity. Their stability is due to their structure. Morpholinos are comprised of nucleotides of which the riboses are transformed into morpholines through the introduction of an amine. The bases (A,T,G,C) are, thus, attached to a morpholine instead of a ribose ([www.gene-tools.com](http://www.gene-tools.com)).

We microinjected a specific Morpholino oligo to block the expression of Emil in mouse oocytes. The sequence of the oligo used was 5'-CG-GGA-CAA-GAA-AGA-CAA-TGT-TAC (triplet corresponding to initiation codon on mRNA)-TT-3'. The identification of the specific sequence took into account that Morpholino oligos work more efficiently when they bind to as much possible of the 5' untranslated region of the target mRNA and when their length is 20-25 bases long. In addition, we made sure that the selected sequence had no self-complementarity to avoid intrastrand pairing. We also took in account that best binding to the mRNA target is obtained when the GC content of the oligo is 40-60%. A higher concentration of GCs was avoided because it reduces solubility in water. The mouse Emil mRNA-specific Morpholino was prepared for us by Gene Tools (OR, USA).

To control for possible non-specific effects of the Emil Morpholino, a control Morpholino was also purchased. The sequence was 5'-CCT-CTT-ACC-TCA-TTA-CAA-TTT-ATA-3'. This oligo has no target and no significant biological activity except in reticulocytes from thalassemic humans. In those cells this oligo will correct a splicing error

and thereby generate a correctly-spliced mRNA which codes for normal beta-globin chains ([www.gene-tools.com](http://www.gene-tools.com)).

## **2.7 Immunolocalisation of Emi1**

Oocytes were fixed in freshly-prepared 4% paraformaldehyde (in PBS pH 7.4, 1mg/ ml polyvinyl alcohol; PVA) for 20 min. After two washes in PBS/PVA the eggs were permeabilised in 0.1% Triton X-100 (in PBS/PVA) for 15 min. The cells were then incubated in blocking buffer (PBS, 3% BSA, 10% normal goat serum) for two hours at room temperature (RT) and then in the rabbit polyclonal anti-human Emi1 antibody (2.5 µg/ml; provided by P. Jackson) in blocking buffer at 4°C over night. The cells were then extensively washed and incubated with a fluorescein-conjugated goat polyclonal anti-rabbit secondary antibody (0.5 mg/ml; Alexa Fluor 488 from Molecular Probes) for one hour at RT. This was followed by extensive washing. Included in the first wash was Hoechst (for DNA staining). The immunostaining was visualised using a LSM 510 META confocal microscope. To ensure that comparisons of immunofluorescence could be made between treatment groups or developmental stages, the different samples were scanned and viewed with identical settings.

## **2.8 Fluorophores**

### **2.8.1 Fluorescence imaging of DNA**

To monitor changes in DNA morphology during the meiotic cell cycle (and in response to a variety of treatments of the oocytes) DNA was stained with the UV excited DNA stain



bisBenzimide (Hoechst 33342). Excitation was obtained by the use of a monochromator and a UV filter set: BP 330-380 nm for excitation, DM 400 nm and LP 450 nm for emission.

### **2.8.2 Imaging of the spindle**

In order to examine the state of the spindle in our experiments, oocytes were microinjected with tetramethylrhodamine-labeled tubulin ( $\alpha/\beta$ -tubulin dimmers from bovine brain; Molecular Probes) to a final concentration inside the oocyte of 0.5 mg/ml. The fluorescence excitation and emission maxima of the tubulin are approximately 555 nm and 580 nm, respectively. After microinjection, the fluorescent tubulin was incorporated into the spindle by replacing the endogenous tubulin dimmers. The oocytes, injected with fluorescent tubulin, were incubated for approximately one hour before imaging or fixing.

### **2.8.3 Measurement of intracellular $[Ca^{2+}]_i$ and photorelease of 'caged-InsP<sub>3</sub>'**

$[Ca^{2+}]_i$  was monitored either with Fura-2 AM, Fura-2 Dextran (10,000 MW) or Fura-red (Molecular Probes, Eugene, OR). Loaded oocytes were placed in a drop of H-KSOM under oil in a chamber and placed on an Axiovert microscope (Zeiss, Welwyn Garden City, UK). The Fura-2 dextran variety is used to minimise compartmentalisation, which can be a potential problem when using non-conjugated dyes (AM) whose efficiency can be reduced in long-term experiments (Schlatterer *et al.*, 1992). In short-term (1-2 hours) experiments, for which the membrane permeable AM varieties' efficiency is satisfactory, Fura-2 AM was preferred in order to avoid the invasive procedure of microinjection. The main advantage of using Fura-2 and Fura Red is that they are ratiometric dyes. This results in a signal that is independent of dye concentration and distribution (Rudolf *et al.*, 2003). Fura-2 is imaged

using a Xenon lamp and was excited by two wavelengths, 350 nm and 380 nm, selected by a monochromator (Till, Germany). A 510 nm dichroic mirror (DM) was used (as for all conventional imaging experiments except the ones with Hoechst) and fluorescence was collected through a 20x 0.75 NA objective. The emitted fluorescence was collected by using a 520 nm long-pass (LP) filter. On binding calcium the excitation efficiency of 350 nm increases and 380 nm decreases. The ratio is obtained by dividing the 350 nm intensity by that of 380 nm (350/380). The emitted light from all the fluorochromes was collected using a cooled CCD camera (MicroMax, Princeton Scientific Instruments, Monmouth Junction, NJ). Although Fura-2 was used for most  $\text{Ca}^{2+}$  imaging experiments, it could not be used for  $\text{IP}_3$  uncaging because Fura-2 is excited by UV wavelengths used to uncage  $\text{IP}_3$  (see below). For this reason, Fura-red AM was preferred. Fura-red is excited at 427 nm and 490 nm, with emitted light monitored with a LP 600 nm filter. Changes in intracellular  $\text{Ca}^{2+}$  concentration are expressed as the ratio between the emission in response to 427 nm and 490 nm excitation (427/490).

$\text{IP}_3$  uncaging was utilised for obtaining single calcium transients of controlled amplitude and duration. Photo-release of caged- $\text{IP}_3$  (Molecular Probes) was performed 30-60 minutes after its microinjection by brief, timed exposures of microinjected oocytes to UV light (360 nm). The exposure times were 1 sec for mature MII eggs and 3 sec for maturing oocytes, since it is well established that sensitivity to  $\text{IP}_3$  is higher in MII eggs than in oocytes. Different exposure times are necessary in order to obtain similar calcium transients, in response to uncaged  $\text{IP}_3$ .

In all imaging experiments using conventional microscopy, data was collected and analysed using Universal Imaging Metafluor and Metamorph software.

#### 2.8.4 Cyclin B1-GFP fusion protein

We have used a cyclin B1-GFP chimera (provided by Jonathon Pines) to follow the behaviour and localisation of cyclin B1 in living mouse oocytes during meiosis. The use of GFP tagged proteins bypasses the problem of artifacts caused by the fixation of cells. Thus, the utilisation of cyclin B1-GFP enabled us to follow the fate of cyclin B1 throughout oocyte maturation or fertilisation in individual single egg. The use of this construct in HeLa cells has shown that cyclin B1-GFP localises correctly through mitosis and that it is specifically degraded at anaphase in parallel with the endogenous cyclin protein (Hagting *et al.*, 1998; Clute and Pines, 1999).

Cyclin B1-GFP is a fusion protein comprised of the human cyclin B1 tagged at the carboxyl terminus with MmGFP. Adding the GFP at the amino terminus renders cyclin indestructible (Hagting *et al.*, 1998). This form of GFP has a series of mutations compared to the wild-type GFP. These modifications have improved the folding of GFP and have altered the chromophore structure (Zernicka-Goetz *et al.*, 1996; Zernicka-Goetz *et al.*, 1997). Due to these changes MmGFP is excited at a longer wavelength (490 nm) than the wild-type protein (395 nm). This is very important, especially for long term experiments and constant imaging, since blue light causes less photodamage to cells than UV light. Furthermore, this form of GFP is stable at 37°C. Wild-type GFP is misfolded and does not fluoresce in temperatures above 30°C (Zernicka-Goetz and Pines, 2001). As MmGFP, the EGFP protein (Clontech) which is used as a control in a number of experiments contains the two major mutations, that enhance the solubility (F64L) and alter the excitation wavelength to 490 nm (S65T) of the GFP (Yang *et al.*, 1996). The MmGFP contains two further mutations (V163A, S175G) responsible for better folding of the protein (Zernicka-Goetz and Pines, 2001).

For imaging cyclin B1-GFP with conventional microscopy, a fluorescein isothiocyanate (FITC) filter set was used: 450-490 nm excitation band pass (BP) filter, DM 510 nm and BP 520 nm for emission. The same settings were used for imaging EGFP (Clontech), Fluorescein Dextran (77.000 MW) and FITC-labelled BSA tagged with a nuclear localising signal (FITC-NLS-BSA; provided by Mark Jackman).

Occasionally, combinations of dyes were used in the same experiment. When FITC-NLS-BSA and Fura-2 dextran were both injected in eggs, the monochromator and an excitation filter wheel were used for the different excitations of the dyes (filter wheel: BP 450-490 nm for the excitation of FITC-NLS-BSA and no filter for Fura-2). The DM and emission filter were the same, as described previously.

## **2.9 Confocal microscopy**

Confocal imaging was preferentially used for immuno-localisation experiments (Emil localisation in oocyte maturation and fertilisation) and short term experiments (1-2h) with living cells (cyclin B1 localisation during GVBD). Long-term experiments can result in photodamage of the cells.

The advantage of confocal light microscopy is that it can collect the light reflected or emitted by a single plane of the specimen. A pinhole conjugated to the focal plane obstructs the light coming from objects outside the plane, so that only light from in-focus objects can reach the detector. A laser beam scans the specimen pixel by pixel and line by line. The pixel data are then assembled into an image that is an optical section through the specimen, distinguished by high contrast and high resolution in x, y and z. In order to reduce

background noise in the obtained images we used the Kalman averaging function of the confocal microscope. Three successive scans of an image were preferred for Kalman averaging.

For cyclin B1 localisation during GVBD, confocal microscopy was performed using a BioRad micro radiance confocal scan head mounted on a Zeiss Axiovert 100TV. Oocytes were placed in a heated chamber (37° C) and cyclin B1-GFP was excited using the 488nm line of an argon laser. The light passed through a DM of 510 and emission LP 520, before resulting in the photon multiplier tube at the detection channel. Fluorescence was collected through a 20x 0.75 NA objective. Laser power was set to 1 or 3% of maximum and images were collected at intervals of 5 or 10 minutes.

A fluorescein-conjugated polyclonal anti-rabbit secondary antibody, injectable rhodamin-labeled tubulin and Hoechst were used for detecting the anti-hEmil antibody, microtubules and chromatin respectively, in the same egg. The LSM 510 confocal system was used for imaging these dyes. It is comprised of a Zeiss Axiovert 200M (equipped with ICS optics and supported by the LSM software) and the LSM laser and scanning module. For the fluorescein-conjugated antibody, confocal images were taken using the 488 nm laser line of an Argon laser and a BP 505-530 nm for emission. The same settings were used for imaging cyclin B1-GFP when detected with confocal microscopy. For rhodamine-labeled tubulin, the 543 nm laser line of a Helion-Neon laser and a BP 560-615 nm for emission were used. For imaging Hoechst, confocal images were obtained by exciting with the 351 nm laser line of a UV laser and emission was collected through a BP 435-485 nm.

For all confocal imaging experiments a pinhole of 2.22 Airy Units was used, giving a calculated optical slice of 3.5µm. The images were analysed using Metamorph software.

## 2.10 Statistical analysis

All t-tests are two-tailed and based upon two samples (unpaired) with similar variance.

Where shown on figures, error bars represent the standard deviation.

**Table 2.2 Spectra of fluorophores used**

<b>Fluorescent agent</b>	<b>Excitation maximum (nm)</b>	<b>Emission maximum (nm)</b>
Fluorescein or GFP	490	510
Fura 2	340/380	510
Fura red	427/490	660
Hoechst	350	450
Rhodamine-labeled tubulin	555	580

**Table 2.3 Final concentrations of microinjected agents inside the oocyte**

<b>Injected agent</b>	<b>Concentration inside cell</b>
Caged IP <sub>3</sub>	20-50 $\mu$ M
Cyclin B1-GFP protein	2-40pg/ cell
EGFP protein	10-20 mg/ ml
hEmi1 protein	0.1 mg/ml
FITC-NLS-BSA	20 $\mu$ M
Fluorescein Dextran (77 KDa)	20-30 pg/ cell
Fura 2 Dextran	2-4 $\mu$ M
Importin $\beta$ <sup>45-462</sup> (provided by Dirk Gorlich)	5-10 $\mu$ M
Morpholinos	30-50 $\mu$ M
WGA	200-500 $\mu$ g/ ml

## 2.4 Reagents and indicators used in treatments

<b>Loaded agent</b>	<b>Concentration</b>	<b>Incubation time (min)</b>	<b>Function</b>
BAPTA salt	2mM	*	Buffers extracellular Ca <sup>2+</sup>
Cycloheximide	10 µM	30*	Protein synthesis inhibitor
Fura 2 AM	0.2-0.5 µM	10	Ca <sup>2+</sup> dye
Fura red AM	4 µM	10	Ca <sup>2+</sup> dye
Hoechst	2 µM	5	Chromatin dye
IBMX	44 µg/ ml	*	GVBD inhibition
Leptomycin B	20 nM	30*	Nuclear export inhibition
MG 132	50 µM	30*	Proteosome inhibition
SrCl <sub>2</sub>	10 mM	*	Parthenogenetic activation
UO 126	50 µM	60*	MEK1 inhibition

pre-incubation, loading is necessary for the duration of the experiment.



### 3. The dynamics of cyclin B1 distribution during meiosis I in mouse oocytes.

#### 3.1 Introduction

In prophase arrested mouse oocytes, CDK1-cyclin B complexes pre-exist in an inactive state (pre-MPF) with cyclin B1 being in a 7-8 fold molar excess over CDK1 (Kanatsu-Shinohara *et al.*, 2000). The abundance of cyclin indicates that cyclin synthesis is not necessary for GVBD. This is demonstrated by the ability of mouse oocytes to undergo GVBD in vitro in the presence of protein synthesis inhibitors (Clarke and Masui, 1983; Hashimoto and Kishimoto, 1988). Thus, activation by de-phosphorylation of the pool of CDK1-cyclin B seems to be an important requirement for entry into MI (Choi *et al.*, 1991). Protein synthesis, however, is necessary for progression to MI since protein synthesis inhibition prevents normal MI spindle formation (Clarke and Masui, 1983; Hashimoto and Kishimoto, 1988). Cyclin B appears to be one of the proteins required for MI progression since the rate of cyclin B synthesis is tightly correlated with the duration of MI and the degree of CDK1-cyclin B activity (Hampl and Eppig, 1995a; Polanski *et al.*, 1998). Moreover, micro-injection of cyclin B mRNA accelerates or delays MI progression depending on the length of the poly-A tail of the mRNA, a mechanism that regulates translational efficiency (Tay *et al.*, 2000; Ledan *et al.*, 2001). These results imply that the levels of cyclin B play a major role in the control of the timing of GVBD and MI progression.

Another mechanism important for the regulation of CDK1-cyclin B activity and NEBD is the localisation of the complex (Pines and Hunter, 1991;Pines, 1999;Takizawa and Morgan, 2000). CDK1-cyclin B is cytoplasmic during interphase and is transported in and out of the nucleus. In somatic cells (Pines and Hunter, 1991;Hagting *et al.*, 1998) and starfish oocytes (Ookata *et al.*, 1992) the complex accumulates in the nucleus late in prophase just prior to nuclear envelope breakdown (NEBD). This translocation is obtained by the phosphorylation of the nuclear export sequence (NES) region of the cyclin partner. Non-phosphorylated NES binds to and is exported from the nucleus by the export factor CRM1 (Hagting *et al.*, 1998;Yang *et al.*, 1998;Toyoshima *et al.*, 1998). Phosphorylation eliminates the affinity of the NES to CRM1 and the CDK1-cyclin B remain nuclear (Hagting *et al.*, 1998;Yang *et al.*, 1998). Besides the decrease of export, nuclear accumulation is controlled by an increase in import (Hagting *et al.*, 1999;Yang *et al.*, 2001). After NEBD, CDK1-cyclin B associates with the mitotic apparatus, including the spindle poles, the microtubules and chromatin (Pines and Hunter, 1991;Clute and Pines, 1999). ✓

There have been no experiments in mammalian oocytes to determine the relationship between cyclin B localisation and GVBD. Here we have used a human cyclin B1-GFP fusion protein (Hagting *et al.*, 1998;Clute and Pines, 1999) to examine the effects of cyclin abundance on GVBD, the dynamics of cyclin B1 localisation during GVBD and the mechanisms underlying the localisation of cyclin B1 during MI in mouse oocytes.

## 3.2 Results

### 3.2.1 Exogenous Cyclin B1-GFP induces premature GVBD

Protein synthesis inhibitors have shown that there is no requirement for cyclin B synthesis for GVBD to occur. To investigate the possibility that GVBD is sensitive to the levels of cyclin B we microinjected cyclin B1-GFP in GV stage oocytes at various concentrations. Since the estimated amount of cyclin B1 in a fully grown oocyte is 10pg (Kanatsu-Shinohara *et al.*, 2000), we microinjected approximately 10, 20 and 40 pg of cyclin B1 into dbcAMP-arrested oocytes. To assess the effects on GVBD and extrusion of the first polar body, oocytes were released from dbcAMP and GVBD was monitored every 15 minutes. Cyclin B1-GFP accelerated GVBD at all concentrations tested (Figure 3.1A). The acceleration was found to be dose dependent; 50% GVBD taking 150 min, 60 min, 45 min and 30 min for controls (n=33) and cyclin injections of 10pg (n=44), 20pg (n=35) and 40pg (n=29), respectively (Figure 3.1A). A similar effect was observed for the maximal level of GVBD, being for controls 180 min, for 10pg injection 90 min, for 20pg 60 min and for 40 pg 45 min (Figure 3.1A).

By measuring H1 kinase activity we ascertained that premature GVBD, after cyclin B1-GFP injection, was attributed to accelerated CDK1-cyclin B activation (Figure 3.1Aii). In injected oocytes, a 9-fold increase over baseline levels in CDK1-cyclin B activity was first detected at 30 minutes after release from arrest. In controls, the first increase was detected after 60 minutes and amounted to a 2-fold increase. Maximum levels of CDK1-cyclin B activity were detected 60 minutes after release in injected oocytes and reached a 25-fold increase. In contrast, control oocytes reached a maximum 4-fold increase in activity after 120 minutes (Figure 3.1 Aii). Accelerated CDK1-cyclin B activation also led to the premature

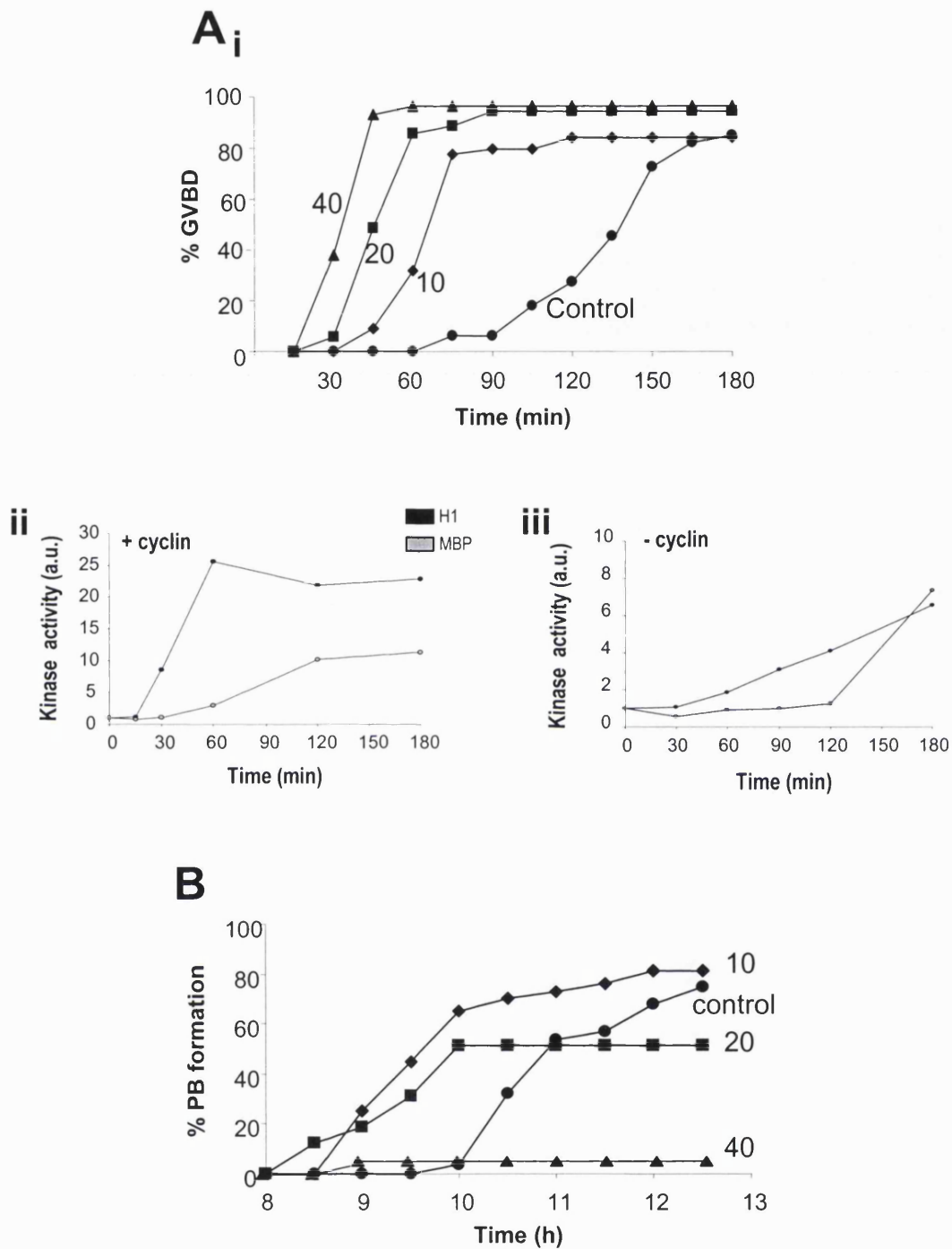


**Figure 3.1 Cyclin B1-GFP accelerates GVBD.** GV stage oocytes were injected with cyclin B1-GFP in the presence of dbcAMP before culture in dbcAMP-free media (A, B). The timing of GVBD (A) and polar body extrusion (B) was monitored using bright field optics. Cyclin B1-GFP accelerated GVBD after microinjection of 10 (◆), 20 (■) or 40 pg (▲) of cyclin B1-GFP compared to controls (●) (A i). H1 kinase and MBP assays for MPF and MAPK activities for cyclin B1-GFP-injected oocytes (A ii) and control oocytes are shown (A iii). Note that the kinase activities increase sooner and to a higher level after injection of cyclin B1-GFP. The effect of cyclin B1-GFP on polar body extrusion was biphasic. Lower doses of 10 and 20pg accelerated polar body extrusion (B) while higher doses increased the proportion of oocytes arrested at MI (B). Data is pooled from 2-3 independent experiments with a total of 44, 35, 29 and 33 oocytes for the 10pg, 20pg, 40pg and uninjected control groups, respectively.

are there any consequences of final pronuclear  
and/or entry into GVB?  
→ normal meiosis +  
fertilisation?

activation of MAPK measured by MBP kinase assays (Figure 3.1Aiii). In cyclin-injected oocytes MAPK activity gradually rose after 30 minutes from injection reaching a maximum 10-fold increase by 120 minutes. In control oocytes, there was no apparent MAPK activity before 120 minutes, rising to an 8-fold increase over basal levels by 180 minutes (Figure 3.1Aiii). Thus, although MAPK activation is accelerated by cyclin injection, there is no substantial effect on the level of activation, contrary to the effect of the injection on CDK1-cyclin B activity.

### 3.2.2 Cyclin B1-GFP has a concentration-dependent effect on extrusion of the 1st polar body

There is a dual effect of cyclin B1-GFP injection on the extrusion of Pb1. The first effect is the acceleration of Pb1 extrusion by 2, 10 and 20 pg of injected cyclin B. The injected oocytes extrude their polar body at 8.5-9 hours after injection whereas controls extrude the Pb1 at about 10 hours after release from dbcAMP (Figure 3.1B). However, there is also a proportion of oocytes that fail to extrude the Pb1 and this proportion rises with the amount of cyclin injected (Figure 3.1B). Oocytes injected with 10 pg of cyclin B1-GFP protein showed similar rates of Pb1 extrusion to controls (80%, 21/25 and 85% 24/28, respectively). Data for 2 pg injections are not shown since they are similar to those for 10 pg. Injection of 20 pg of cyclin, however, resulted in 50% Pb1 extrusion (12/24;  $P < 0.05$  compared to controls), while only 5% of oocytes injected with 40 pg extruded a polar body (1/19;  $P < 0.01$  compared to controls). Similar results were also observed by Ledan et al., 2001, who microinjected cyclin B1 mRNA with poly-A tails of different lengths. However, mRNA injection can not show the dose-dependent effect observed in our work.

4.5 hrs  
increased  
what  
are  
the other  
time  
regulatory  
factors?

### **3.2.3 Cyclin B1 overrides cAMP-mediated arrest in germinal vesicle stage mouse oocytes**

Ledan et al., (2001) showed that over-expression of cyclin B1 after microinjection of cyclin B1 mRNA, was sufficient to override cAMP-mediated arrest. The observation that exogenous cyclin B1 accelerated the rate of GVBD suggests that excess cyclin B1 is a potent stimulus for meiotic resumption. In our work (performed prior to the publication of Ledan and co-workers, 2001) we determined whether cyclin B1-GFP injection could override cAMP-mediated arrest. Oocytes were cultured in M2 media containing 250  $\mu$ M dbcAMP to inhibit resumption of meiosis. The oocytes were retained in dbcAMP for 2h and then injected with cyclin B1 protein (40 pg). Injected and control oocytes were then cultured with and without dbcAMP and GVBD was monitored every 15 minutes. Cyclin-injected oocytes in the presence and absence of dbcAMP started to undergo GVBD around 30 minutes after injection (Figure 3.2A). The maximum level of GVBD was reached at around 60 minutes for both cyclin injected groups compared to 120 minutes for uninjected controls cultured in the absence of dbcAMP (Figure 3.2A). As expected, uninjected control oocytes remained in the GV stage during the 3 hour incubation (Figure 3.2A). Thus, oocytes injected with cyclin underwent GVBD with similar kinetics as those in the absence of dbcAMP. However, dbcAMP did prevent a proportion of oocytes from undergoing GVBD. After 3 hours 60% (41/69) of the cyclin-injected oocytes had undergone GVBD in the presence of dbcAMP which was significantly less than the 90% that had undergone GVBD in its absence ( $P < 0.01$ ). To determine if the non-responding oocytes were able to undergo GVBD, dbcAMP was removed after three hours and the oocytes were cultured in dbcAMP-free medium. These

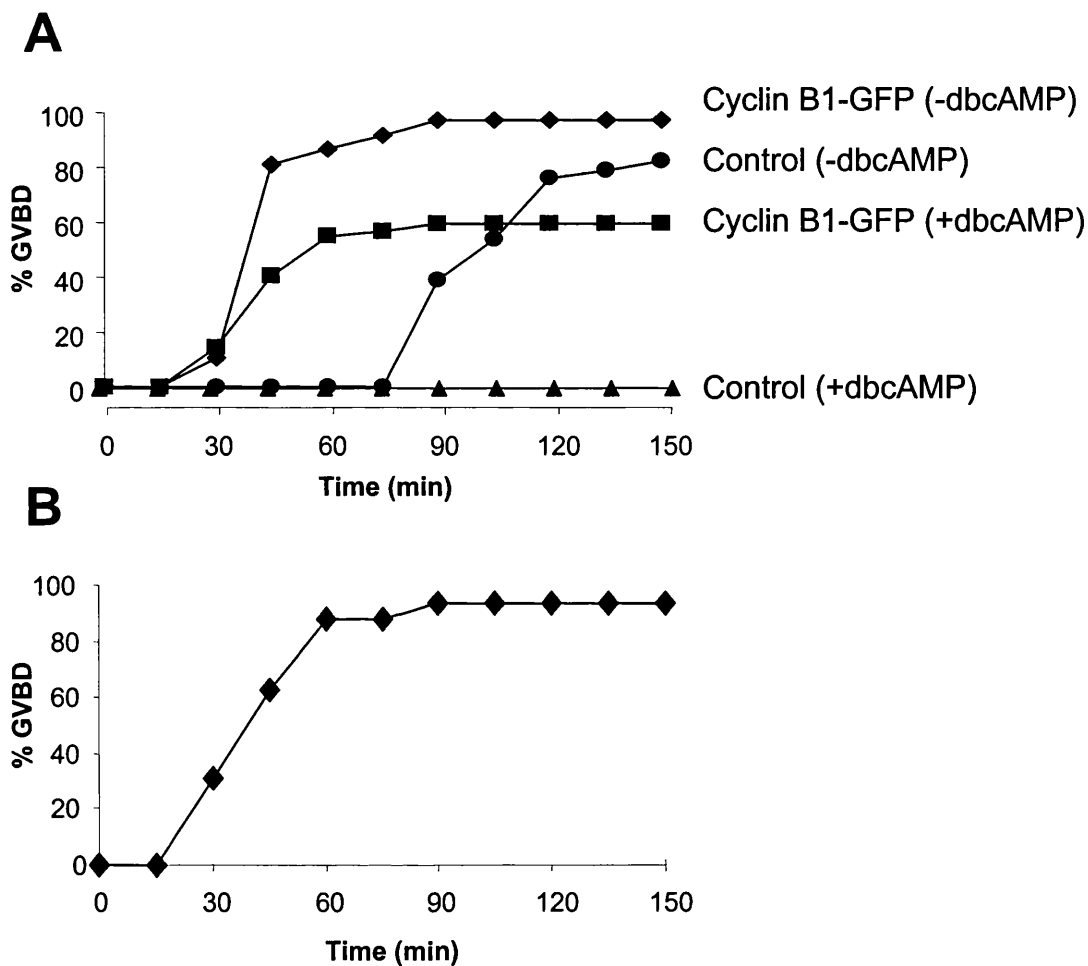


**Figure 3.2 Cyclin B1-GFP overrides cAMP-mediated meiotic arrest.** In *A*, GV stage oocytes were microinjected with 40pg of cyclin B1-GFP in the presence of dbcAMP. The rate of GVBD was then monitored in the continued presence of dbcAMP (■) (n=69) or after release from dbcAMP (◆) (n=37). Non-injected control oocytes cultured in the presence (▲) (n=43) or absence (●) (n=67) of dbcAMP were included for comparison. Cyclin B1-GFP-injected oocytes that failed to undergo GVBD (n=23) in the presence of dbcAMP were released from cAMP and monitored for the presence of a GV (*B*). Data are pooled from 2-4 separate experiments.

oocytes underwent GVBD within 60 minutes (87%, 21/24), similar to the timing of GVBD in the absence of dbcAMP (Figure 3.2B).

### **3.2.4 GVBD is associated with nuclear localisation of cyclin-GFP**

In mammalian mitotic cells it is shown that cyclin B is found in the cytoplasm during interphase, only to enter the nucleus at prophase, just prior to NEBD (Hagting *et al.*, 1998; Pines, 1999). Unlike mitosis, in meiosis the cell cycle is not continuous and the oocytes are arrested in prophase. Thus, it was of interest to investigate the localisation of the protein in the arrested state and determine how cyclin B is distributed during GVBD. In order to examine this, we microinjected mouse oocytes arrested at prophase with dbcAMP with 40 pg cyclin B1-GFP protein. The oocytes were then released from the prophase block and cyclin distribution was observed using confocal microscopy. Initially, cyclin B1-GFP localisation is cytoplasmic with no traces of the protein in the nucleus. A focal localisation is observed close to the nuclear membrane (Fig 3.3A arrow). These accumulations (one or two) resemble the localisation on centrosomes of mitotic cells (Hagting *et al.*, 1998) and they are most possibly microtubule organising centres, the equivalent of centrosomes in meiosis. In the mouse the first signs of cyclin B1-GFP entering the nucleus are observed after 20 minutes from injection and maximal nuclear accumulation is seen at about 40 minutes (Fig 3.3A,B). GVBD occurs within 10 minutes from peak nuclear localisation. After GVBD, cyclin is redistributed to the cytoplasm with a higher concentration remaining on the condensed chromosomes. In order to ascertain whether cyclin B1-GFP localises on the chromatin in other stages of meiosis, 20 pg of cyclin B1-GFP were microinjected in MII arrested eggs. Confocal microscopy showed that cyclin B can localise on the chromosomes and spindle



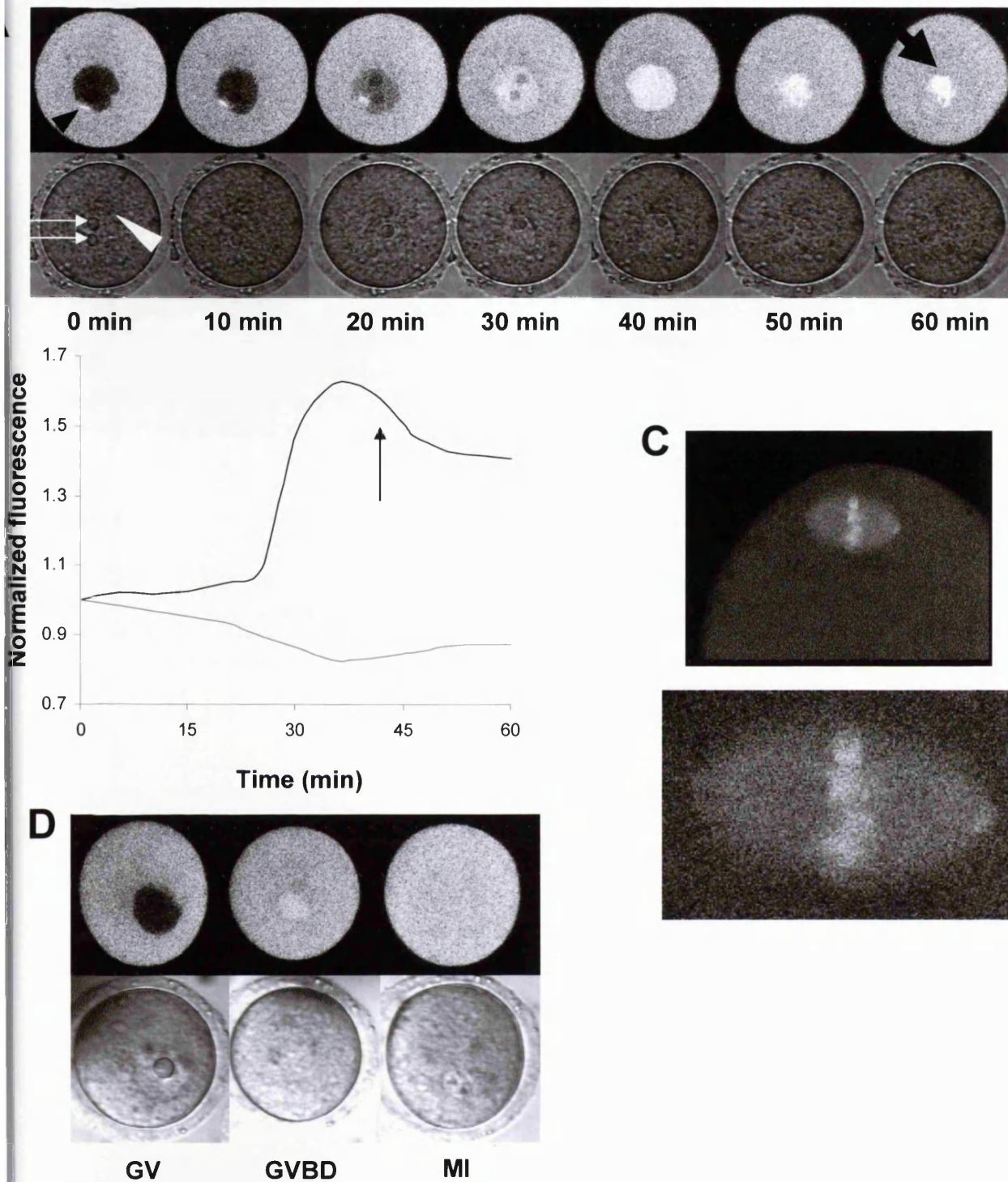


**Figure 3.3 Cyclin B1-GFP enters the GV just prior to GVBD.** Oocytes were microinjected with 40 pg cyclin B1-GFP and confocal microscopy was used to determine its localisation. In *A*, confocal scans of cyclin B1-GFP recorded every 10 minutes are shown in the top panel with corresponding bright field images in the lower panel. The black arrows in the first image of the top panel highlight a concentration of cyclin B1-GFP (see Results) that is apparent in all oocytes examined ( $n=15$ ). The large arrowhead on the first image of the lower panel points to the GV while the thin arrows point to the nucleoli. A plot of the fluorescence intensities in the nucleus and cytoplasm during the course of the experiment is shown in *B* (representative of 12 oocytes examined). The arrow signifies the time that GVBD was confirmed. In *C*, MII stage oocytes were injected with cyclin B1-GFP to determine whether it localised to the metaphase chromosomes. Note that cyclin B1-GFP attaches to the MII spindle including the metaphase plate. In *D*, oocytes were microinjected with 70kDa fluorescein dextran and monitored through GVBD with confocal microscopy ( $n=8$ ). Images are shown when oocytes are at the GV stage, at GVBD and one hour after GVBD. Note that fluorescence in the region of the germinal vesicle was only detected after GVBD.

microtubules (Figure 3.3C). Identical localisation is observed when cyclin B1-GFP is injected any time during MI (data not shown).

In order to confirm the observed pattern of nuclear entry and that it is specific for cyclin B, we microinjected oocytes with a 70kDa fluorescein dextran and compared its localisation to that of the 97 kDa cyclin B1-GFP (Figure 3.3D). The molecular weight of the dextran was chosen to be high to avoid passive entry of the protein in the nucleus, through the nuclear pore complexes. The dextran was excluded from the GV prior to GVBD, only to diffuse in the nuclear area after nuclear membrane breakdown. In addition, there was no peri-nuclear accumulation of fluorescence as observed in cyclin B1-GFP-injected oocytes.

### 3.2.5 Cyclin B1 is actively exported from the germinal vesicle

In mitotic cells, although cyclin enters the nucleus in interphase, due to its nuclear export signal, it is rapidly exported via the CRM1 nuclear export pathway and retained in the cytoplasm (n=8). In order to investigate whether the same nuclear export mechanism is observed in meiosis we microinjected cyclin B1-GFP in the GV of oocytes arrested at prophase. Imaging of the GFP-tagged protein revealed that cyclin B is gradually exported from the GV immediately after injection (Figure 3.4A, D). Bright field observations of the oocytes showed that, during the measurements, the GVs were intact. In addition, this gradual loss of cyclin from the nucleus can not be compared with the abrupt loss seen at GVBD. Thus, the export observed can not be attributed to GVBD, but to active nuclear export.

Furthermore, in order to ascertain that the export pattern observed is attributed to cyclin and not GFP, we injected GVs with EGFP (n=10). The GFP, due to its small size, was not retained in the nucleus, leading to similar concentrations of GFP both in the nucleus and

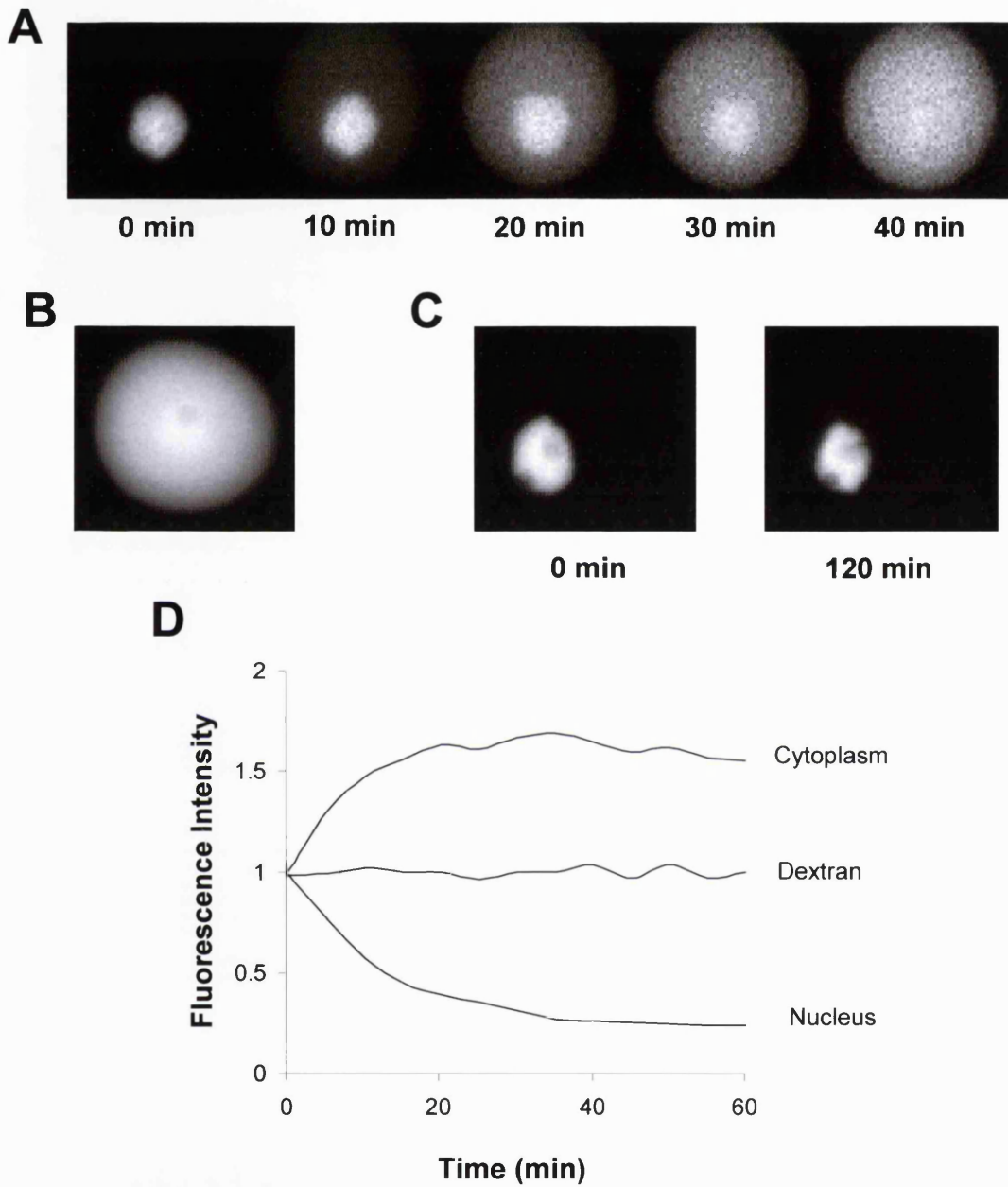


**Figure 3.4 Cyclin B1-GFP is actively exported from the germinal vesicle.** Cyclin B1-GFP was injected into the germinal vesicle of oocytes maintained in dbcAMP and the redistribution was monitored using confocal microscopy (A). The export of cyclin B1-GFP is specific because nuclear injection of GFP (B) and 70kDa fluorescein dextran (C) do not show similar redistribution. A plot of the fluorescence intensities of cyclin B1-GFP in the nucleus and cytoplasm can be compared to the constant level of nuclear fluorescence after injection of 70kDa fluorescein dextran (D). No data is provided for GFP as it had diffused from the GV in the 3-5 minutes between injection and imaging. Data presented is representative of 8 cyclin B1-GFP-injected oocytes, 10 fluorescein dextran-injected oocytes, and 10 GFP-injected oocytes.

the cytoplasm (Figure 3.4B). To further test that the measured export was specific to cyclin B and that it is not due to simple diffusion, we injected GVs with a 70 kDa fluorescein dextran (n=10). The dextran was retained in the nucleus for the duration of the experiment (two hours) (Figure 3.4C, D).

### **3.2.6 Inhibition of nuclear export accelerates accumulation of nuclear cyclin-GFP**

Besides nuclear export, we wanted to investigate the kinetics of cyclin B during nuclear import. Since cyclin B is constantly exported from the nucleus at prophase arrest, measuring the rate of import at this stage had to involve blocking the nuclear export pathway. Thus, we used leptomycin B in order to inhibit the CRM1-dependent nuclear export (Fornerod *et al.*, 1997; Hagting *et al.*, 1998). When oocytes were incubated with 20 nM of leptomycin B, injected with low amounts of cyclin B1-GFP (2-3 pg) and then monitored, nuclear accumulation was apparent from the start of imaging the oocytes (Figure 3.5Ai, B). On the contrary, oocytes not incubated with the drug did not show any nuclear import in the first 20 minutes of observation (Figure 3.5Aii, B). The rate, however, of cyclin import just prior to GVBD is higher than the rate of the leptomycin B-driven nuclear import. To quantify the different rates of import we compared the change in the ratio of the fluorescence intensity in the first 10 minutes of the experiment using the formula  $(F_{10min} - F_{0min}) / F_{0min}$ . The analysis confirmed that the rate of cyclin import in the first 10 minutes of measurement was greater in the leptomycin B treated oocytes compared to the controls, but lower than the nuclear import rate observed at the 10 minutes prior to GVBD (Figure 3.5C). These results imply that the accumulation of cyclin B in the nucleus prior to GVBD involves mechanisms that cause acceleration of import in addition to the inhibition of nuclear export.

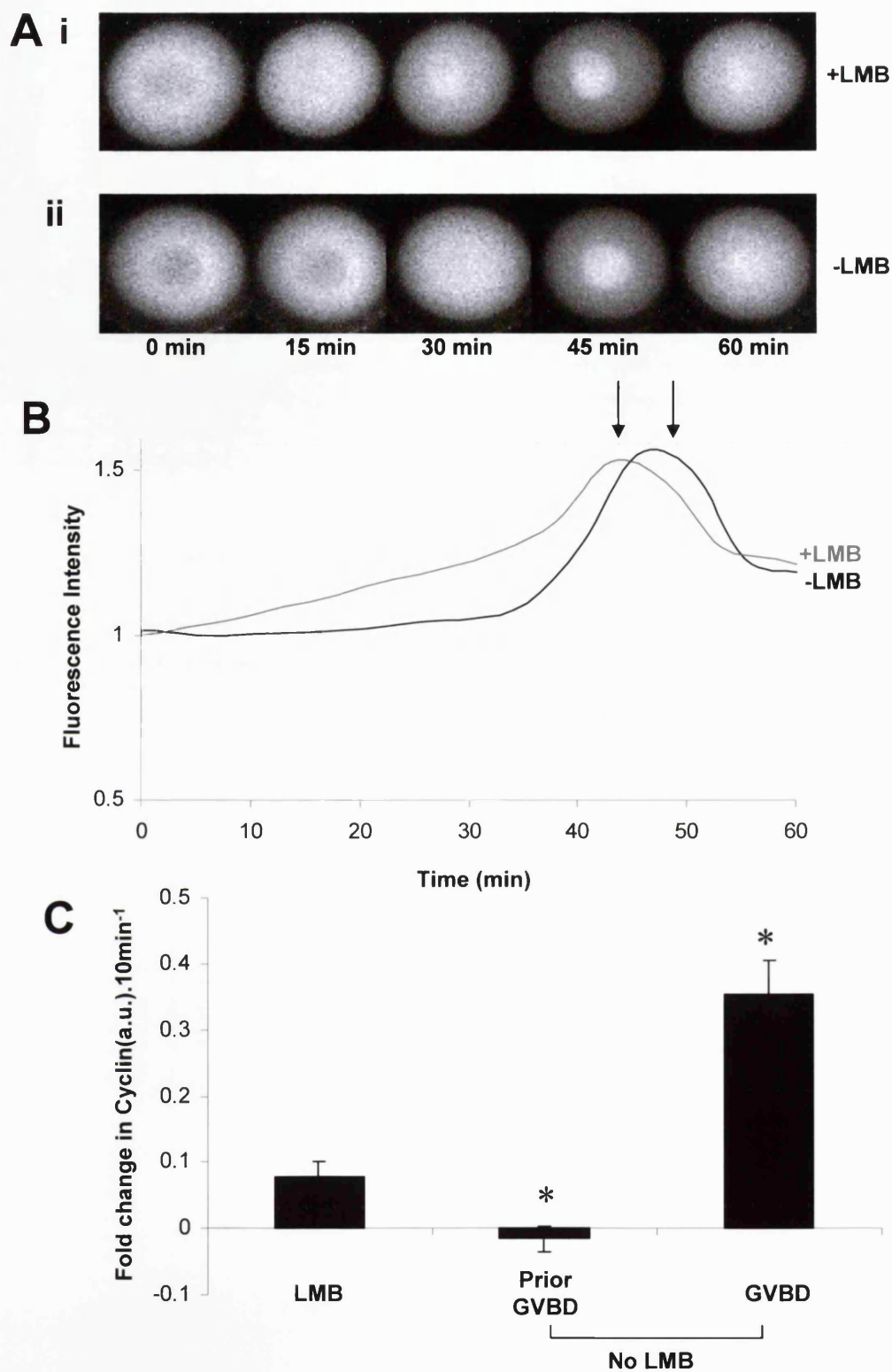


**Figure 3.5 Inhibition of nuclear export leads to nuclear accumulation of cyclin B1-GFP.** Oocytes were injected with cyclin B1-GFP (2-3pg) and the time course of accumulation in the GV was monitored over 60 minutes in the presence (Ai) (n=12) or absence (Aii) (n=11) of leptomycin B. Fluorescence intensity plots (B) and the representative images (A i, ii) show the temporal and spatial redistribution of cyclin B1-GFP. The arrows on B show the time that GVBD was confirmed. Note that in the presence of leptomycin B cyclin B1-GFP accumulates in the GV from the start of the recording. This is quantified in C by determining the ratio of the change in nuclear fluorescence in the first 10 minutes and during the nuclear transport stage in the absence or presence of leptomycin B (n=12). The \* above the columns indicates significantly different compared to rate of import in the presence of LMB ( $P < 0.05$  at least).

### 3.3 Discussion

#### 3.3.1 Effects of cyclin abundance on GVBD

The ability of cyclin B1-GFP to override cAMP-mediated meiotic arrest and to accelerate GVBD indicates that entry into meiosis is sensitive to the abundance of cyclin B. The fact that exogenous cyclin injection accelerates MPF activation to 25 fold of controls is consistent with the acceleration of GVBD and the overriding of cAMP-mediated arrest. The effects of exogenous cyclin were published during the course of our studies by Ledan and co-workers (2001) who micro-injected cyclin B1 and B2 mRNA and anti-sense oligonucleotides. The same effect of cyclin abundance is apparent in *Xenopus* (Pines and Hunt, 1987) and bovine oocytes (Levesque and Sirard, 1996). The big difference however between these systems and mouse oocytes is that, unlike the mouse (Clarke and Masui, 1983), cyclin synthesis is required for GVBD in the *Xenopus* and bovine oocyte. Moreover, the cyclin B concentration in mouse GV oocytes is reported to be 7 times higher than that of CDK1 (Kanatsu-Shinohara *et al.*, 2000). Although the existing cyclin B pool in the oocyte does not affect GV arrest, injection of exogenous cyclin does. Therefore, the big question that arises from our results is how does exogenous cyclin B lead to the activation of MPF.

One explanation for this paradox is that although cyclin B is theoretically abundant in the oocyte, it may not have access to CDK1. The endogenous cyclin B1 protein may be sequestered and, thus, unavailable for activating CDK1 (Westendorf *et al.*, 1989; de Vanter *et al.*, 1997; Terasaki *et al.*, 2003). Alternatively, not cyclin B alone, but the CDK1-cyclin B complex may be sequestered as has recently been shown in starfish oocytes. In this system, CDK1-cyclin B is present in aggregates that disperse at the time of CDK1-cyclin B activation

(Terasaki *et al.*, 2003). Increases in available cyclin may initiate a small degree of activation of the pre-existing CDK1-cyclin B complexes (pre-MPF). This activation can then extend to CDC25 through the CDK1-cyclin B auto-amplification loop leading to rapid CDK1-cyclin B activation (Hoffmann *et al.*, 1993; Lincoln *et al.*, 2002). Recently, a bi-stable switch model has been proposed that ensures oscillations form an interphase to an M-phase state (Pomerening *et al.*, 2003). Thus, small increases in cyclin levels can cause a switch-like activation of CDK1-cyclin B from an inactive interphase state to an active M-phase one. This may provide the explanation for the accelerated GVBD seen in our results. A switch-like model has also been proposed for MAPK activation (Ferrell, Jr. and Machleder, 1998). In mouse oocytes, switch-like MAPK activation may be dependent on CDK1-cyclin B since exogenous cyclin-induced CDK1-cyclin B activation caused the earlier activation of MAPK. This switch is unaffected by CDK1-cyclin B levels of activity since there is no change in the maximum levels of MAPK activity in injected and control oocytes. This suggests that MAPK is activated in an 'all or none' response.

In addition, although cyclin B production is not necessary for mouse GVBD in vitro, the importance of cyclin synthesis in vivo has not been determined. The surge of LH and follicle stimulating hormone (FSH) is known to lead to a significant rise in the production of cAMP in the somatic cells of the follicle (Richards, 1980). It's possible that cAMP is transferred to the oocyte through the multiple gap junctions that connect it to the rest of the follicle's cells and may explain the slower kinetics of oocyte maturation in vivo. Cyclin synthesis could be important for GVBD in vivo for overcoming an elevated cAMP concentration. New in vitro culture systems for intact follicles where the oocyte is more accessible may provide a means of investigating these questions.

has this premature extrusion  
of the affected quality  
of the oocyte  
(interesting to know whether  
other body around cyclin B  
will have the (any known  
effect),

### 3.3.2 Effects of cyclin abundance on first polar body extrusion

As a result of cyclin B1-GFP injection, meiotic maturation and Pb1 extrusion are accelerated. Even in low doses of cyclin, Pb1 extrusion occurs earlier than it would normally do. This is consistent with observations by other researchers using cyclin B1 mRNA (Polanski *et al.*, 1998; Ledan *et al.*, 2001) and is in agreement with the finding that progression through MI is dependent on translation of cyclin B (Hampl and Eppig, 1995b; Polanski *et al.*, 1998).

Another effect of excess cyclin injection was the dose dependent inhibition of polar body extrusion. The saturation of mechanisms for cyclin destruction during MI probably explains this inhibitory effect. This finding shows that, unlike *Xenopus* oocytes where cyclin destruction is not necessary for the progression from MI to MII (Peter *et al.*, 2000; Taieb *et al.*, 2001), cyclin B needs to be degraded for mouse oocytes to exit MI. Recently, this was demonstrated more clearly by using non-destructable cyclin B1-GFP in mouse oocytes (Herbert *et al.*, 2003). The oocytes remained arrested in metaphase and the disjunction of homologous chromosomes was inhibited. Nevertheless, securin degradation was not affected. Thus, in mammals, there is a dual system of regulating exit from MI that involves the proteolysis of both securin and cyclin B.

### 3.3.3 Localisation of cyclin-B1 GFP in GVBD

In the present study we show the first observations of the relationship between the dynamics of cyclin localisation and the timing of GVBD in mammalian oocytes. Cyclin B1-GFP can be accepted as a valid marker for endogenous cyclin since it behaves similarly to endogenous cyclin observed by immunofluorescence experiments in somatic cells (Pines and Hunter,



1991;Hagting *et al.*, 1998) starfish oocytes (Ookata *et al.*, 1992) and porcine oocytes (Casas *et al.*, 1999).

Primarily, cyclin B1-GFP is localised in the cytoplasm and is associated with two accumulations in the peri-nuclear region. In somatic cells these accumulations were identified as the centrosomes, which are responsible for the formation of the mitotic spindle (Hagting *et al.*, 1988;Clute and Pines *et al.*, 1999). More recently, the centrosomes have been identified as the sites where CDK1-cyclin B activation is initiated (Jackman *et al.*, 2003), consistent with the idea that CDK1-cyclin B is first activated in the cytoplasm (Peter *et al.*, 2002b). In meiosis, there are no centrosomes. Instead, there are microtubule organising centres (MTOCs) that do not contain centrioles but are responsible for spindle formation (Verlhac *et al.*, 1993). Therefore it is likely that the observed accumulations are MTOCs where cytoplasmic activation of CDK1-cyclin B is initiated in mammalian meiosis.

The other important accumulation of cyclin B1-GFP occurs in the germinal vesicle just prior to GVBD. This nuclear accumulation is tightly related to the timing of GVBD indicating a significant effect of cyclin accumulation in the nucleus on GVBD. This is further supported by the fact that cyclin remains exclusively cytoplasmic during cAMP-mediated arrest. In *Xenopus* oocytes the importance of cyclin entry in the GV was shown directly. In *Xenopus* oocytes exogenous cyclin B is sufficient to drive GVBD in the absence of progesterone but a phosphorylation mutant (cyclin B1<sup>ala</sup>) that does not undergo nuclear translocation (Li *et al.*, 1997) is not. The addition of an NLS to cyclin B<sup>ala</sup> restores nuclear accumulation and the capacity to stimulate GVBD (Li *et al.*, 1997).

### 3.3.4 Cyclin transport

In somatic cells (Hagting *et al.*, 1998; Hagting *et al.*, 1999) and *Xenopus* oocytes (Yang *et al.*, 1998) cyclin nuclear accumulation is mediated by the blocking of nuclear export and an increase in import. As in the other cell types, intra-nuclear injection of cyclin B1-GFP in mouse GVs showed that the protein is actively exported from the nucleus. Injection of a dextran molecule that remains in the nucleus was used as a control. In addition, treatment with Leptomycin B blocked export and enabled us to measure the rate of nuclear import of cyclin injected in the cytoplasm. These experiments showed that during GV arrest in mammals, the cytoplasmic localisation of cyclin B is obtained by nuclear export of cyclin being almost two times faster than cyclin B import.

Just prior to GVBD (10-15 minutes) the balance of cyclin transport is shifted towards import resulting in cyclin B accumulation in the nucleus. In somatic cells, this is obtained both by blocking nuclear export and accelerating import (Hagting *et al.*, 1998). Recent work has revealed that nuclear import of cyclin is accelerated by the phosphorylation of four serine residues, while nuclear export is blocked by the phosphorylation of a fifth serine (Hagting *et al.*, 1999; Yang *et al.*, 1999; Yang *et al.*, 2001). Our experiments show that the rate of cyclin B-GFP import prior to GVBD is significantly enhanced. This, in combination with the block of export, leads to cyclin B accumulation in the nucleus. In somatic cells, the nuclear accumulation of CDK1-cyclin B1 leads to the phosphorylation of nuclear lamins, an important step in initiation of nuclear envelope disassembly (Peter *et al.*, 1990).

This work shows the importance of cyclin B localisation for the regulation of GVBD and MI. Since protein synthesis is not necessary for progression to GVBD, cyclin B transport may be controlling the timing of GVBD. Future experiments may provide the mechanisms

that link up the induction of GVBD in vivo and CDK1-cyclin B activation and nuclear translocation.

## **4. Ca<sup>2+</sup> oscillations at fertilisation of mouse oocytes maintain a persistent rate of cyclin B degradation that is exclusive to exit from meiosis II.**

### **4.1 Introduction**

Exit from mitosis requires the destruction of cyclin B, the regulatory partner of the mitotic kinase CDK1 (Draetta *et al.*, 1989; Labbe *et al.*, 1989; Murray and Kirschner, 1989; Gautier *et al.*, 1990). Cyclin destruction is controlled by the activity of a multi-subunit complex with ubiquitin ligase activity known as the anaphase promoting complex (APC). In a regulated manner, the APC ubiquitinates cyclin in its destruction box and targets it for destruction by the proteasome (Glotzer *et al.*, 1991; Fang *et al.*, 1999; Zachariae and Nasmyth, 1999; Peters, 2002). The resultant fall in CDK1-cyclin B activity together with APC-mediated destruction of additional mitotic regulators provides a co-ordinated exit from mitosis.

In vertebrate oocytes the cell cycle is arrested at metaphase II. This arrest is maintained by a partial inhibition of APC-mediated cyclin B destruction in the presence of continued cyclin B synthesis (Kubiak *et al.*, 1993). This balance between synthesis and destruction results in the maintenance of high CDK1-cyclin B activity. The brake on cyclin destruction is provided by the Mos/MAPK pathway, which is a component of the egg specific activity known as cytotstatic factor (CSF) (Sagata *et al.*, 1989b; Hashimoto *et al.*, 1994; Colledge *et al.*, 1994; Tunquist and Maller, 2003). CSF activity is assayed on the basis of its ability to cause metaphase arrest in blastomeres of dividing embryos (Sagata *et al.*,

1989b; Tunquist and Maller, 2003). In *Xenopus* oocytes it has been established that downstream of MAPK is the activation of p90rsk and Bub1 which are necessary for initiating the metaphase arrest, perhaps through mechanisms analogous to those of the spindle assembly check point (Bhatt and Ferrell, Jr., 1999; Gross *et al.*, 2000; Schwab *et al.*, 2001). In addition to the Mos/MAP kinase/p90Rsk/Bub1 pathway at least two other proteins have been shown to contribute to CSF activity, namely, CDK2-cyclin E and Emi1 (Gabrielli *et al.*, 1993) (Reimann and Jackson, 2002). The outcome of this CSF arrest is that exit from meiosis II is under external control.

In MI, a prolonged metaphase leads to the extrusion of the first polar body and subsequent arrest at MII. The utilisation of cyclin B-GFP mRNA in MI has shown that during the MI-MII transition, the degradation of cyclin B occurs during a 1-2 hour period prior to polar body extrusion (Ledan *et al.*, 2001).

At fertilisation, in all oocytes, exit from arrest at meiosis I (ascidians) or II (vertebrates) is triggered by a sperm-induced increase in the concentration of intracellular  $Ca^{2+}$ . In different species the pattern of  $Ca^{2+}$  signalling can take the form of a single  $Ca^{2+}$  transient (*Xenopus*) or  $Ca^{2+}$  oscillations lasting tens of minutes (ascidians) or hours (mammals) (Stricker, 1999; Swann *et al.*, 2001; Runft *et al.*, 2002). The increase in cytosolic  $Ca^{2+}$  relieves the meiotic arrest, presumably by promoting cyclin B destruction, but the mechanism and the significance of the different patterns of  $Ca^{2+}$  signalling are not known. Some insight into  $Ca^{2+}$ -stimulated cyclin destruction at fertilisation has been provided in recent experiments where the levels of cyclin B1-GFP have been monitored during fertilisation. In ascidian eggs (that arrest at meiosis I) the fertilisation induced  $Ca^{2+}$  transients initiate a steady increase in the rate of cyclin B1 destruction after a delay of 3 minutes

(Levasseur and McDougall, 2000). In contrast, mouse eggs expressing the same cyclin B1-GFP, show an immediate onset of cyclin B1 destruction that can not be distinguished from the timing of the onset of the first  $\text{Ca}^{2+}$  transient. Subsequent  $\text{Ca}^{2+}$  transients result in additional incremental decreases in cyclin B1-GFP fluorescence leading to the conclusion that multiple  $\text{Ca}^{2+}$  transients are needed in mammals to ensure continued cyclin B1 destruction during exit from meiosis II (Nixon *et al.*, 2002). It remains unclear how  $\text{Ca}^{2+}$  drives cyclin destruction and why such differences in the dynamics of cyclin destruction exist in different species. Q

An additional important question is why CSF mediated arrest in vertebrate eggs occurs at meiosis II but not in meiosis I. The Mos/MAPK pathway is active during meiosis I and is able to slow the destruction of cyclin during MI as shown by a 50% increase in the rate of cyclin destruction in the presence of UO126, an inhibitor of MAPK kinase. Nevertheless, despite the presence of the Mos/MAPK pathway, cyclin B destruction is induced during the transition from MI to MII. The difference in MI and MII may arise due to the presence of additional factors in meiosis II, such as CDK2-cyclin E or Emi1 that may be not be present at meiosis I. Alternatively, a signal may be generated at MI, analogous to that generated at fertilisation that is able to override any components of CSF activity present during MI. Q! Ann 21/10/08

Here we address the kinetics of  $\text{Ca}^{2+}$ -dependent cyclin B destruction in mouse oocytes undergoing fertilisation and whether there is a role for  $\text{Ca}^{2+}$  in MI. We find that a single  $\text{IP}_3$ -induced  $\text{Ca}^{2+}$  transient is sufficient to increase the rate of cyclin destruction for at least 30 minutes in MII eggs and that similar transients have no effect on cyclin B1 destruction during meiosis I. Thus, in MI,  $\text{Ca}^{2+}$  has no effect on the stimulation of cyclin B RFS,

destruction. At fertilisation, we show that the decrease in fluorescence seen in oocytes containing cyclin B1-GFP consists of two components, one slow increase in the rate of decline that is sensitive to MG132, a proteasome inhibitor, and a series of incremental steps that are insensitive to MG132. However, these steps appear to be an artefact and not actual cyclin degradation since they are also evident in autofluorescence that overlaps with the excitation/emission spectrum of GFP. We conclude that  $\text{Ca}^{2+}$  transients at fertilisation lead to an MII-specific release of the CSF-mediated brake on cyclin B synthesis.

## 4.2 Results

### 4.2.1 Cyclin destruction in MI is not associated with a detectable $\text{Ca}^{2+}$ transient

Cyclin destruction and CDK1-cyclin B inactivation is necessary for progression through the first meiotic division (Hashimoto and Kishimoto, 1986; Ledan *et al.*, 2001) but it is not known how the increase in cyclin destruction is initiated. Here we have monitored cyclin destruction in oocytes progressing through MI using cyclin B1-GFP. We confirm previous findings of Ledan *et al.* (2001) that cyclin destruction takes place over a window of approximately 2 hour preceding the first meiotic division as determined by the time of polar body extrusion (Figure 4.1A, black line, B). Given the recent reports that APC-mediated cyclin destruction is not necessary for progression from MI to MII in *Xenopus* oocytes, we have used the proteasome inhibitor, MG132, to determine whether inhibition of cyclin destruction is sufficient to inhibit the MI-MII transition. MG132 effectively inhibited the decrease in fluorescence confirming that the cyclin B1-GFP fusion protein is destroyed by the proteasome (Figure 4.1A, grey line, B). This inhibition of cyclin B1 destruction was associated with arrest at MI suggesting that proteasome-mediated cyclin destruction was necessary for progression to MII.

In mouse and *Xenopus* eggs arrested at MII, cyclin destruction is initiated by an increase in intracellular  $\text{Ca}^{2+}$ . We tested the possibility that  $\text{Ca}^{2+}$  transients during MI led to the initiation of cyclin destruction. Oocytes were injected with Fura 2-dextran approximately 4 hours after release from the follicle and  $\text{Ca}^{2+}$  was monitored through to extrusion of the first polar body. Of 15 oocytes monitored through polar body extrusion (Figure 4.1C) only one was seen to generate a small  $\text{Ca}^{2+}$  transient. Thus, a detectable  $\text{Ca}^{2+}$  transient is not



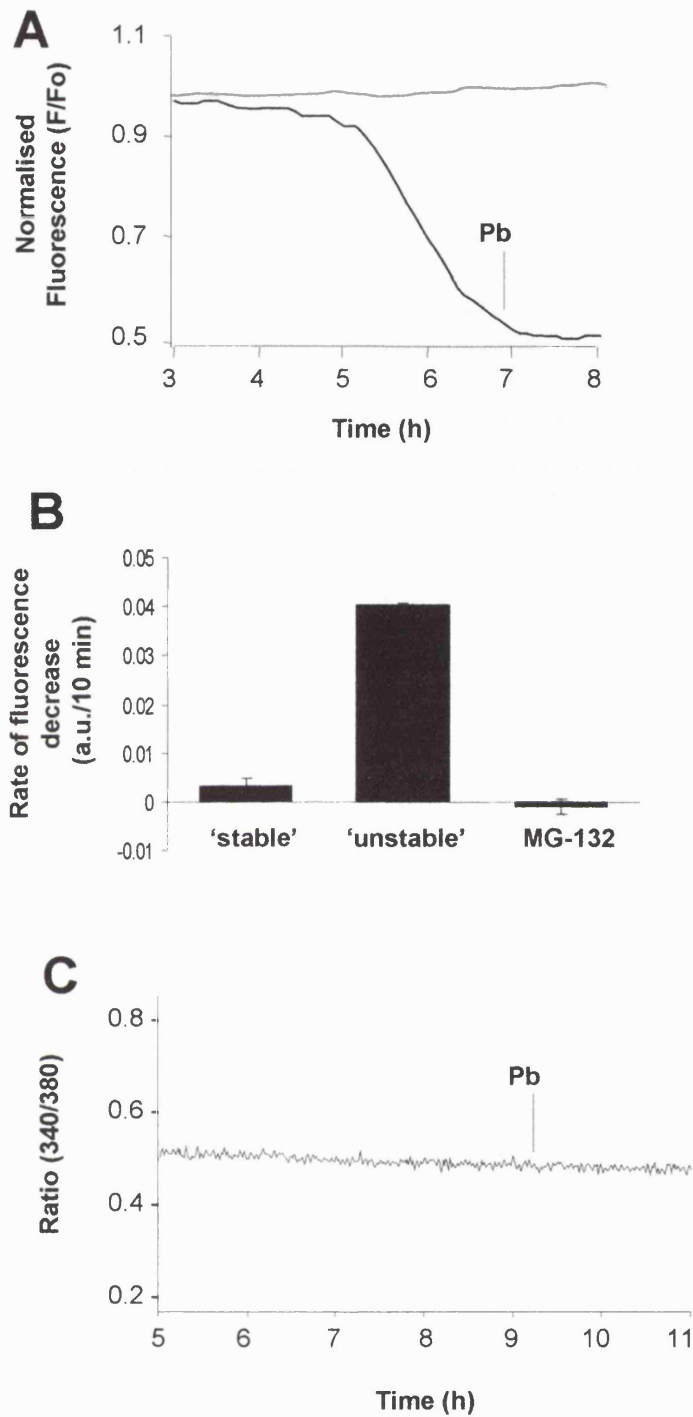


**Figure 4.1 Destruction of cyclin B1 and progression through MI is independent of  $Ca^{2+}$ .** (A, B) GV stage oocytes were microinjected with cyclin B1-GFP protein and released from IBMX-induced arrest. The oocytes were monitored from three-five hours after release. The fluorescence is stable until about 5 hours after release when an increase in the rate of cyclin B1-GFP destruction is detected and continues for 1-2 hours (black line) (n=20). Pb shows the time within 30 minutes that the polar body was extruded. In B, the rate of loss of cyclin B1-GFP is measured during the early 'stable' period and during the increase in 'instability' at MI. Incubation of the oocytes with MG132 abolishes the decrease in fluorescence and maintains a stable level of cyclin B1-GFP fluorescence for the duration of the recording (grey line) (n=16) (A,B). (C) Oocytes were microinjected with Fura-2 dextran and  $Ca^{2+}$  was monitored from 5h after release from IBMX. In 29 oocytes that were examined 15 extruded the polar body and 14 of these showed no perturbations of baseline  $Ca^{2+}$  while one oocyte showed a single  $Ca^{2+}$  transient. Pb indicates time of polar body extrusion within 30 minutes. The difference in the timing of Pb extrusion between A and C is accounted for by the fact that exogenous cyclin accelerates meiosis I (Ledan *et al.*, 2001; Marangos and Carroll, unpublished observations).

associated with the onset of cyclin destruction or the resulting metaphase to anaphase transition in MI.

#### **4.2.2 Ca<sup>2+</sup> dependent cyclin destruction only occurs in MII arrested oocytes**

We next addressed the question of whether an increase in intracellular Ca<sup>2+</sup> was sufficient to cause cyclin destruction during MI. In order to perform this experiment we photoreleased IP<sub>3</sub> in maturing and mature MII stage oocytes. We found that for the same exposure to UV light and IP<sub>3</sub> uncaging we obtained lower levels of Ca<sup>2+</sup> release, ascertained by the generation of Ca<sup>2+</sup> transients of smaller size in maturing oocytes compared to MII eggs. Thus, we established conditions in which we could photorelease caged IP<sub>3</sub> such that a Ca<sup>2+</sup> transient of similar magnitude was generated (3 seconds exposure to UV light for MI compared to 1 second for MII) (Figure 4.2A). To monitor cyclin destruction in these conditions oocytes were injected with caged IP<sub>3</sub> and cyclin B1-GFP. In maturing oocytes, the release of IP<sub>3</sub> resulted in a transient decrease in fluorescence that recovered to resting levels after which the fluorescence from cyclin B1-GFP remained stable (Figure 4.2B, Ci). This pattern in the change of fluorescence was surprising since the oocytes were injected with cyclin B1-GFP protein and no recovery of fluorescence would be expected. This suggests that the transient decrease in fluorescence is not a result of cyclin B1-GFP destruction but rather a result of a change in another component of the fluorescence signal. The decrease was Ca<sup>2+</sup> dependent since no deviation in fluorescence was apparent in the absence of caged IP<sub>3</sub>. One explanation for the unexpected decrease in fluorescence is contamination of the cyclin B1-GFP fluorescence with a Ca<sup>2+</sup>-dependent decrease in autofluorescence. Irrespective of the origin

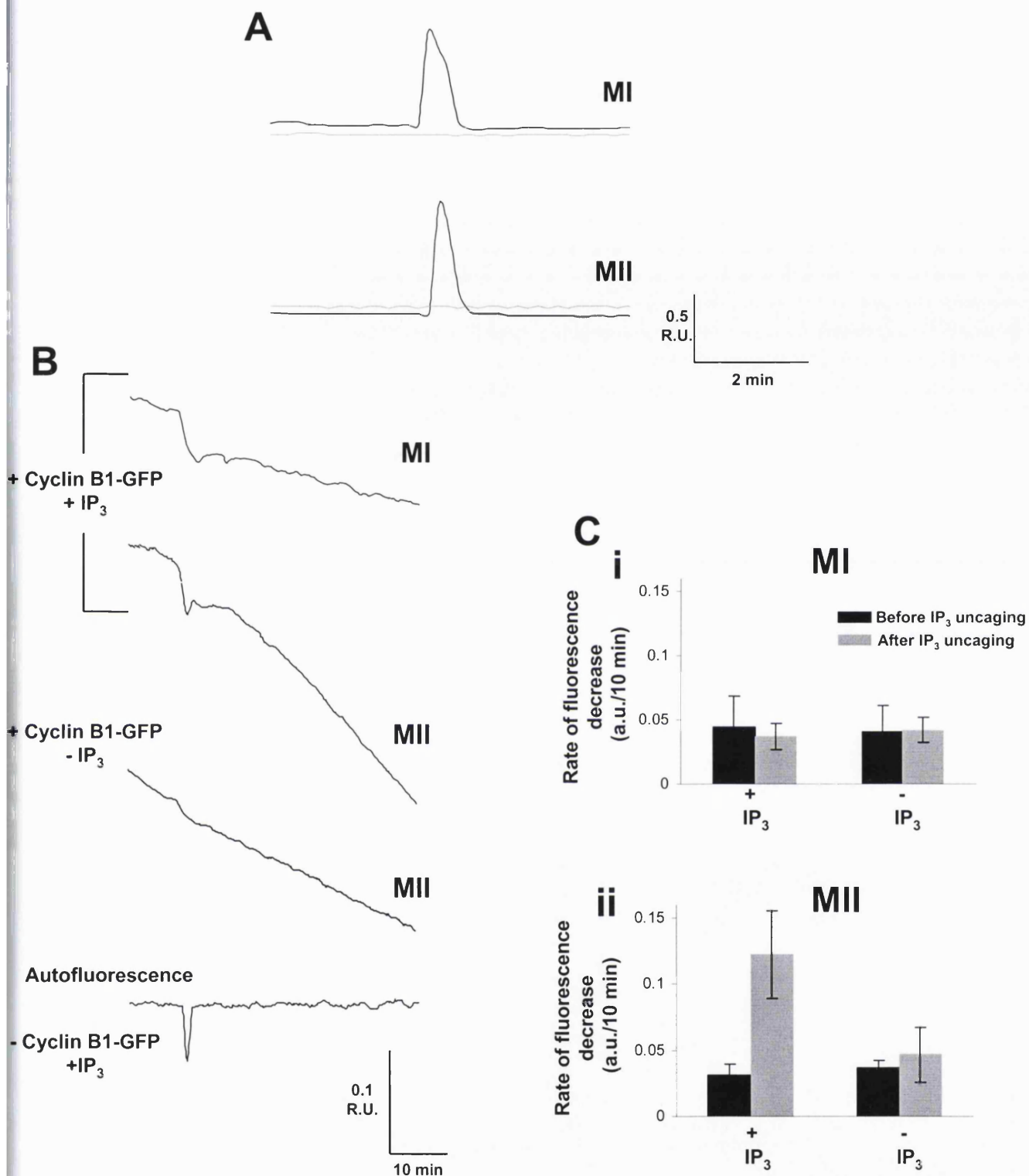


**Figure 4.2**  $\text{Ca}^{2+}$ -stimulated cyclin destruction is specific to oocytes arrested in an MII-like state. (A) Maturing MI stage and MII arrested oocytes were microinjected with caged  $\text{InsP}_3$  and loaded with Fura-red AM ( $5\mu\text{M}$ ) to monitor  $\text{Ca}^{2+}$ . Three seconds of UV exposure in MI generated a  $\text{Ca}^{2+}$  transient similar to that induced by a 1 second UV exposure in MII eggs. No  $\text{Ca}^{2+}$  transient was observed in non-injected oocytes (grey line). (B) In maturing oocytes injected with caged  $\text{InsP}_3$  and cyclin B1-GFP, uncaging  $\text{InsP}_3$  had no effect on the overall rate of degradation of cyclin B1-GFP, although a short-lived transient decrease in fluorescence was apparent immediately after the release of  $\text{InsP}_3$  ( $n=14$ ). Similar to maturing oocytes, the photorelease of  $\text{InsP}_3$  in cyclin B1-GFP injected MII stage oocytes was accompanied by an immediate transient decrease in fluorescence. In addition, note the accelerated rate of fluorescence decrease after the release of  $\text{Ca}^{2+}$  ( $n=16$ ) (B, Cii). The increased rate of loss of fluorescence and the rapid, short-lived change were dependent on the release of  $\text{InsP}_3$ . (B) Control oocytes exposed to a similar  $\text{InsP}_3$ -induced transient also showed an immediate transient decrease in fluorescence, but no gradual decreases were seen.

of this transient decrease in fluorescence, the experiments show that an increase in  $\text{Ca}^{2+}$  during MI does not elicit any detectable change in the rate of cyclin destruction.

In MII eggs, the uncaging of  $\text{IP}_3$  and resultant  $\text{Ca}^{2+}$  increase led to an initial step-like decrease in fluorescence that was followed by an acceleration of cyclin destruction as determined by an increase in the rate of decline of fluorescence from cyclin B-GFP (Figure 4.2B, Cii). The increased rate of cyclin destruction was apparently maintained for at least the duration of the experiment, 30-50 minutes. This suggests that a single increase in  $\text{Ca}^{2+}$  is sufficient to induce a persistent acceleration of the rate of cyclin destruction in MII oocytes. This acceleration of cyclin destruction was not caused by the uncaging protocol since control oocytes injected with cyclin-GFP but not caged  $\text{IP}_3$  showed no change in the rate of cyclin destruction after applying an identical uncaging procedure. The initial step-wise decrease in fluorescence that accompanied the release of  $\text{IP}_3$  was dependent upon the release of  $\text{Ca}^{2+}$  since it was only seen in the presence of caged  $\text{IP}_3$ . This is reminiscent of the apparent autofluorescence change in maturing oocytes and also the reported  $\text{Ca}^{2+}$ -dependent incremental cyclin B1 degradation recently reported in fertilising mouse eggs (Nixon *et al.*, 2002).

#### 4.2.3 Cyclin B destruction at fertilisation

The data described above suggest a single  $\text{Ca}^{2+}$  transient is sufficient to induce an increase in the rate of cyclin destruction in MII eggs. Furthermore, an  $\text{IP}_3$ -induced  $\text{Ca}^{2+}$  transient is associated with a rapid stepwise decrease in fluorescence, similar to that in maturing oocytes. Given the similarity of the decrease in apparent cyclin B1-GFP fluorescence seen in response

to  $IP_3$  with that reported at fertilisation we have revisited the question of how cyclin B1-GFP is degraded at fertilisation. At fertilisation, sperm trigger a series of  $Ca^{2+}$  transients (Figure 4.3A). In cyclin B1-GFP injected oocytes (2-5 pg) that are exposed to sperm we detected changes in fluorescence that appeared to consist of two components: an incremental decrease that occurred with a frequency consistent with that reported for fertilisation-induced  $Ca^{2+}$  transients (Nixon *et al.*, 2002) and a rate of  $0.085 \text{ au}\cdot\text{min}^{-1}$ . These incremental steps of decrease were a component of an overall gradual decline in the level of fluorescence ( $0.012 \text{ au}\cdot\text{min}^{-1}$ ) (Figure 4.3B). In the absence of sperm the only detectable change in fluorescence was a slow rate of decline consistent with basal cyclin B1-GFP turnover in mature oocytes (rate of decrease:  $0.005 \text{ au}\cdot\text{min}^{-1}$ ) (Figure 4.3Biii). Therefore, we interpret the additional changes in fluorescence in the presence of sperm to be dependent upon sperm-induced  $Ca^{2+}$  oscillations.

However, the fluorescence level after each step often showed partial recovery (Figure 4.3B, grey line). In studies where mRNA was microinjected this recovery could be attributed to newly synthesised protein (Nixon *et al.*, 2002). This is not the case in our experiments since we introduced cyclin B1-GFP protein. To define the exact contribution of cyclin B to the changes in fluorescence observed at fertilisation, we monitored fertilised eggs injected with similar amounts (2-5 pg) of purified EGFP. We did not see any gradual loss in the injected eggs either before or after fertilisation (Figure 4.3C). However, we observed the transient steps. Thus, the gradual loss of fluorescence may be attributed to cyclin B1-GFP destruction, whereas the steps appear to be a result of autofluorescence changes that are induced by  $Ca^{2+}$ .

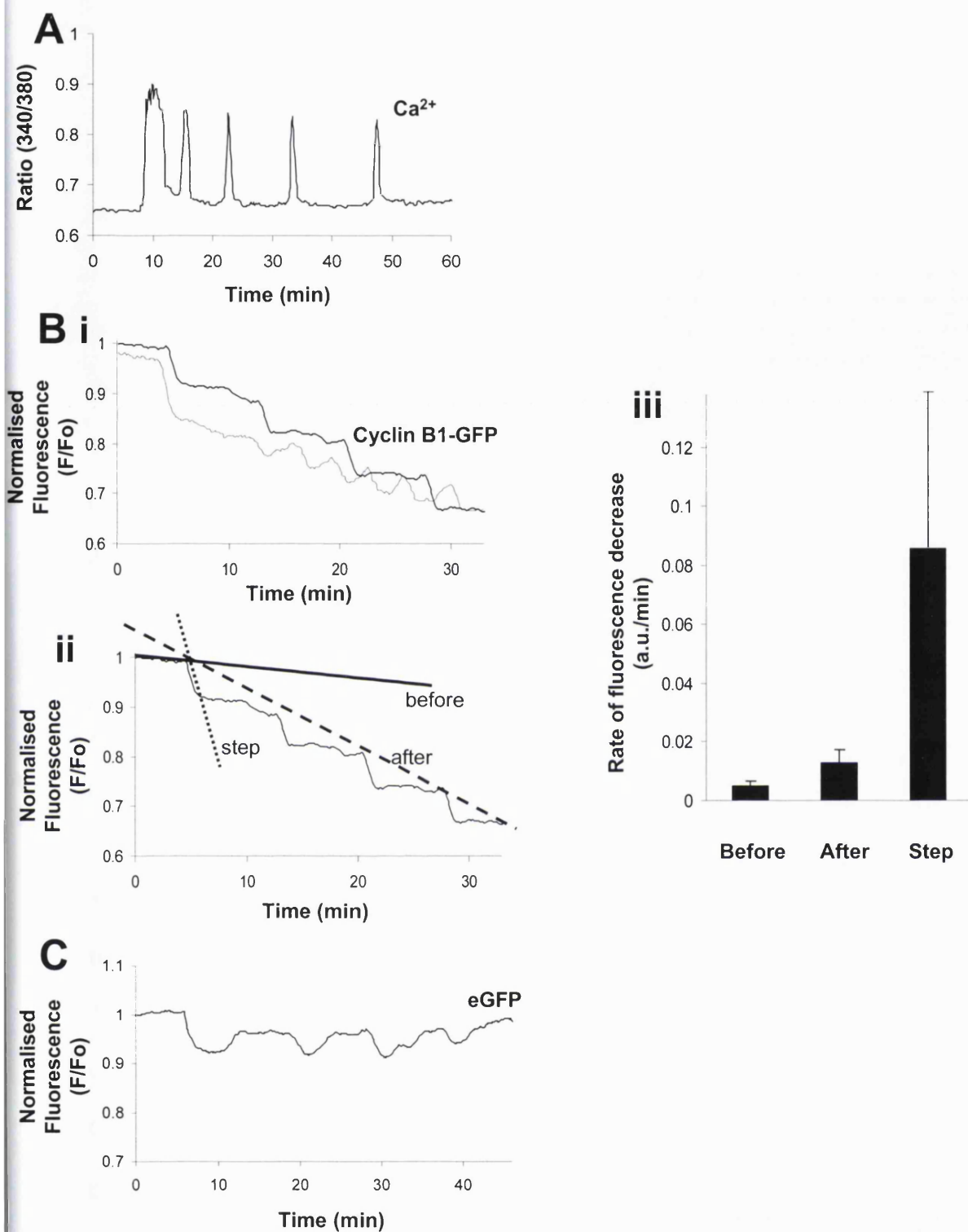


**Figure 4.3** The dynamics of Ca<sup>2+</sup>-induced cyclin B1-GFP degradation at fertilisation. MII-arrested eggs were loaded with Fura-2 and Ca<sup>2+</sup> was monitored at fertilisation. The addition of sperm leads to a long lasting series of Ca<sup>2+</sup> oscillations (A). In B, MII oocytes were microinjected with cyclin B1-GFP (2-5pg) and fertilised. Black line: single egg showing a stepwise decrease in fluorescence. Gray line: an example of another egg where the first step is larger than subsequent decreases. Note also that in this egg the fluorescence shows a partial recovery. In all cases there is a net increase in the rate of fluorescence decrease after fertilisation (Bi). The rates of the decrease in fluorescence was measured *before* fertilisation, *after* fertilisation and during the downward slope of the *step* (Bii and iii) (n=15). Data show the mean  $\pm$  s.d. (C) Eggs were microinjected with eGFP (2-5pgs) and monitored during fertilisation. All eGFP-injected eggs examined showed a small oscillation in baseline fluorescence (n=6).

#### **4.2.4 Sr<sup>2+</sup> containing medium also induces incremental fluorescence changes and oscillations in autofluorescence**

To investigate whether cyclin destruction and autofluorescence changes were specific to fertilisation we have used a fertilisation-independent means of inducing Ca<sup>2+</sup> oscillations. In the mouse, Ca<sup>2+</sup> oscillations can be induced by Sr<sup>2+</sup>-induced egg activation (Cheek *et al.*, 1993; Bos-Mikich *et al.*, 1995). Eggs microinjected with cyclin B1-GFP and activated in Sr<sup>2+</sup>-containing medium generate incremental steps similar to those seen in fertilised eggs (Figure 4.4A). As in fertilisation, the gradual decline is cyclin-specific and the steps are possibly caused by autofluorescence since eggs injected with EGFP and activated by Sr<sup>2+</sup> show a series of oscillations of fluorescence but not a net decrease in fluorescence (Figure 4.4B). Thus, the fertilisation-induced changes in cyclin B1-GFP and autofluorescence can be replicated by an independent means of inducing Ca<sup>2+</sup> oscillations.

#### **4.2.5 The proteasome is necessary for the increased rate of cyclin B destruction but not the incremental steps**

To further examine the involvement of cyclin B1-GFP degradation on the fluorescence changes seen at fertilisation, we added MG132, a proteasome inhibitor, after the beginning of Ca<sup>2+</sup> oscillations or before fertilisation had started. In both procedures, MG132 inhibited the gradual decrease in fluorescence but did not affect the generation of the transient stepwise changes in fluorescence (Figure 4.5). Thus, it is apparent that the proteasome is important for cyclin degradation at fertilisation, whereas the incremental changes in fluorescence occur independently.

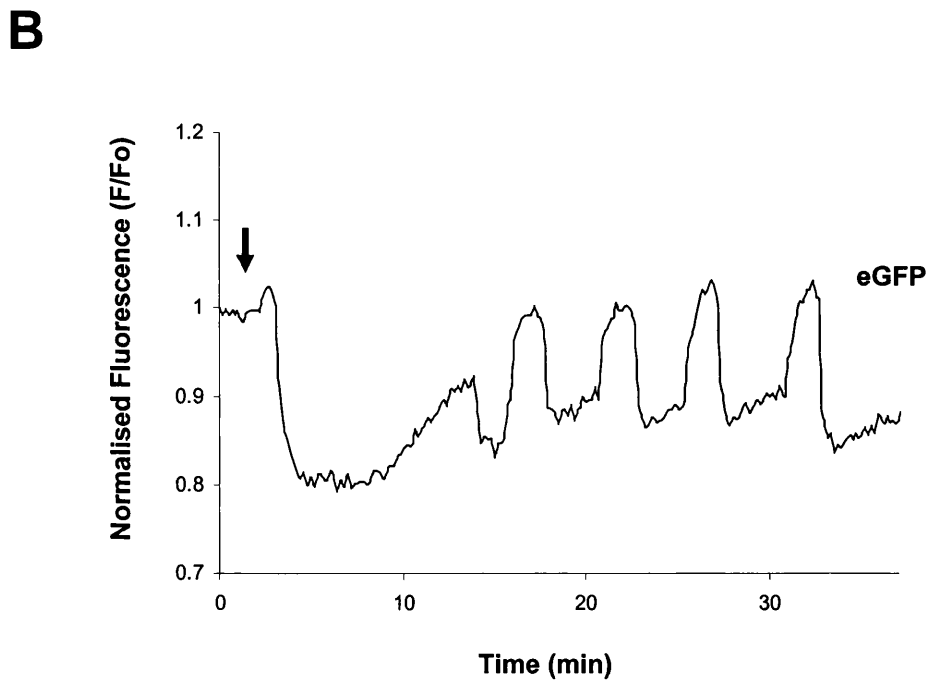
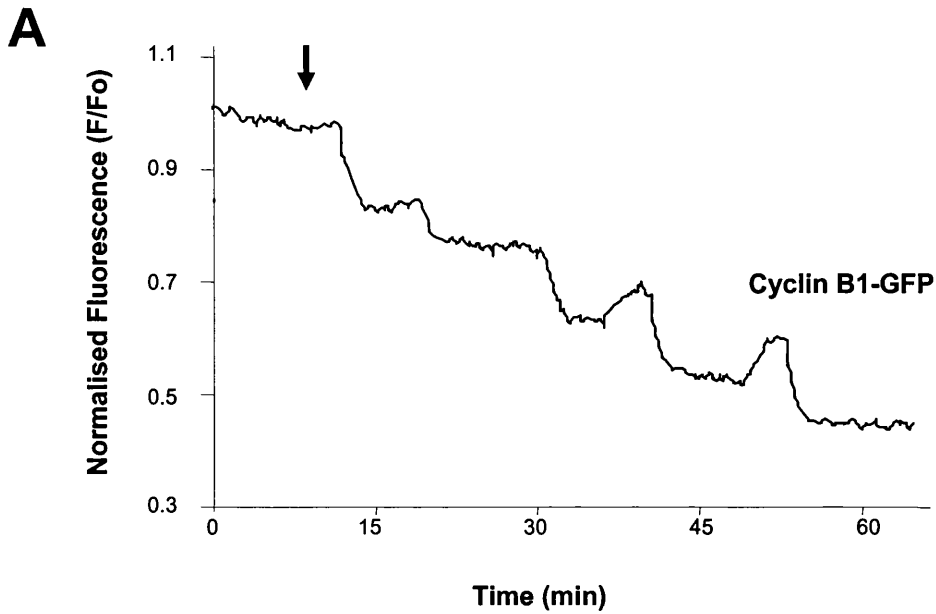


**Figure 4.4**  $\text{Sr}^{2+}$ -containing medium causes fluorescence decreases similar to fertilisation in cyclin B1-GFP injected eggs. MII oocytes were injected with cyclin B1-GFP (A) or eGFP (B) and fluorescence was monitored during exposure to  $\text{Ca}^{2+}$ -free H-KSOM containing 20mM  $\text{Sr}^{2+}$ . Note that the pattern of the decrease in fluorescence invoked by  $\text{Sr}^{2+}$  is similar to that seen at fertilisation. Decremental changes were seen in all cyclin B1-GFP injected eggs (n=26). Control eggs injected with eGFP showed oscillations in fluorescence but no net decrease in fluorescence (n=15). The arrow indicates the time of  $\text{Sr}^{2+}$  addition.



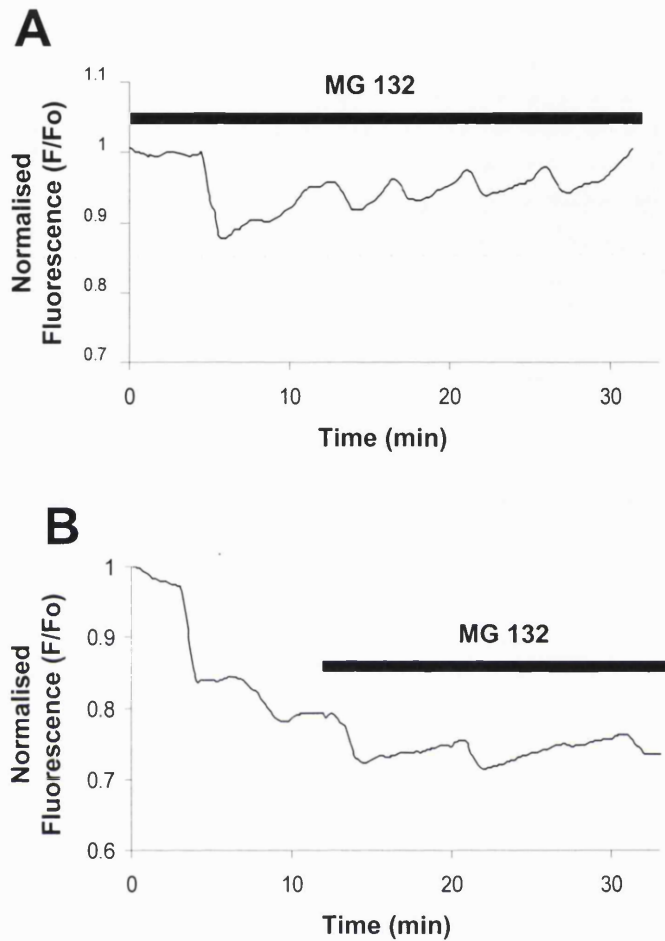


**Figure 4.5** Inhibition of the proteasome inhibits the gradual decrease in cyclin B1-GFP fluorescence but not the oscillations. MII oocytes were microinjected with cyclin B1-GFP and fluorescence was monitored during fertilisation. The proteasome inhibitor MG132 (50  $\mu$ M) was added prior to (A) or during (B) fertilisation (n=20 and 12, respectively). Note that in the presence of MG132 there is no net decrease in cyclin B1-GFP fluorescence but that oscillations in baseline fluorescence persist.

#### 4.2.6 Fertilisation induces Ca<sup>2+</sup>-dependent oscillations in autofluorescence

To investigate the origin of the stepwise, transient changes in Ca<sup>2+</sup> we have monitored autofluorescence in fertilising eggs. For an improved autofluorescence signal we increased the acquisition time of the CCD camera. The addition of sperm to these eggs resulted in a series of oscillations of decreases in the autofluorescence signal (Figure 4.6A). The absence of any other indicators confirms that these changes are due to autofluorescence. To determine the requirement for Ca<sup>2+</sup> oscillations in the induction of these oscillations in autofluorescence we added 2mM BAPTA to buffer extracellular Ca<sup>2+</sup> (1.7mM). After an initial increase in autofluorescence, the removal of Ca<sup>2+</sup> caused the cessation of all autofluorescence oscillations. This effect was reversible as shown by the re-initiation of the autofluorescence changes when the Ca<sup>2+</sup> is returned to the media (Figure 4.6B).

The origin of the oscillations is most likely a result of mitochondrial FAD<sup>+</sup>, the excitation and emission spectra of which overlaps with that of GFP (Chen *et al.*, 2002; Duchen *et al.*, 2003). To compare the spectra of autofluorescence and EGFP in our system we used a monochromator to provide a series of excitation wavelengths between 430 and 490 nm at 5 nm intervals. The same conditions used for monitoring cyclin B1-GFP were used in this experiment in order to monitor eggs injected with EGFP or uninjected eggs. The excitation spectra were similar with only a 10 nm difference in their maxima (480 nm for EGFP, 470 for autofluorescence) (Figure 4.6C) making it practically impossible to separate the two signals.

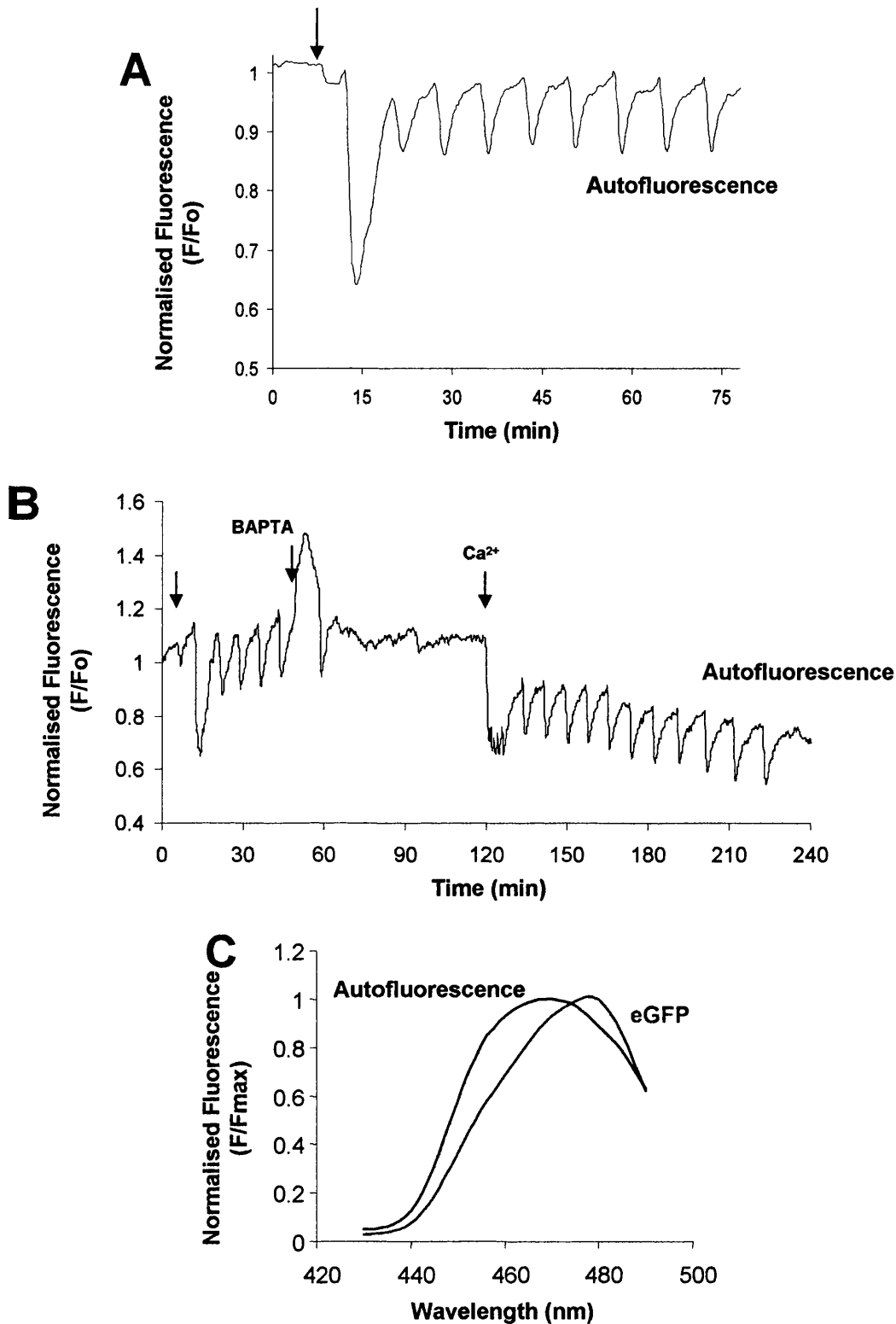


**Figure 4.6 Fertilisation stimulates oscillations in autofluorescence that are Ca<sup>2+</sup>-dependent.** MII arrested oocytes were placed on the microscope stage and fertilised in the absence of any fluorescent probes or indicators. Using the same filters as for cyclin B1-GFP the fluorescence was monitored and an oscillating autofluorescence signal was detectable (A). Addition of 2mM BAPTA to the chamber to chelate extracellular Ca<sup>2+</sup> caused the oscillations to stop in a reversible manner. Readdition of 2mM CaCl<sub>2</sub> stimulated a resumption of the oscillations (B). In *A* and *B* the arrow is the time of sperm addition. Data are representative of 25 eggs undergoing fertilisation and an additional 9 eggs were exposed to Ca<sup>2+</sup>-free medium. In *C*, the intensity of the emitted fluorescence (normalised to the maximum) for autofluorescence (grey line) and eGFP (black line) were sampled across a range of wavelengths from 430–490 nm. The overlapping curves show that the excitation spectra of autofluorescence and eGFP are inseparable.

## 4.3 Discussion

### 4.3.1 Autofluorescence oscillations at fertilisation of mouse eggs

Our results show that fertilisation stimulates a progressive increase in the rate of destruction of cyclin B1-GFP. Our initial observations (see Figure 1B) and those published previously indicated a  $\text{Ca}^{2+}$ -driven incremental decrease in cyclin B1, however, a number of observations raised questions of such a pattern of cyclin B1 destruction. For example, some eggs showed a small recovery of fluorescence after the incremental decrease that could not be accounted for by new synthesis of cyclin B1-GFP, since fluorescence was being recorded from recombinant protein. Also, the rate and magnitude of the destruction seen on the fall of the step would require around 10% of the exogenous cyclin B1-GFP to be ubiquitinated and destroyed in the time it takes for the  $\text{Ca}^{2+}$  to increase, about 20 seconds. Finally, more direct experiments on the source of the fluorescence changes seen in fertilising eggs show the persistence of oscillations but not the steady decrease in fluorescence in the presence of MG132 and that, oscillations in fluorescence are also seen in GFP-injected eggs and in eggs containing no fluorescent probes. As such, the fluorescence records obtained in cyclin B1-GFP injected eggs represent a combination of GFP and autofluorescence. We interpret our fluorescence records to indicate that  $\text{Ca}^{2+}$  oscillations drive an increase in the rate of cyclin B1-GFP destruction and that the incremental steps are a result of contaminating autofluorescence. This observation raises a number of important questions relating to, firstly, the source of the autofluorescence, secondly, the role of  $\text{Ca}^{2+}$  oscillations in cyclin B1 destruction and thirdly, the mechanism of  $\text{Ca}^{2+}$ -induced cyclin destruction.

The source of the contaminating autofluorescence is likely to be a result of mitochondrial  $\text{Ca}^{2+}$  uptake resulting in the stimulation of the mitochondrial dehydrogenases.  $\text{Ca}^{2+}$ -induced increases in mitochondrial activity have been described in a number of different systems (Hajnoczky *et al.*, 1995; Rutter *et al.*, 1996; Robb-Gaspers *et al.*, 1998). This activation of mitochondrial function results in increased conversion of fluorescent  $\text{FAD}^+$  to less fluorescent  $\text{FADH}$ . The excitation / emission spectra of flavoproteins (470/540) and GFP (480/520), combined with the use of low levels of cyclin B1-GFP so as to ensure minimal interference with the cell cycle appear to be two important factors that have allowed us to uncover this previously unnoticed  $\text{Ca}^{2+}$  dependent change in autofluorescence at fertilisation. In recent years, the impact of  $\text{Ca}^{2+}$  signalling on mitochondrial function has received much attention. It provides a mechanism of matching metabolic demand with activity in the cell (Hajnoczky *et al.*, 1995; Rutter *et al.*, 1996; Robb-Gaspers *et al.*, 1998). Conversely, by virtue of the buffering effects of mitochondria on cytosolic  $\text{Ca}^{2+}$ , mitochondria have an impact on the dynamics of  $\text{Ca}^{2+}$  signalling.

#### **4.3.2 Cyclin B degradation at fertilisation**

The conclusion that  $\text{Ca}^{2+}$ -dependent destruction of cyclin B1-GFP is a simple increase in rate rather than incremental has important implications as to the role of  $\text{Ca}^{2+}$  oscillations in driving cyclin B destruction and exit from meiotic arrest. Our data suggest that the increase in  $\text{Ca}^{2+}$ , marked by the first rapid down-stroke of the autofluorescence, initiates an increased progressive rate of cyclin degradation. The first transient is sufficient to induce this decline.

Although not directly examined here, the subsequent oscillations may shape and perhaps sustain the exponential destruction of cyclin B.

An important question is how does an increase in  $\text{Ca}^{2+}$  stimulate cyclin B1 destruction in the presence of CSF. Two possibilities include, first, activation of the APC and second, stimulation of the 26S proteasome. It is relatively simple to delineate between these possibilities since it is well established that CSF-induced cyclin B1 stability is due to a CSF-mediated inhibition of the APC, not the proteasome (Tunquist and Maller, 2003). Therefore, in CSF arrested MII oocytes it is the APC that is required to be targeted by  $\text{Ca}^{2+}$  in order to increase the rate of cyclin B1 destruction. The question is how does  $\text{Ca}^{2+}$  increase the activity of the APC. One possibility is that  $\text{Ca}^{2+}$  may act by directly stimulating the APC, thereby, bypassing CSF-mediated inhibition of the APC. Alternatively, an increase in  $\text{Ca}^{2+}$  may relieve the effects of an APC inhibitor, of which CSF is the best candidate. The molecular identity of CSF has not been fully characterised but a number of the main players has been identified. In the current model for CSF action, the *mos*/MAPK/*rsk*/*bub1* pathway and cyclin E/*cdk2* provide a brake on the APC (Tunquist *et al.*, 2002) and that this brake is reinforced by proteins such as *Emi1*, *Mad1* and *Mad2* that also bind and inhibit the APC activator, *Cdc20* (Kallio *et al.*, 1998; Lorca *et al.*, 1998; Fang *et al.*, 1998b; Reimann and Jackson, 2002). It is not known, which of these CSF components, if any, may interact with  $\text{Ca}^{2+}$  so as to relieve inhibition of the APC.

V

### 4.3.3 Ca<sup>2+</sup> has no effect on cyclin B degradation at MI

Some insight into the mechanisms of Ca<sup>2+</sup> induced cyclin B1 destruction is provided by our experiments on oocytes progressing through MI. The APC is activated and cyclin B1-GFP is destroyed during MI in the absence of any increase in Ca<sup>2+</sup>. Further, APC activity is not sensitive to Ca<sup>2+</sup> during MI since we were unable to increase the rate of cyclin destruction by imposing Ca<sup>2+</sup> transients that would be sufficient to accelerate cyclin B1 destruction in arrested MII eggs. More evidence illustrating that meiosis I is independent of large increases in intracellular Ca<sup>2+</sup> is provided by the finding that intracellular BAPTA (a Ca<sup>2+</sup> chelator) does not abolish polar body extrusion as it does at MII (Tombes *et al.*, 1992). Thus, during MI, APC activity and destruction of cyclin B1-GFP can take place independently of increases in intracellular Ca<sup>2+</sup>. Furthermore, this Ca<sup>2+</sup>-independent cyclin B1 destruction during MI takes place in the presence of an active Mos/MAP kinase pathway. This shows that the Mos/MAPK pathway and other components with CSF activity that are present at MI do not sufficiently suppress the APC so as to sustain a prolonged metaphase arrest.

Taken together, these observations suggest that between MI and MII factors are required that provide both a strong inhibition of the APC and a sensitivity of the APC to increases in Ca<sup>2+</sup>. Candidate proteins include spindle assembly checkpoint proteins Bub1 and Mad2, the Cdc20 inhibitor, Emil (Kallio *et al.*, 1998; Lorca *et al.*, 1998; Fang *et al.*, 1998b; Reimann and Jackson, 2002). To date the identity of such proteins has not been elucidated but it is an attractive possibility that the same protein may serve both functions; MII specific CSF activity and sensitivity to Ca<sup>2+</sup>.

## 5. The role of Emil in mouse oocytes

### 5.1 Introduction

In vertebrates, meiosis is characterised by specific pauses at various stages of oocyte maturation. The resumption of meiosis, at G2/M transition, is accompanied by the activation of CDK1-cyclin B followed by MAPK. CDK1-cyclin B is responsible for chromatin condensation, GVBD and spindle formation. GVBD is followed by a lengthy first metaphase during which the levels of the two kinases rise (Verlhac *et al.*, 1994; Hampl and Eppig, 1995a). Separation of the homologous chromosomes at anaphase I only occurs after inactivation of CDK1-cyclin B, which is achieved by cyclin B degradation (Hashimoto and Kishimoto, 1986; Hampl and Eppig, 1995a; Winston, 1997; Herbert *et al.*, 2003). CDK1-cyclin B increases immediately after MI and remains active during the MII arrest (Kubiak *et al.*, 1993; Masui, 2001). MAPK activity remains elevated throughout MI and MII and is necessary for sustaining MII arrest (Ferrell, Jr. *et al.*, 1991; Verlhac *et al.*, 1993; Verlhac *et al.*, 1994). This ability to sustain M-phase arrest suggests that MAPK is a component of CSF.

Progression out of MI and MII is controlled by regulated proteolysis. Proteolysis controls two subsequent steps. The initial step involves the separation of chromosomes or chromatids and is regulated by the proteolytic degradation of securin (Zur and Brandeis, 2001). Securin destruction releases separases which destroy the meiosis-specific cohesin, Rec8, from the chromosome arms (Zachariae and Nasmyth, 1999; Siomos *et al.*, 2001). Rec8



remains protected at the centromeric regions by the newly identified protein Sgo1, thus enabling sister chromatid cohesion after the MI/MII transition (Kitajima *et al.*, 2004). The subsequent step is the exit from metaphase and is controlled by cyclin B destruction (Murray *et al.*, 1989). Destruction of securin and cyclin B is determined by their ubiquitination which makes them accessible to the proteasome. Ubiquitination of these M-phase regulatory proteins is the result of an E3 ubiquitin ligase, the anaphase promoting complex (APC) (Zur and Brandeis, 2001; Raff *et al.*, 2002; Hagting *et al.*, 2002).

The APC remains inactive in MI until the metaphase/anaphase transition by which time all the chromosomes are aligned at the metaphase plate. Inhibition of APC activity is mediated by spindle assembly checkpoint proteins such as Mad2 and Bub1, which sequester the APC activator, Cdc20 (Fang *et al.*, 1998b; Hilioti *et al.*, 2001; Fang, 2002). Mad2, for example, binds Cdc20 on unattached kinetochores to inhibit APC activity until the chromosomes align at the metaphase plate. After alignment, Mad2 releases Cdc20 resulting in the activation of the APC (Kallio *et al.*, 1998; Fang *et al.*, 1998b). The resultant destruction of securin and cyclin B coordinates the exit from M-phase. Other proteins have been found that also act to inhibit APC by binding and sequestering Cdc20. One of these is the recently identified Emi1 (Reimann *et al.*, 2001a; Reimann *et al.*, 2001b; Reimann and Jackson, 2002).

In *Xenopus* oocytes, Emi1 is initially expressed in G2/prophase and its levels increase further after progesterone addition reaching their maximum level by GVBD. After GVBD, Emi1 levels remain high for the duration of maturation (Reimann and Jackson, 2002). In MII-arrested eggs *Xenopus* Emi1 levels are high and persist after fertilisation through the longer first interphase, during pronucleus migration only to decrease in the first mitotic division. In somatic cells, Emi1 levels increase in S-phase and decrease at

prometaphase (Reimann *et al.*, 2001a;Hsu *et al.*, 2002;Reimann *et al.*, 2001b). The importance of Emil for the early events of M-phase is shown by the fact that immunodepletion of the protein in *Xenopus* cycling extracts blocks cyclin B accumulation and prevents mitotic entry (Reimann *et al.*, 2001a). Similarly, loss of the Emil homolog Rcal prevents mitotic entry in *Drosophila* embryos (Dong *et al.*, 1997).

In addition, there is evidence that Emil is important for the maintenance of CSF activity. Firstly, in *Xenopus* extracts, excess Emil inhibits the destruction of cyclins A and B and blocks mitotic exit. The protein also causes M-phase arrest if injected in blastomeres of 2-cell embryos (Reimann *et al.*, 2001a). Furthermore, Emil addition in CSF extracts prevents  $Ca^{2+}$ -induced destruction of cyclin B and Mos and the inactivation of MAPK keeping the extracts in the arrested state (Reimann and Jackson, 2002). Finally, Emil depletion in CSF extracts induces cyclin B and Mos destruction and exit from M-phase in the absence of  $Ca^{2+}$  (Reimann and Jackson, 2002). It is not known how fertilisation-induced  $Ca^{2+}$  release activates the APC in the presence of Emil. One mechanism may involve the phosphorylation of Cdc20 or, alternatively, the phosphorylation of Emil that leads to the dissociation from Cdc20.

From the data described above it is evident that Emil is a good candidate for the regulator of CSF activity in *Xenopus*. However, there are well documented differences in APC action between *Xenopus* and mammalian eggs and it is not known if Emil plays a similar role in mammalian oocytes. For example, cyclin B degradation during the MI/MII transition is only partial in *Xenopus* (Kobayashi *et al.*, 1991), but almost complete in mouse oocytes (Kubiak *et al.*, 1993;Winston, 1997). Furthermore, cyclin B destruction and APC<sup>Cdc20</sup> activation are not necessary during *Xenopus* MI (Peter *et al.*, 2001;Taieb *et al.*,

2001). In contrast, excess cyclin B (chapter 1;Ledan *et al.*, 2001) or indestructible cyclin B (Herbert *et al.*, 2003) in the mouse cause metaphase arrest.

We have investigated the role of Emil in mouse meiosis. Firstly, we find that Emil is present in mouse oocytes and that the distribution of the protein changes during meiotic progression. Furthermore, we find that excess Emil delays Pbl<sup>1</sup> extrusion and exit from MII arrest. Finally, preventing Emil synthesis during maturation leads to abnormal spindles suggesting a role in spindle assembly. In MII, blocking Emil synthesis leads to spontaneous egg activation.

## 5.2 Results

### 5.2.1 Localisation of Emil during meiosis of mouse oocytes

The existence and localisation of Emil in mouse oocytes was examined by immunocytochemistry. We used an affinity purified rabbit polyclonal anti-human Emil antibody to label Emil in mouse oocytes. This antibody has been extensively characterised and used for Western blot analysis and immunofluorescence of Emil in HeLa cells (Hsu *et al.*, 2002)

Consistent with observations in *Xenopus* somatic cells in interphase (Reimann *et al.*, 2001a), GV stage mouse oocytes show a perinuclear accumulation of immunoreactivity and a punctuate pattern of localisation in the cytoplasm (Figure 5.1A). After GVBD, in prometaphase, Emil begins to localise to the area surrounding the chromatin and the microtubules, which have not yet evolved into an organised spindle (Figure 5.1B). At metaphase of the first meiotic division, at which time the spindle is formed and most of the chromosomes are aligned at the metaphase plate, there is a ring of Emil immunoreactivity in the area surrounding the spindle (Figure 5.1C). This localisation shows similarities to the distribution of endoplasmic reticulum (ER) and mitochondria (Bavister and Squirrell, 2000; FitzHarris *et al.*, 2003) implying that Emil may be membrane-bound and localised on these organelles. When the spindle translocates to the oocyte periphery, at the end of metaphase I, Emil remains surrounding the spindle and is particularly concentrated at the spindle poles (Figure 5.1D). In anaphase, most of the protein has disappeared from the spindle region with only a small concentration localising at the spindle pole area, where the chromosomes are gathered (Figure 5.1E). At the time of the formation of the first polar body, Emil can only be observed at the midbody (Figure 5.1F).

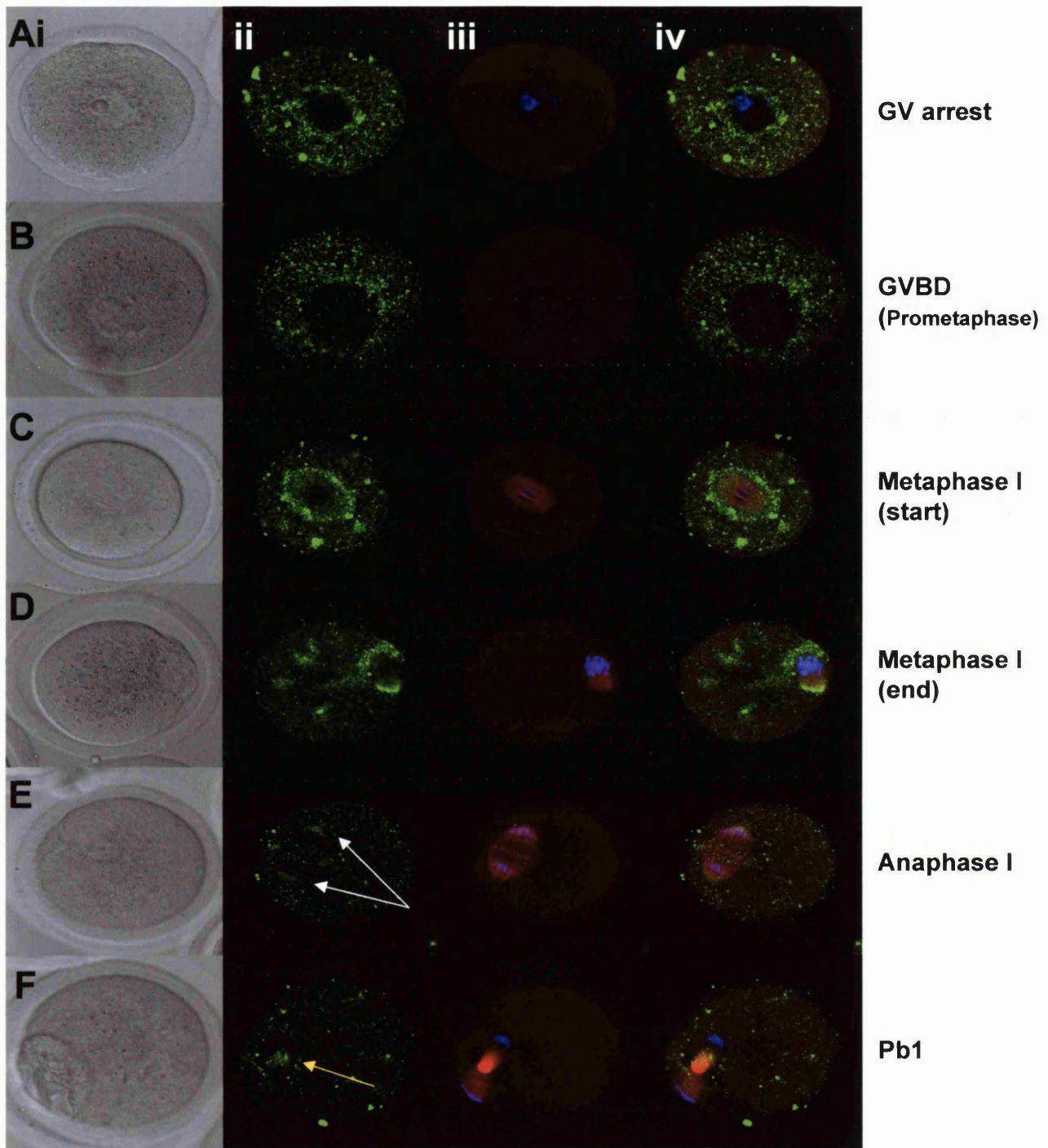


**Figure 5.1 Emi1 localisation during oocyte maturation.** GV stage oocytes were released from prophase arrest and fixed for immunocytochemistry at different times during maturation (A: fixed during arrest, B: fixed 2h after release, C: 6h, D: 8h, E-F: 10h). Column (i) represents the transmission images of the fixed oocytes. Column (ii) shows the staining of Emi1 (green) with an anti-hEmi1 antibody. Column (iii) shows the staining of microtubules (red) and chromatin (blue) obtained with an anti-tubulin- $\alpha$  antibody and Hoechst respectively. Column (iv) is the merge between columns (ii) and (iii). It is obvious that Emi1 is localised at the peri-spindle area at metaphase only to disappear at anaphase. White arrows: spindle pole localisation, yellow arrow: midbody localisation. The immunocytochemistry experiments were carried out with approximately 20 oocytes per group.

seems like Emil is  
anywhere but level of  
spindle

In MII arrested eggs, as in MI, Emil is again concentrated around the spindle (Figure 5.2A). After fertilisation, at anaphase II, most of the protein disappears with some immunoreactivity evident at the poles close to the separated chromatids (Figure 5.2B). Eventually, during the formation of the second polar body, Emil can only be seen concentrated at the midbody region (Figure 5.2C). The formation of the polar body is associated with loss of immunoreactivity (Figure 5.2D).

Why not do Rht?  
antibody injection  
to confirm

### 5.2.2 Emil depletion causes spindle formation inhibition and arrest at MI

The data described above suggest that Emil is present in mammalian meiosis and its localisation is dependent on the stage of meiosis. To examine the role of Emil in mammalian meiosis we have used morpholino oligonucleotides to deplete Emil (see chapter 2). The morpholino-injected oocytes were cultured for 16-18h in the presence of IBMX before being released from arrest and the effects on the first meiotic division were determined. A significant inhibition of Pb1 extrusion was observed in Emil morpholino-injected oocytes (9% Pb1 extrusion; 7/78 oocytes) compared to control morpholino-injected oocytes (79%; 48/61;  $P < 0.001$ ) (Figure 5.3A).

It was then necessary to verify that Emil had been depleted by treatment with the Emil morpholino. Emil and control morpholino-injected oocytes were fixed 6h after release from prophase arrest and the presence of Emil was determined by immunocytochemistry. The level of Emil depletion was determined by measuring the average intensity of an area of the same size in the cytoplasm and peri-spindle area of 22 control morpholino-injected and 18 Emil morpholino-injected oocytes. We observed a 5-fold decrease of Emil in the cytoplasm ( $P < 0.001$ ) and a 4-fold decrease at the peri-spindle area ( $P < 0.001$ ) (Figure 5.3B,

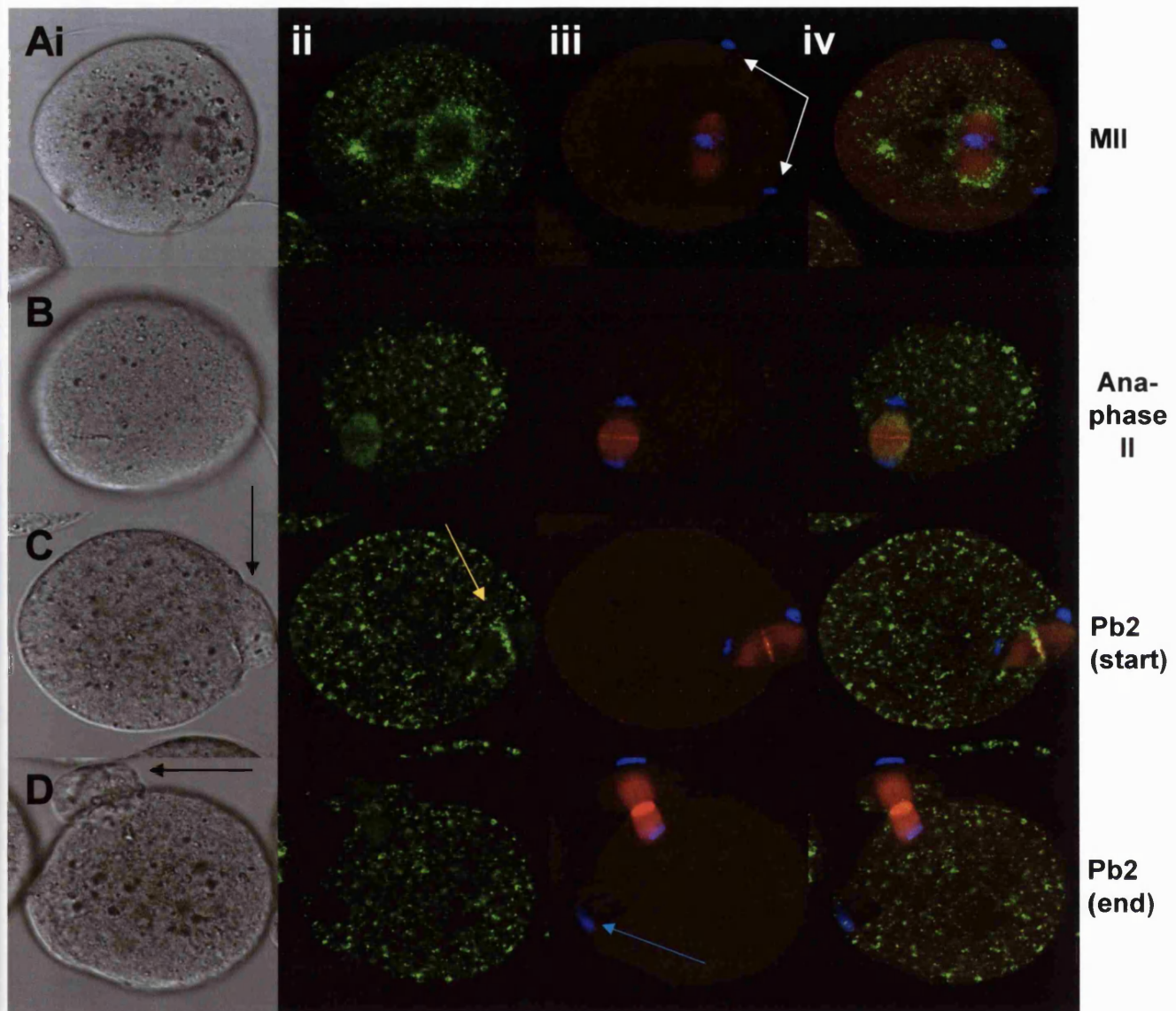
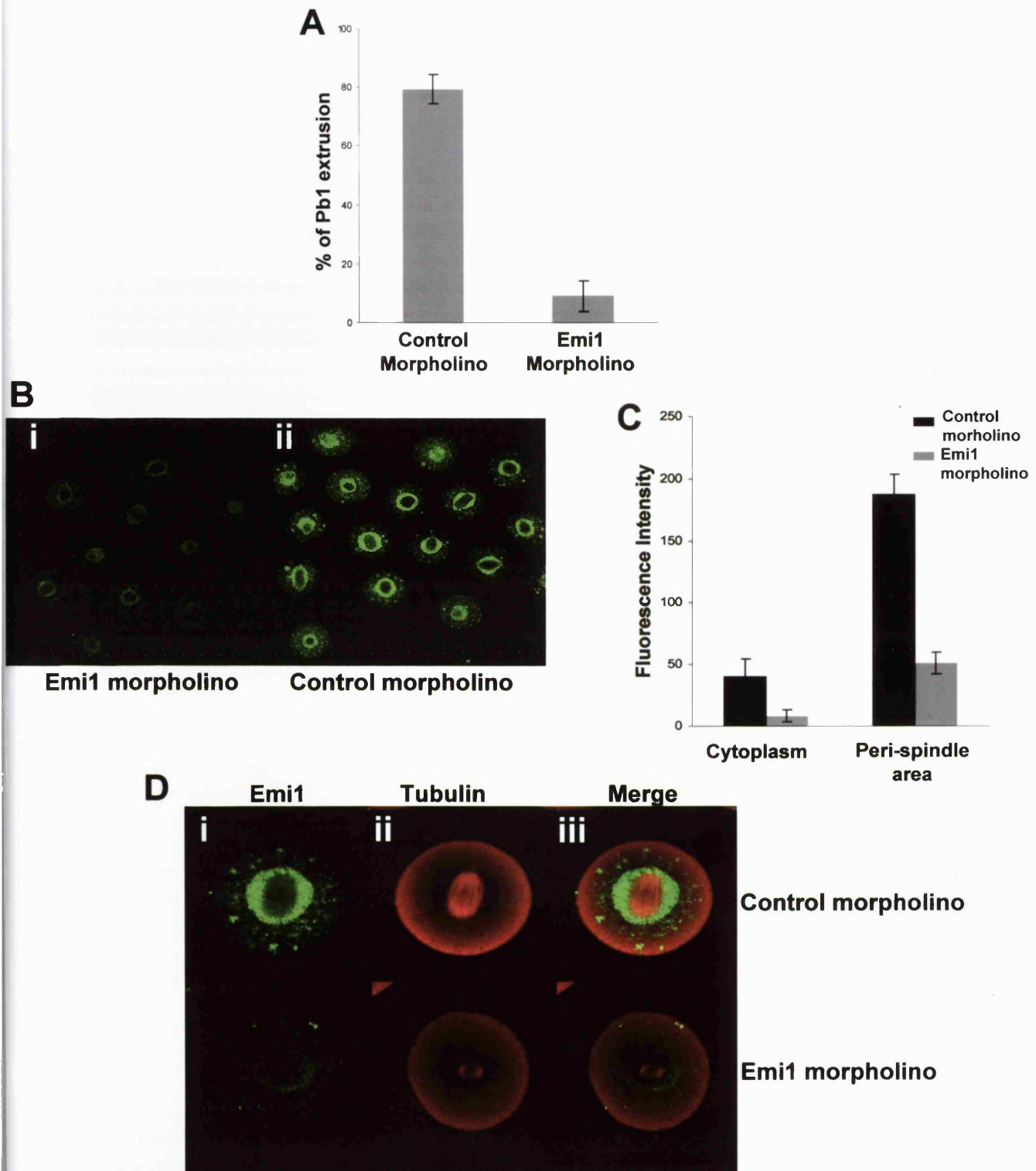


**Figure 5.2 Emi1 localisation at fertilisation.** Eggs were fixed for immunocytochemistry at different times during fertilisation (A: fixed prior to fertilisation, B: fixed at 1h after sperm addition, C-D: 1.5h). Emi1 is localised around the spindle at MII arrest. After release from metaphase arrest, Emi1 can be seen at the spindle pole and midbody (yellow arrow) areas. Columns (i) to (iv) as in Fig 6.1. White arrows: sperm attached to egg, blue arrow: decondensing sperm chromatin, black arrows: Pb2. The immunocytochemistry experiments were carried out with 18-20 eggs per group.





C). This result also provides further support that the antibody is specifically recognising Emi1 in mouse oocytes.

In order to explore the reason for the inhibition of Pb1 extrusion after Emi1 depletion, Emi1 morpholino-injected (n=18) and control morpholino-injected oocytes (n=22) were microinjected with rhodamine-tubulin 1h before fixing for immunocytochemistry. In Emi1 morpholino-injected oocytes there was a severe disruption of the formation of the first meiotic spindle. Only one oocyte had the normal barrel-shaped spindle. From the rest, seven did not show any signs of spindle formation, while 10 oocytes had very small abnormal spindles where the tubulin was accumulated at the spindle poles and spindle microtubules were almost completely absent. In contrast, the control morpholino-injected oocytes had normal barrel-shaped MI spindles by six hours from the initiation of oocyte maturation (Figure 5.3D). Thus, depletion of Emi1 from the first meiotic cell division disrupts spindle assembly and as result Pb1 extrusion.

Attempts to reverse the effect of the Emi1-morpholino injection were performed by injecting Emi1 protein. These attempts were unsuccessful since polar body extrusion could not be reversed. A possible explanation could be that the exogenous protein does not localise or behave in a similar manner to the endogenous protein.

### **5.2.3 Excess Emi1 blocks Pb1 extrusion**

As seen from the localisation experiments, Emi1 seems to disappear from the spindle during Pb1 extrusion. To investigate the significance of the loss of Emi1 in the first meiotic division we examined the effects of excess Emi1 protein on meiotic maturation of mouse oocytes. GV stage oocytes were microinjected with human Emi1 protein (0.1 mg/ml inside egg) and

released from prophase arrest. Interestingly, similar to depletion of Emi1, excess Emi1 had the effect of inhibiting Pbl extrusion. 18 hours after release from prophase arrest, only 16% (6/37) of Emi1 injected oocytes had extruded a polar body compared to 85% (37/44;  $P < 0.001$ ) of control oocytes injected with water (Figure 5.4A). To determine the stage of oocyte maturation at which the oocytes were blocked, we examined the condition of the spindle of the arrested Emi1 injected oocytes by microinjecting oocytes with rhodamine-tubulin 16-18h after release from GV arrest (Figure 5.4B). We found that the arrested oocytes have an intact spindle. The chromosomes can be identified as dark regions at the metaphase plate showing that anaphase has not occurred. Thus, excess Emi1 causes the arrest of maturing oocytes at MI.

#### **5.2.4 Emi1 depletion causes spontaneous activation of MII arrested eggs**

In order to understand the role of Emi1 in MII, we microinjected eggs with the Emi1 morpholino oligonucleotide (30-50  $\mu\text{M}$  inside the oocyte). Injection of the morpholino can be useful for testing if Emi1 is important for maintaining CSF activity. Depletion of Emi1 from MII eggs should lead to spontaneous resumption of meiosis as seen in *Xenopus* extracts after Emi1 immunodepletion (Reimann and Jackson, 2002). Groups of oocytes were also injected with the control morpholino which, as we showed earlier (5.2.2) does not cause Emi1 depletion. The eggs were assessed 16-18h after microinjection by which time most of the endogenous protein was expected to have disappeared, assuming a similar half-life as we observed in MI oocytes (chapter 5.2.2, Figure 5.3B). From eight experiments there was a significant effect of Emi1 depletion in five. In the three experiments that did not show any effect of the morpholino, there were no signs of activation in either the control or the Emi1

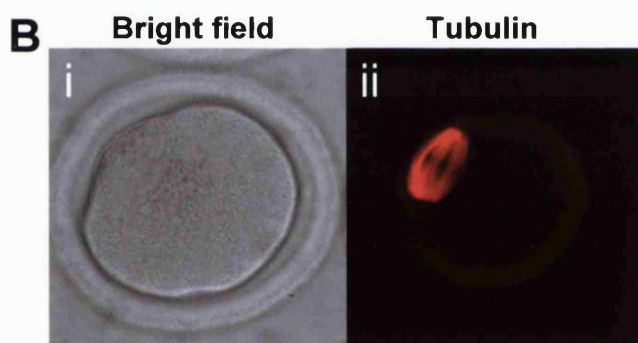
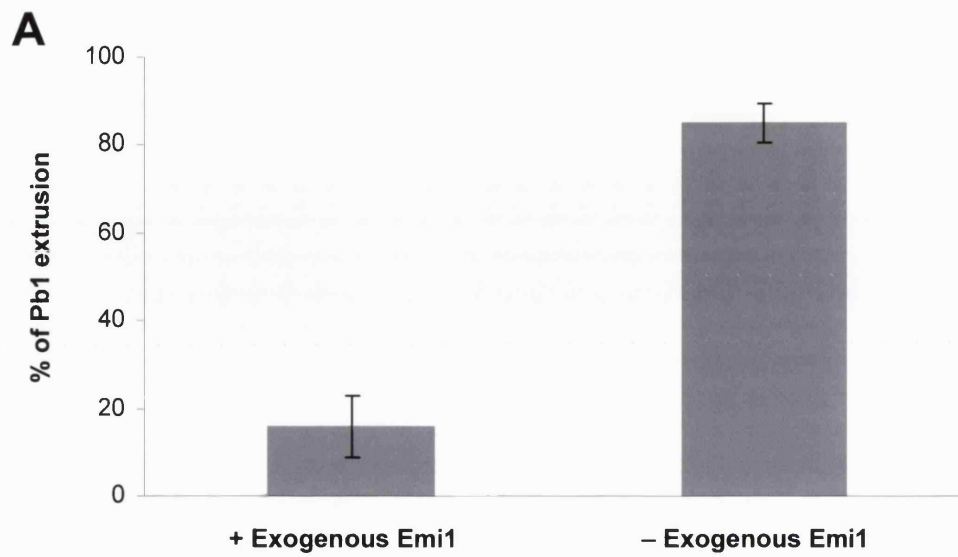


**Figure 5.4 Excess Emi1 blocks Pb1 extrusion.** GV stage oocytes were injected with human Emi1 protein and release from prophase arrest. Excess Emi1 caused a 5-fold decrease in Pb1 extrusion (A, 3 experiments). The injected oocytes were arrested at metaphase as revealed by the presence of an intact MI spindle 16-18h after release from GV arrest (Bii). Error bars: standard deviation.

morpholino group. From the five experiments in which there was an effect, 75% (70/93) of the eggs injected with the Emi1 morpholino showed signs of activation (Figure 5.5A). The activated state was determined by features reported for the parthenogenetic activation of Mos or MAPK deficient MII eggs (Hirao and Eppig, 1997;Phillips *et al.*, 2002): presence of second polar bodies (7%), pronuclei (48%), cleavage to the 2-cell stage (11%) and fragmentation (caused by atypical cytokinesis and imperfect control of cleavage sites; 34%). In contrast, in control morpholino-injected eggs, the rate of activation was 16% (12/74;  $P < 0.001$ ) (Figure 5.5A). Similar levels of activation were observed in buffer-injected controls (data not shown). There was no sign of spontaneous activation in uninjected eggs. Thus, the low rate of activation seen in the control morpholino-injected eggs may be attributed to the microinjection procedure.

If Emi1 depletion is responsible for increasing the rate of spontaneous activation, the effect should be reversed by injecting excess Emi1 protein (0.1 mg/ml inside the egg). Emi1 was injected 30 minutes prior to injecting the Emi1 morpholino. From two experiments 92% (22/24) of the Emi1 morpholino-injected eggs were activated 16-18h after injection. In contrast, the degree of activation was significantly lower in the Emi1 morpholino-injected eggs that were injected with excess protein (35%; 10/28;  $P < 0.001$ ). This was similar to control morpholino-injected eggs (33%; 6/18;  $P < 0.001$ ) (Figure 5.5B). The high rate of activation in the control group reflects the double injection with the control morpholino and the buffer solution. This experiment shows that the effects of the Emi1 morpholino at MII can be rescued by the injection of Emi1 protein.

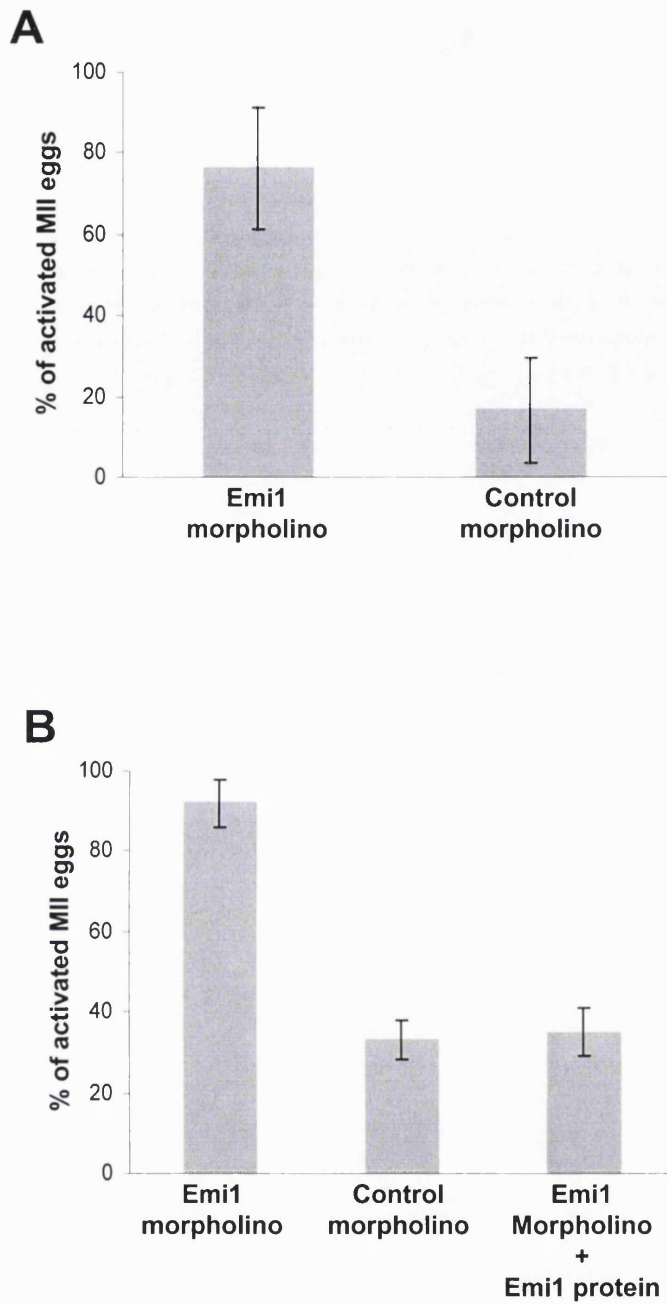


**Figure 5.5 Emi1 depletion causes spontaneous activation of MII eggs.** MII mouse eggs were microinjected either with a Emi1-specific morpholino or a standard inactive morpholino. 16-18h after injection there was an approximately 5-fold greater level of activation observed in the Emi1 morpholino injected eggs (A). The morpholino used is specific for Emi1 since Emi1 protein injection prevents egg activation (B). Error bars: standard deviation.

### **5.2.5 Excess Emi1 delays fertilisation**

The ability of Emi1 morpholino to induce egg activation suggests that endogenous Emi1 may contribute to the stability of arrest at MII. In order to determine whether Emi1 can maintain MII arrest we microinjected Emi1 protein in MII arrested eggs prior to fertilisation in vitro. We found that eggs injected with Emi1 show a significant delay in Pb2 extrusion compared to controls injected with injection buffer. 1h and 2h after sperm addition, 32% (15/42) and 98% (41/42), respectively, of control eggs had extruded the second polar body (Figure 5.6A; black line). In contrast, the first signs of Pb2 extrusion in Emi1 injected eggs was seen 3h after sperm addition (15%; 6/38) (Figure 5.6A; grey line). In order to identify at which stage of the cycle the eggs are delayed, we stained the chromatin with Hoechst and examined the eggs 90 minutes after sperm addition. We found that the chromosomes had not yet separated, but remained at the metaphase plate (Figure 5.6A inset). Thus, excess Emi1 causes a delay in the onset of anaphase at fertilisation by approximately 3 hours.

### **5.2.6 Excess Emi1 delays egg activation caused by UO126**

The Mos/MAPK pathway is necessary for initiating MII arrest (Verlhac *et al.*, 1996; Wianny and Zernicka-Goetz, 2000). Furthermore, inhibition of the pathway in MII-arrested eggs, by the addition of the MEK inhibitor UO126, causes egg activation suggesting, in mice, that the Mos/MAPK pathway is also necessary for the maintenance of MII arrest (Phillips *et al.*, 2002). In order to investigate the possibility of Emi1 involvement in this pathway, MII eggs microinjected with Emi1 were incubated with 50 $\mu$ M UO126 and monitored for signs of activation. Activation was determined as in 5.2.4 by the presence of Pb2, pronuclei, 2-cell stage embryos and fragmentation. We found that although half of the control eggs (52%;

28/54) in UO126 were activated by 6h from addition of the drug, it was not until 10h when Emil-injected eggs showed similar levels of activation (44%; 17/39) (Figure 5.6B). By that time, there was almost complete activation in control eggs (91%; 49/54). This result shows that excess Emil is able to maintain the MII arrested state when the Mos/MAPK pathway is inhibited.

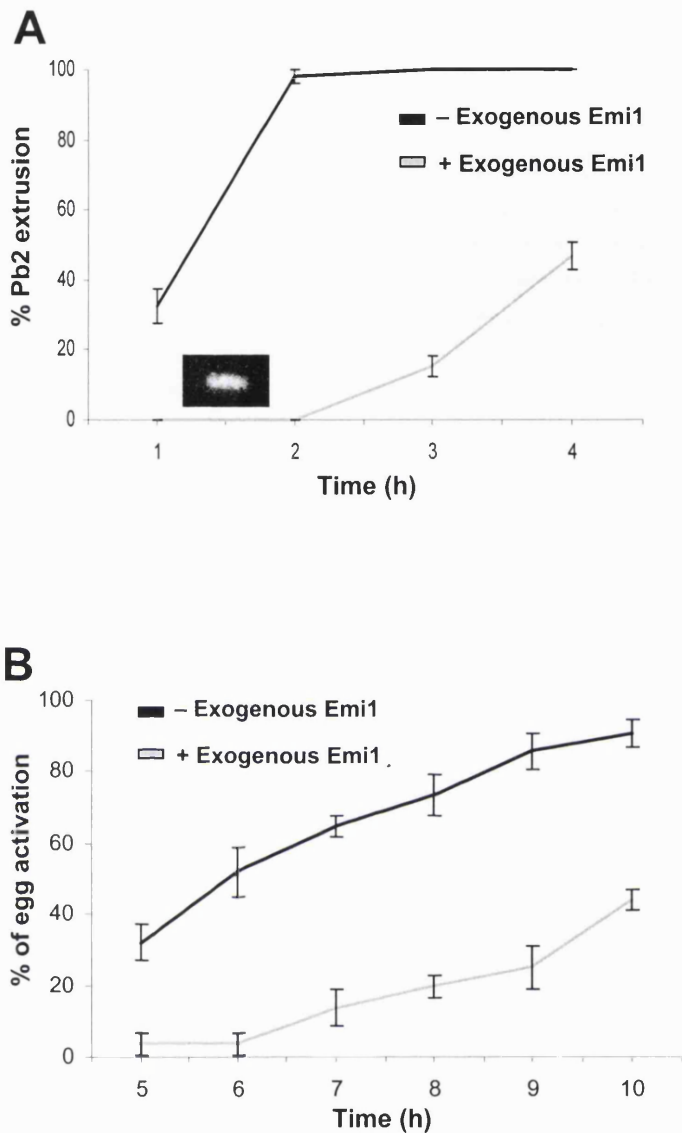


**Figure 5.6 Excess Emi1 delays fertilisation and egg activation.** When MII eggs are microinjected with Emi1 protein prior to fertilisation, Pb2 extrusion is delayed by approximately 3h (2 experiments).  $t=0$  the time of sperm addition (A). Hoechst staining of Emi1-injected eggs 90 minutes after sperm addition shows that the eggs remain at MII arrest (A inset). (B) MII eggs were injected with Emi1 and then incubated with UO126. Egg activation is delayed by approximately 5h in Emi1-injected eggs (3 experiments).  $t=0$  the time of addition of UO126. Error bars: standard deviation.



## 5.3 Discussion

### 5.3.1 Emil1 persists during MI in mouse oocytes

#### 5.3.1a Emil1 localisation during meiotic maturation

Our immunofluorescence experiments show that Emil1 is present in mouse oocytes during maturation and is strongly localised at the area surrounding the spindle at metaphase I and II. This localisation suggests a role for Emil1 in mammalian meiosis. No Emil1 localisation experiments have been performed in eggs of other species. Localisation experiments, however, have been done in *Xenopus* somatic cells (Reimann *et al.*, 2001a). These experiments have shown that in interphase, the protein localises in a punctuate pattern in the nucleus and the cytoplasm with some perinuclear concentration. Our experiments in GV stage arrested mouse oocytes also shows perinuclear and punctuate cytoplasmic localisation, but no nuclear concentration. This difference may be due to the fact that the oocytes are not arrested in interphase, but in prophase. In early mitosis, Emil1 is found throughout the cells and particularly at the spindle (Reimann *et al.*, 2001a). In mouse oocyte maturation, we find that Emil1 is also localised throughout the cytoplasm, but with strong peri-spindle localisation similar to the localisation of the ER and mitochondria (Bavister and Squirrell, 2000; FitzHarris *et al.*, 2003). In contrast to *Xenopus* somatic cells, the spindles did not show Emil1 immunoreactivity. The pattern of Emil1 localisation during maturation implies that the protein may be membrane-bound. As such, the differences in Emil1 localisation in mitosis and meiosis may reflect differences in the organisation of the ER and mitochondria. The difference in spindle localisation may reflect differential action or dynamics of Emil1 in mitosis and meiosis.

At the end of MI we find that Emi1 translocates from the spindle surrounding area to the midbody and spindle poles. At the final stage of cytokinesis and Pb1 extrusion there are no signs of any Emi1 immunoreactivity. The timing of this loss from the spindle area suggests it may be related to the release of Cdc20 and APC activation at the metaphase-anaphase transition. The presence of Emi1 at the spindle poles and the midbody region, at polar body extrusion, suggests it may play a role in promoting the inhibition of degradation of key proteins that are important for the completion of meiosis.

### 5.3.1b *Emi1 and cyclin A in meiosis and mitosis*

Unlike meiosis where we find Emi1 throughout oocyte maturation in both mouse (our work) and *Xenopus* (Reimann and Jackson, 2002), in somatic cells, Emi1 accumulates in S-phase and is degraded at prophase/prometaphase. In mitosis, Emi1 degradation is responsible for cyclin A destruction at that stage (den Elzen and Pines, 2001; Hsu *et al.*, 2002; Margottin-Goguet *et al.*, 2003). Degradation of Emi1 causes the release of Cdc20 resulting in activation of the APC and the initiation of cyclin A degradation (Reimann *et al.*, 2001a; Reimann *et al.*, 2001b; Margottin-Goguet *et al.*, 2003). The persistence of Emi1 during oocyte maturation is consistent with the observation that, unlike mitosis, cyclin A also persists through MI in the mouse (Sweeney *et al.*, 1996; Winston *et al.*, 2000).

Thus, in MI, Emi1 may be responsible for the prolonged metaphase by inhibiting APC-dependent destruction of cyclin A. This is supported by the observation that, in mitosis, cyclin A overexpression causes a delay in chromosome alignment and sister chromatid segregation (den Elzen and Pines, 2001). This phenotype suggests cyclin A may be

responsible for the prolonged metaphase I where the chromosomes do not align at the metaphase plate until 3-4 hours after GVBD (Brunet *et al.*, 1999).

Thus, in mitosis and meiosis, Emi1 kinetics seem to follow those of cyclin A, which is consistent with Emi1 being the main regulator of APC-dependent cyclin A degradation. The question that arises is why Emi1 should be so important for protecting cyclin A from degradation, when other APC inhibitors are also present in M-phase. However, Mad2, a protein that also sequesters Cdc20 and inhibits the APC (Kallio *et al.*, 1998; Fang *et al.*, 1998b) is not capable of inhibiting APC-dependent cyclin A ubiquitination and destruction (Geley *et al.*, 2001; den Elzen and Pines, 2001; Reimann *et al.*, 2001b). Although addition of Mad2 to cycling *Xenopus* extracts prevents cyclin B destruction, it does not affect that of cyclin A (Margottin-Goguet *et al.*, 2003). This possibly occurs because Emi1 and Mad2 follow distinct mechanisms for APC activation. A differential APC activation hypothesis is supported by the fact that Emi1 and Mad2 sequester Cdc20 by binding to different regions of the APC activator (Margottin-Goguet *et al.*, 2003). Further experiments clarifying the relationship between Emi1, cyclin A and MI are necessary to understand the significance of Emi1 persistence during MI.

### **5.3.2 Emi1 is necessary for progression through oocyte maturation**

In order to ascertain the importance of Emi1 for oocyte maturation we depleted the endogenous protein by using a morpholino oligonucleotide designed to deplete Emi1 mRNA. Depletion of Emi1 resulted in the formation of small abnormal spindles that did not support normal progression into MI. Immunofluorescence experiments verified that Emi1 was depleted in the arrested oocytes. Furthermore, microinjection of a control morpholino did not

affect normal spindle formation, as seen by immunofluorescence, and extrusion of Pb1. Thus, these experiments show that Emi1 is essential for progression through MI.

The fact that spindle assembly is controlled by CDK1-cyclin B raises the possibility that low CDK1-cyclin B levels may be responsible for the phenotype observed in our morpholino experiments. This is consistent with the known role of Emi1. Depletion of Emi1 would lead to premature release of Cdc20 and activation of the APC resulting in cyclin B destruction preventing mitotic entry (Reimann *et al.*, 2001a;Reimann *et al.*, 2001b). This mechanism is also supported by experiments showing that in strains of mice where the rate of cyclin B synthesis is higher, Pb1 extrusion occurs faster and, thus, the levels of cyclin B determine the duration of MI (Polanski *et al.*, 1998). Alternatively, our data suggest a previously unknown role for Emi1 in spindle assembly. It is not known if such a role is direct or the result of Emi1 affecting other proteins such as cyclin A.

Our data also point to a difference in the regulation of Emi1 destruction in mitosis and meiosis. As discussed earlier, in mitosis, Emi1 is destroyed in prophase (Hsu *et al.*, 2002;Margottin-Goguet *et al.*, 2003). The destruction of Emi1 at this stage shows that the protein is not necessary for the progression of M-phase. In meiosis, the prolonged presence of Emi1 through to MI may be the result of a delayed activation of factors involved in its degradation. Emi1 degradation is APC-independent since APC immunodepletion prevents cyclin B destruction but not that of Emi1 (Reimann *et al.*, 2001a). It has recently been discovered that Emi1 ubiquitin-dependent destruction is regulated by Emi1 phosphorylation by CDK1 and the subsequent recognition of Emi1 by the SCF E3 ubiquitin ligase (Margottin-Goguet *et al.*, 2003). The different timing of Emi1 destruction in meiosis and mitosis suggests that Emi1 destruction may be regulated differently in meiosis. Either a higher

threshold of CDK1 activity is necessary for Emi1 phosphorylation, Emi1 is protected or the SCF ligase is inactive until some time after formation of the MI spindle.

### 5.3.3 Excess Emi1 causes arrest at MI

To investigate the necessity for Emi1 degradation or relocation at the end of M-phase, we examined the effect of excess Emi1 by microinjecting the protein in maturing oocytes. We found that maturation progresses normally until the end of metaphase I, as shown by the translocation of the spindle at the oocyte periphery, at which stage the oocytes arrest and Pbl is not extruded. The mechanism of Emi1 action is likely to be through an inhibition of the APC preventing securin and cyclin B destruction. This result also supports the work of Herbert and co-workers (2003) which suggests that the APC is important for the MI/MII transition in the mouse.

### 5.3.4 Emi1 is involved in CSF activity

After identifying Emi1 as an important regulator of oocyte maturation, we wanted to investigate whether Emi1 is present in MII and whether it was important for CSF activity. As described above, we find that Emi1 is present in MII arrested eggs and localised around the spindle. Since Emi1 disappears from the spindle area at Pbl extrusion, this accumulation may be the result of new protein synthesis or translocation of Emi1 from the cytoplasm to the newly formed MII spindle.

The most direct way to show whether a protein is a component of CSF or not is to deplete this protein from MII eggs. The absence of a protein that is sufficient for maintaining CSF should lead to premature egg activation in the absence of  $Ca^{2+}$ . In order to determine the

role of Emi1 in CSF-mediated MII arrest, we depleted Emi1 by injecting the Emi1 mRNA-specific morpholino oligonucleotide in MII eggs. Unfortunately, the absence of sufficient amounts of Emi1 antibody did not allow us to confirm Emi1 depletion using immunofluorescence. Similar treatment, however, of maturing oocytes resulted in a 5-fold loss of Emi1 protein. From this line of experiments, it was discovered that Emi1 depletion caused a significant loss of CSF activity. This was determined by the fact that a significant percentage of Emi1-depleted eggs underwent parthenogenic activation. This result was apparently specific to Emi1 depletion, since the addition of Emi1 protein could rescue the eggs from spontaneous activation. This Emi1 action was evident in eggs that were more susceptible to activation, since in three out of eight experiments, where no spontaneous activation was seen in controls, no loss of CSF activity was seen. The ability of morpholinos to release eggs from MII arrest suggests Emi1 is necessary for the maintenance of CSF. The requirement for Emi1 in MI, as described earlier, prevents us from determining whether Emi1 is necessary for establishing CSF activity.

Our results in isolated mouse eggs are consistent with the data obtained from *Xenopus* egg extracts. Reimann and Jackson (2002) have shown that immunodepletion of Emi1 in *Xenopus* CSF extracts leads to cyclin B degradation and exit from M-phase in the absence of intracellular  $Ca^{2+}$  rises. In this work, constitutively active CaMKII, the major  $Ca^{2+}$  mediator of CSF release, did not trigger cyclin B degradation, Mos destruction or M-phase exit in CSF extracts in the presence of excess Emi1. This implies that Emi1 acts downstream of CaMKII. Similar to these data, we find that addition of exogenous Emi1 protein in mouse oocytes preserves CSF arrest after fertilisation.

Another well documented pathway involved in CSF-mediated MII arrest is the Mos/MAPK pathway. This pathway is required for establishing the CSF state in mouse MII eggs. For example, unfertilised oocytes from *mos*<sup>-/-</sup> mice undergo parthenogenetic activation in the absence of any Ca<sup>2+</sup> stimulus (Hashimoto *et al.*, 1994; Colledge *et al.*, 1994; Verlhac *et al.*, 1996). Spontaneous activation is also observed by the use of RNA interference against Mos mRNA in mouse oocytes (Wianny and Zernicka-Goetz, 2000). In addition, the Mos/MAPK pathway is necessary for the maintenance of CSF arrest in mouse MII eggs since blocking the pathway by incubating MII eggs with UO126 causes spontaneous activation (Phillips *et al.*, 2002).

Thus, in mouse oocytes, Mos and Emi1 both appear to be important for the maintenance of CSF during the MII arrest. The ability of Emi1 to, significantly, delay UO126-induced activation provides some further information about the part played by Emi1 with respect to the Mos/MAPK pathway in regulating CSF arrest. Since Emi1 can sustain CSF activity in the absence of MAPK, it appears that Emi1 is not part of the Mos/MAPK pathway. Thus, Emi1 is a Mos/MAPK-independent pathway. This means that both Mos/MAPK and Emi1 inhibit APC<sup>cdc20</sup> independently. At fertilisation, Ca<sup>2+</sup> release leads to CaMKII activation, which then could cause Emi1 inactivation and possibly APC activation through a yet unknown pathway. APC activation is then responsible for cyclin B degradation, subsequent CDK1-cyclin B inactivation and exit from meiosis.

## 6. Ca<sup>2+</sup> oscillations at fertilisation in mammals are regulated by the formation of pronuclei

### 6.1 Introduction

In all organisms examined, sperm-egg fusion at fertilisation triggers an intra-cellular Ca<sup>2+</sup> release which is responsible for the resumption of meiosis and the transition from oocyte to embryo (Stricker, 1999;Runft *et al.*, 2002). For many species, like *Xenopus*, sea urchin and starfish, calcium signalling at fertilisation begins and ends with the explosion of Ca<sup>2+</sup> release in the form of a single long monotonic transient (Stricker, 1999). However, in mammalian eggs and a handful of other organisms, like ascidians and nemertean worms, an initial long transient is followed by a series of Ca<sup>2+</sup> oscillations lasting, in mammals, for 3-4 h.

It has been recently realised that the M-phase kinases may regulate the ability to generate Ca<sup>2+</sup> transients and thereby govern the temporal pattern of calcium signalling at fertilisation. These kinases are CDK1-cyclin B and MAPK. During MII arrest, both kinases are active. CDK1-cyclin B is responsible for sustaining M-phase. As it has already been shown from our work and from others, exit from MI is inhibited by high levels of CDK1-cyclin B activity (see chapter 3;Polanski *et al.*, 1998;Ledan *et al.*, 2000;Hampl and Eppig, 1995a). The MAPK pathway is, at least in part, responsible for CSF arrest at MII by maintaining high CDK1-cyclin B activity levels by inhibiting the APC.



At fertilisation, however, both kinase activities need to be downregulated. The sperm-induced  $\text{Ca}^{2+}$  transients trigger the degradation of cyclin B and the subsequent loss of CDK1-cyclin B activity. This leads to the completion of meiosis as indicated by the extrusion of Pb2 about 90 minutes after sperm-egg fusion. There seems to be a correlation between the timing of  $\text{Ca}^{2+}$  oscillations and M-phase. One demonstration of this correlation is that oscillations only occur during fertilisation at MI (ascidians) or MII (mammals) when M-phase kinase activities are high. Monotonic transients are predominantly seen in prophase of meiosis (clam) or mitosis (sea urchin) when the kinases are inactive. One exception is the fertilisation of *Xenopus* eggs where only a monotonic transient occurs in MII, releasing the eggs from arrest. In ascidians, there is a very strong correlation between  $\text{Ca}^{2+}$  oscillations and CDK1-cyclin B activity (Levasseur and McDougall, 2000).  $\text{Ca}^{2+}$  oscillations stop after cyclin destruction in MI, restart at MII when CDK1-cyclin B appears and cease at the time of CDK1-cyclin B inactivation at Pb2 extrusion. Moreover, the microinjection of a non-destructible form of cyclin B which keeps CDK1-cyclin B activity high causes  $\text{Ca}^{2+}$  oscillations during the transition from MI to MII that continue after the extrusion of Pb2 (Levasseur and McDougall, 2000). This correlation does not extend to MAPK since, during the MI/MII transition, MAPK remains active and does not affect the pattern of the oscillations. In addition, the oscillations are not affected by the MEK inhibitor UO126 indicating that the MAPK activity is not regulating the oscillations (Levasseur and McDougall, 2000).

Correlation between M-phase and  $\text{Ca}^{2+}$  oscillations is also observed in mammals. Treatment of fertilised MII eggs with microtubule depolymerising agents like colcemid and

nocodazole that arrest eggs in M-phase, causes long-lasting  $\text{Ca}^{2+}$  oscillations, mirroring the effects of excess cyclin B in ascidian eggs (Jones *et al.*, 1995). Furthermore, inactivation of CDK1-cyclin B by roscovitine blocks  $\text{Ca}^{2+}$  oscillations. However, roscovitine also inhibits  $\text{Ca}^{2+}$  release by  $\text{IP}_3$  and the  $\text{Ca}^{2+}$ -pump inhibitor thapsigargin (Deng and Shen, 2000). However, the  $\text{Ca}^{2+}$  transients do not stop at Pb2 extrusion when CDK1-cyclin B is inactivated (Verlhac *et al.*, 1994; Moos *et al.*, 1995), but continue for a further 2-3 hours, terminating at around pronucleus formation (Jones *et al.*, 1995).

Nuclear transfer and cell-fusion experiments have shown that pronuclei are important for the regulation of  $\text{Ca}^{2+}$  release. The transfer of pronuclei from fertilised embryos to MII eggs causes  $\text{Ca}^{2+}$  oscillations and activation of the eggs (Kono *et al.*, 1995). On the contrary, when pronuclei from parthenogenetically activated eggs are transferred to MII eggs, the MII eggs remain arrested and no  $\text{Ca}^{2+}$  changes are detected. The fusion of fertilised or parthenogenetically activated eggs to MII arrested eggs gives similar results. Only the fertilised eggs cause a  $\text{Ca}^{2+}$ -dependent resumption of meiosis in the MII eggs (Zernicka-Goetz *et al.*, 1995). Furthermore,  $\text{Ca}^{2+}$  transients after NEBD of the first embryonic cell cycle are only observed in fertilised but not parthenogenetically activated embryos and the transfer of pronuclei from fertilised embryos to parthenogenetic embryos causes the generation of  $\text{Ca}^{2+}$  oscillations (Kono *et al.*, 1996). These experiments imply that a sperm-derived  $\text{Ca}^{2+}$ -releasing activity is localised in the pronuclei causing the cessation of the fertilisation-induced  $\text{Ca}^{2+}$  transients. However, there are also experiments suggesting that there is no correlation of pronucleus formation and the cessation of  $\text{Ca}^{2+}$  oscillations. Nucleate and

anucleate halves from fertilised embryos bisected prior to pronucleus formation stop oscillating at about the same time (Day *et al.*, 2000).

The observations in mouse and ascidian eggs suggest two possible mechanisms for  $\text{Ca}^{2+}$  regulation at fertilisation. Firstly,  $\text{Ca}^{2+}$  releasing activity may be controlled by the M-phase kinases and secondly the activity ceases as a result of Pn formation. In this chapter I describe the experiments in which we dissociate these two mechanisms. I show that  $\text{Ca}^{2+}$  oscillations continue after the M-phase kinases are both inactivated, while pronucleus formation is blocked. Our results suggest a compartmentalisation-regulated mechanism by which  $\text{Ca}^{2+}$  oscillations are controlled at fertilisation.

## 6.2 Results

### 6.2.1 The relationship between $\text{Ca}^{2+}$ transients, pronucleus formation and CDK1-cyclin B and MAP kinase at fertilisation

The duration of  $\text{Ca}^{2+}$  signalling and the activities of Cdk1-cyclin B and MAPK at fertilisation have been studied in independent experiments (Jones *et al.*, 1995; Moses and Kline, 1995; Moos *et al.*, 1995; Schultz and Kopf, 1995; Moos *et al.*, 1996; Day *et al.*, 2000), but not previously in the same series of experiments. Here we have measured kinase activities and monitored the cessation of  $\text{Ca}^{2+}$  oscillations after fertilisation in order to examine the relationship in more detail. CDK1-cyclin B and MAPK activities were measured in unfertilised eggs, in eggs that had extruded the second polar body (2 hours after insemination) and after pronucleus formation (4-6 hours after fertilisation). The activities of CDK1-cyclin B and MAPK were highest in unfertilised eggs. After polar body formation, CDK1-cyclin B activity was reduced to about 10-15% of that of the unfertilised egg while MAPK activity remained at pre-fertilisation levels (inset Figure 6.1A). After pronucleus formation, CDK1-cyclin B activity remained at 10% and MAPK activity had also declined to 10% of unfertilised levels (inset Figure 6.1A). Thus, similar to previous studies we show that CDK1-cyclin B activity declines about the time of second polar body extrusion while MAPK activity decreases around the time of pronucleus formation.

To monitor the time that the sperm-induced  $\text{Ca}^{2+}$  transients ceased, we recorded intracellular  $\text{Ca}^{2+}$  while examining, by using two techniques, the time of pronucleus formation. Firstly, we used bright field images every 10-15 minutes to view the pronucleus (Figure 6.1A, Bi, C). The second approach involved the use of a fluorescent nuclear-targeted marker, FITC-NLS-BSA. This peptide enters the nucleus from the very early stages of nuclear formation, being

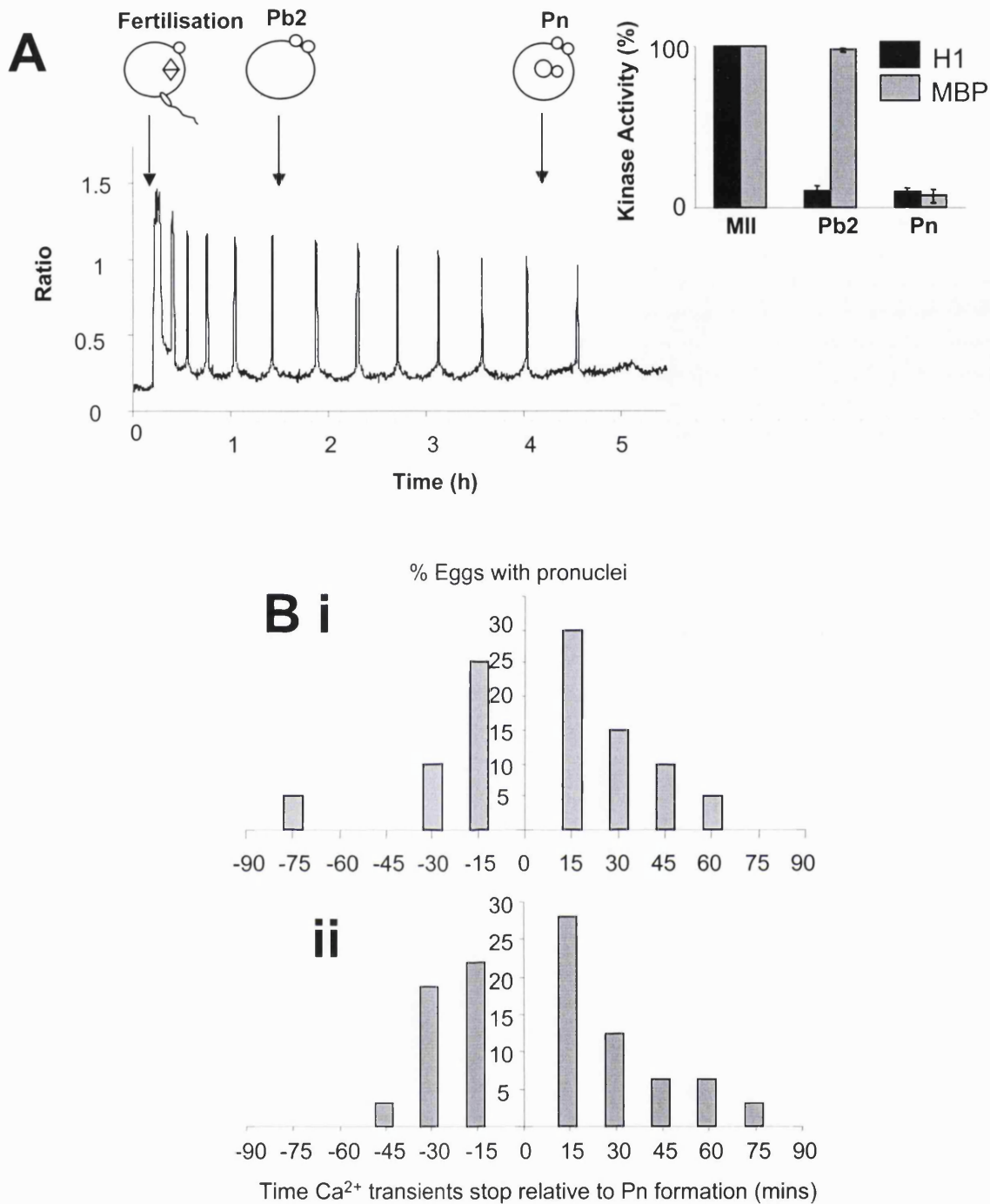


**Figure 6.1 The correlation between  $Ca^{2+}$  transients, Cdk1-cyclin B, MPF and MAPK activities and pronucleus (Pn) formation.**

(A) Fertilisation stimulates a series of  $Ca^{2+}$  transients that persist for about 4 hours, stopping close to the time of pronucleus formation. The schematics show the state of the eggs during the time course of the  $Ca^{2+}$  oscillations, CDK1-cyclin B activity was determined by measuring H1-kinase activity and MAPK activity by measuring phosphorylation of myelin basic protein (MBP). Kinase activities were recorded in unfertilised oocytes arrested at MII, in fertilised eggs that had extruded the second polar body (Pb2) within 2 hours of insemination and after Pn formation 4-6 hours after insemination. Data are from two experiments each with two replicates. Data are normalized to 100% activity in unfertilised eggs. The time that the  $Ca^{2+}$  oscillations stopped relative to the time of Pn formation is shown in Bi ( $n=20$ ) and Bii ( $n=18$ ). The zero time point is defined as the point at which the pronuclei were visible under bright-field observation (Bi) or by accumulation of FITC-NLS-BSA (Bii). (C-following page) Fluorescent images of FITC-NLS-BSA (left column) and bright-field images (right column) illustrating the assessment of Pn formation. The sperm fusion site, or fertilisation cone, can be seen in the first bright-field image (arrow). The first evidence of Pn formation is evident in the FITC-NLS-BSA image (arrows, Cii). The first evidence of pronuclei in the bright field optics is some 20 minutes later (arrow, Civ).

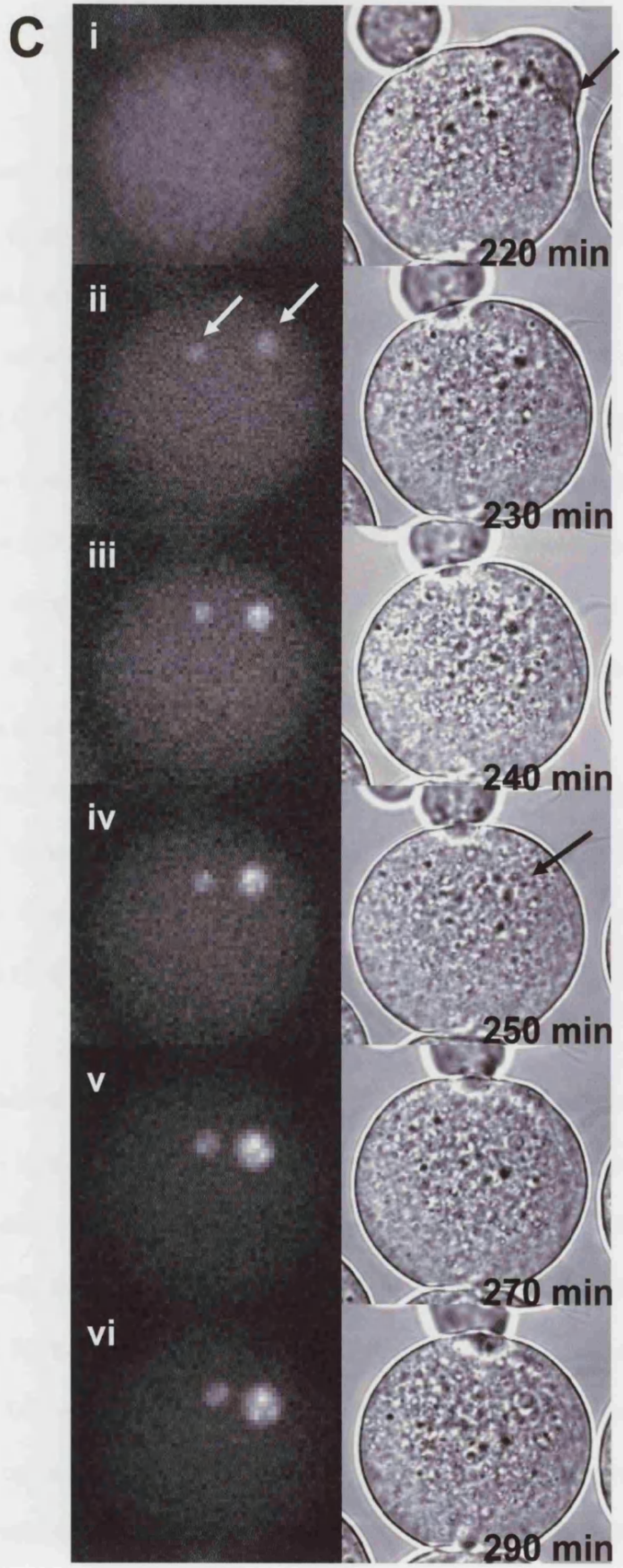


Figure 6.1 continued

more accurate and allowing the simultaneous imaging of  $\text{Ca}^{2+}$  transients and pronucleus formation (Figure 6.1Bii, C). This technique reported pronucleus formation 15-20 minutes earlier than bright-field microscopy (Figure 6.1C). Both techniques, however, revealed that in the 15 minutes either side of pronucleus formation 50-55% of fertilised eggs stopped generating  $\text{Ca}^{2+}$  transients while at 30 minutes the proportion reached 80%. The window of 30 minutes is not long if considering that the mean interspike interval between the last two oscillations is  $29 \pm 7$  minutes (Figure 6.1B). In both techniques, only 2 of 38 eggs stopped oscillating more than 30 minutes before pronucleus formation, while in the FITC-NLS-BSA technique, only 4 of 18 eggs showed two transients and 1 of 18 three, after the first signs of pronucleus formation.

The finding that  $\text{Ca}^{2+}$  oscillations cease in a window either side of pronucleus formation is consistent with previous observations (Day *et al.*, 2000). The close association between pronucleus formation and the cessation of  $\text{Ca}^{2+}$  transients correlates with MAPK activity rather than CDK1-cyclin B.

### **6.2.2 Inhibition of MAPK activity has no effect on $\text{Ca}^{2+}$ oscillations**

In order to investigate the effect of MAPK on the fertilisation-induced  $\text{Ca}^{2+}$  oscillations we used the MEK inhibitor UO126 (Duncia *et al.*, 1998; Favata *et al.*, 1998; Gross *et al.*, 2000). The eggs were incubated in the inhibitor for one hour prior to fertilisation. At that point, eggs were used for kinase assays for determining the effect of the drug on CDK1-cyclin B and MAPK. CDK1-cyclin B1 was not affected, but MAPK was severely inhibited with its activity dropping to about 10-15% from the maximum level (Figure 6.2A). Kinase assays during fertilisation showed that CDK1-cyclin B activity dropped at about the time of second

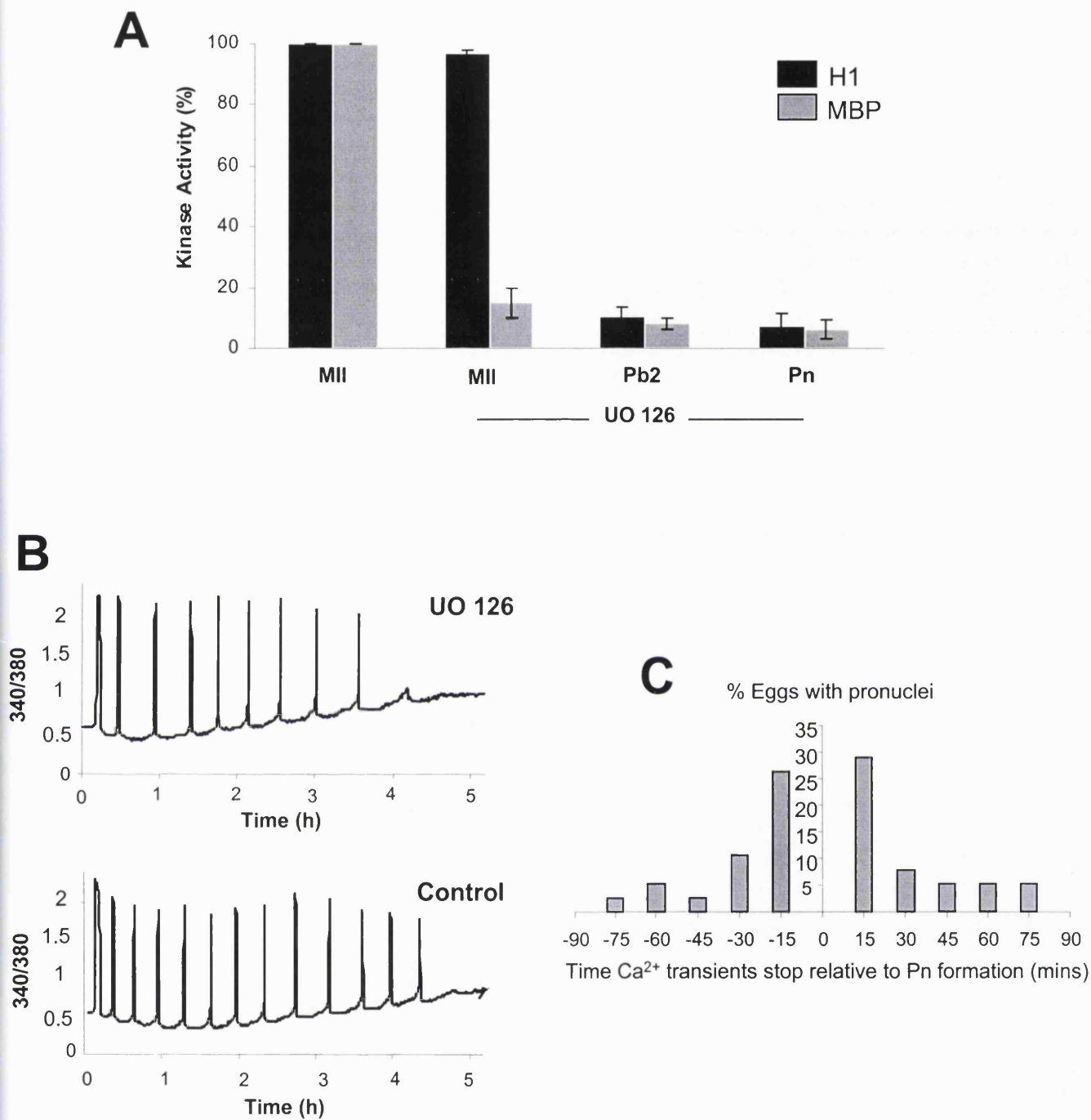


**Figure 6.2 Inhibition of MAP-kinase activity does not inhibit Ca<sup>2+</sup> oscillations.** Treatment with UO126 inhibited MAPK activity in MII eggs and maintained low levels of MAPK up until Pn formation when it would normally decline. Kinase assays as for Figure 6.1. Ca<sup>2+</sup> oscillations in UO126-treated eggs ( $n=38$ ) were similar to controls (B). The cessation of oscillations correlated tightly with Pn formation (C) (compare with Figure 6.1C, see Table 6.1).



polar body extrusion, both in controls and UO126-treated eggs. At fertilisation, MAPK activity did not rise when the eggs remained in UO126 (Figure 6.2A).

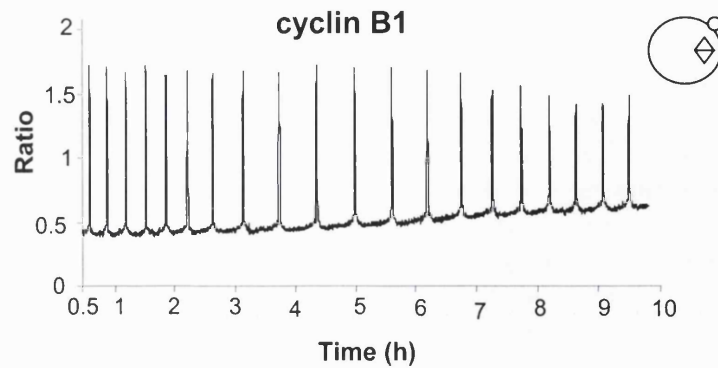
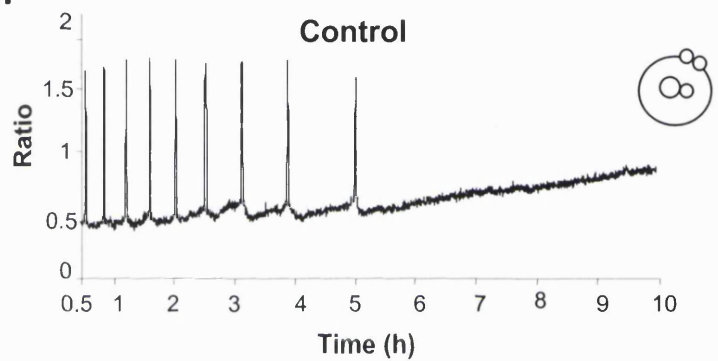
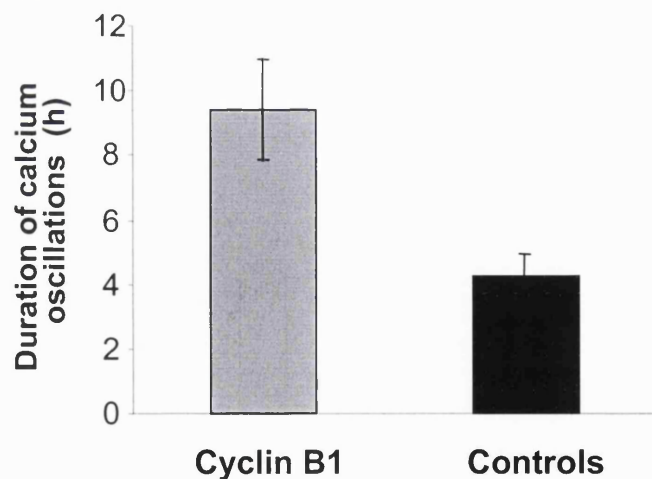
Fertilised eggs, treated with UO126, were monitored to measure the effect of MAPK inhibition of  $\text{Ca}^{2+}$  oscillations. The oscillations were initiated in the same way as in controls and they continued until the time of pronucleus formation although MAPK kinase was inhibited (Figure 6.2B). Similar to controls (see Figure 6.1Bi), 55% of the eggs stopped oscillating 15 minutes either side of pronucleus formation and 74% within 30 minutes (Figure 6.2C; Table 6.1). These experiments showed that MAPK is not responsible for the generation or cessation of the fertilisation-induced  $\text{Ca}^{2+}$  oscillations.

### **6.2.3 Injection of cyclin B1-GFP can lead to persistent $\text{Ca}^{2+}$ oscillations**

The experiments described previously show that the two major meiotic kinase activities, CDK1-cyclin B and MAPK are not responsible for the maintenance of the sperm-induced  $\text{Ca}^{2+}$  oscillations at fertilisation. In a first glance, this seems contradictory to the fact that maintaining high levels of the activities and thus meiotic arrest, by treating fertilised eggs with nocodazole, leads to long-lasting oscillations (Jones *et al.*, 1995). In order to confirm that this effect is not specific to the drug, we micro-injected cyclin B1-GFP in eggs prior to fertilisation and monitored the duration of the  $\text{Ca}^{2+}$  oscillations. The injected eggs did not extrude a second polar body or form pronuclei indicating that meiotic arrest is established by high levels of CDK1-cyclin B activity (as indicated in the schematic diagrams in Figure 6.3A). In addition, the oscillations show a pattern similar to that seen with nocodazole and they last for a mean time of  $9.5 \pm 1.5$  hours (n=15) compared to  $4.2 \pm 0.5$  hours in controls

**Table 6.1 The relationship between pronucleus formation and the time when sperm induced Ca<sup>2+</sup> oscillations stop**

	n	% of eggs that stop oscillating (time from Pn formation)	
		± 15 min	± 30 min
Control	20	55	80
UO 126	38	55.2	73.6
CHX	17	47	82.2
Cyclin B1-GFP	15	0	0
WGA	16	0	0

**A i****ii****B**

**Figure 6.3** Injection of excess cyclin B1-GFP leads to long-lasting  $\text{Ca}^{2+}$  oscillations. Cyclin B1-GFP fusion protein was microinjected into eggs prior to monitoring  $\text{Ca}^{2+}$  at fertilisation. Cyclin-injected eggs produced long-lasting  $\text{Ca}^{2+}$  oscillations at fertilisation (A). The schematic diagrams show the state of the eggs under bright-field observation. Cyclin-injected eggs showed no sign of second polar bodies or pronuclei (A). The duration of  $\text{Ca}^{2+}$  signalling in cyclin-injected eggs ( $n=15$ ) is significantly longer than in controls ( $n=18$ ) (B). Data show the mean $\pm$ s.d.

(mean  $\pm$  s.d.; n=18; P < 0.001) (Figure 6.3). This shows that exogenous cyclin B supports the maintenance of Ca<sup>2+</sup> oscillations at fertilisation (Table 6.1).

#### **6.2.4 Low cycling levels of CDK1-cyclin B can not explain the maintenance of Ca<sup>2+</sup> transients**

Cyclin B synthesis is responsible for the maintenance of high CDK1-cyclin B activity and meiotic arrest in MII eggs (Kubiak *et al.*, 1993). Although there is a degree of cyclin B destruction, this destruction is controlled and restrained by the Mos/MAPK pathway so that CDK1-cyclin B retains its high levels of activity (Hashimoto *et al.*, 1994; Colledge *et al.*, 1994).

After Pb2 extrusion, there is the possibility that continuous cyclin B synthesis in the presence of MAPK, may lead to a low level of CDK1-cyclin B activity responsible for the maintenance of Ca<sup>2+</sup> oscillations. To test this hypothesis, we incubated fertilised eggs in the protein synthesis inhibitor cycloheximide (CHX) (Moses and Kline, 1995; Moos *et al.*, 1996) and monitored the Ca<sup>2+</sup> oscillations in the absence of any cyclin B synthesis. The effectiveness of the drug was confirmed by its ability to cause parthenogenetic activation of aged MII eggs (80%; not shown). The treatment of eggs that had extruded Pb2, with CHX did not affect the correlation of Pn formation with Ca<sup>2+</sup> oscillations. 47% stopped oscillating 15 minutes either side of Pn formation and 82% at 30 minutes (Figure 6.4A; Table 6.1).

We also used a second approach to identify the possibility of low cycling levels of CDK1-cyclin B activity to maintain the sperm-induced Ca<sup>2+</sup> transients after Pb2. If the activity is cycling, its levels being elevated prior to each oscillation, it is expected that it could be possible to identify the level of the activity, if a large number of eggs was

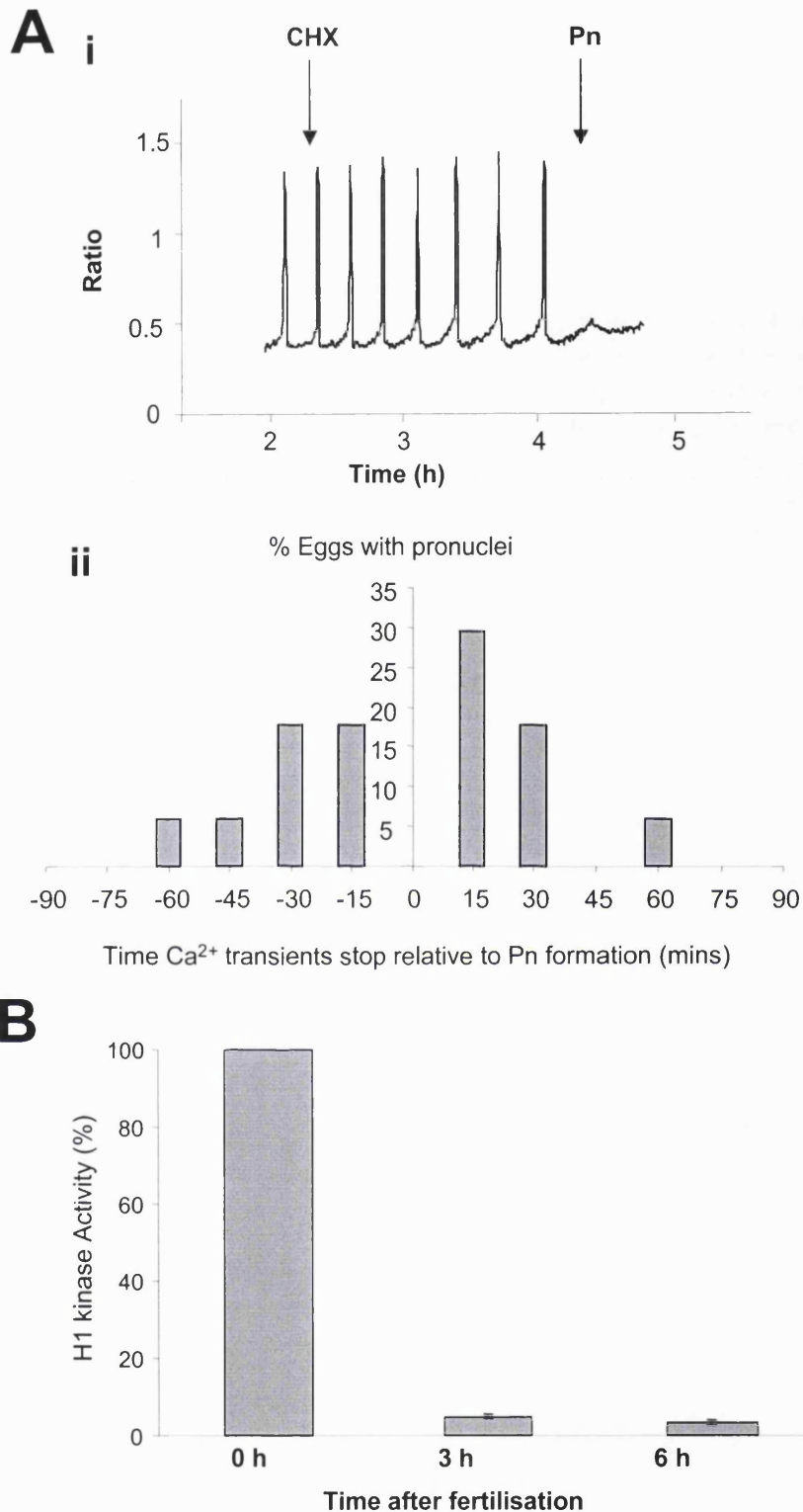


**Figure 6.4 Low levels of CDK1-cyclin B activity do not explain persistent  $\text{Ca}^{2+}$  oscillations after extrusion of the second polar body.** To inhibit cyclin synthesis after polar body extrusion, cycloheximide (CHX) was added to eggs 90 minutes after fertilisation. In the presence of CHX,  $\text{Ca}^{2+}$  transients were generated as in controls (Ai). The time that the  $\text{Ca}^{2+}$  oscillations stop relative to Pn formation is shown in Aii ( $n=17$ ). Note that the distribution is similar to that shown for controls in Figure 6.1Bii (see also Table 6.1). CDK1-cyclin B activity was measured in groups of 50 unfertilised eggs and in eggs 3 hours after fertilisation that had extruded a second polar body and 6 hours after fertilisation when they had formed pronuclei. Data are from two experiments, each with two replicates. No significant difference in CDK1-cyclin B activity is seen before and after Pn formation (B).

examined. Thus, we assayed samples of 50 eggs for their kinase activity levels expecting to identify possible differences before and after Pn formation. We found that CDK1-cyclin B levels immediately after Pb2 extrusion when MAPK activity is high were similar to the levels measured after Pn formation when MAPK is low (Figure 6.4B). These results imply that the hypothesis of oscillating levels of CDK1-cyclin B activity after Pb2 extrusion is unlikely to explain the maintenance of  $Ca^{2+}$  transients until Pn formation.

### **6.2.5 Inhibition of pronucleus formation leads to persistent $Ca^{2+}$ oscillations**

From the previous experiments, we have shown that maintaining high levels of the meiotic kinase activities causes long-lasting  $Ca^{2+}$  oscillations. However, the inhibition of CDK1-cyclin B or MAPK does not lead to premature cessation of the transients. Instead, under all the different conditions used in our work, the timing of the cessation of the oscillations seemed to coincide with the formation of the pronucleus. Thus, we examined the effect of Pn formation on the oscillations. In order to investigate the role of Pn formation, we microinjected eggs, prior to fertilisation, with wheat germ agglutinin (WGA). WGA binds to nucleoporins, thus inhibiting nuclear import in cells with an intact nucleus (Yoneda *et al.*, 1987; Newmeyer and Forbes, 1988; Vautier *et al.*, 2001) and blocking Pn formation in bovine eggs (Sutovsky *et al.*, 1998). In our experiments, WGA injection in mouse eggs (Figure 6.5A), inhibited Pn formation but did not affect Pb2 extrusion or the normal timecourse of inactivation M-phase kinases (Figure 6.5B). In this way, it was possible to determine the role of the Pn formation independently of the activities of CDK1-cyclin B and MAPK. Monitoring  $Ca^{2+}$  oscillations during fertilisation, showed that in WGA injected eggs, the inhibition of Pn formation leads to persistent  $Ca^{2+}$  transients although the M-phase kinases

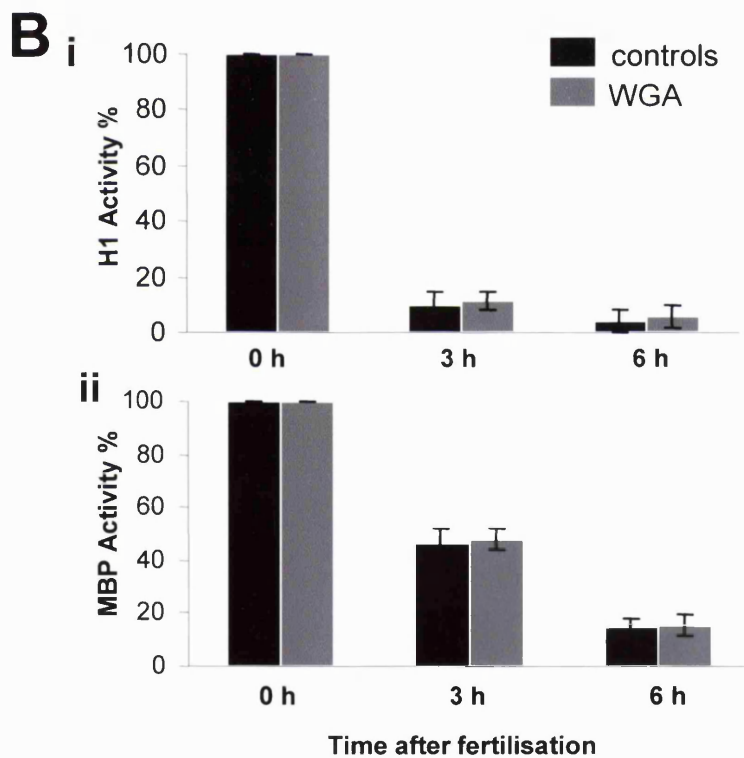
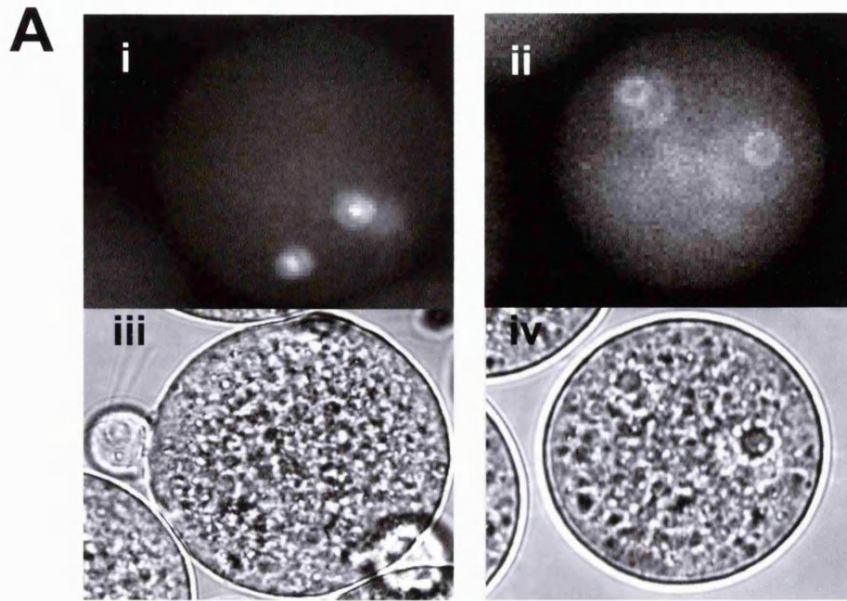


**Figure 6.5 Inhibition of Pn formation leads to persistent  $Ca^{2+}$  oscillations after inactivation of CDK1-cyclin B and MAPK.** Microinjection of WGA inhibits Pn formation in mouse oocytes (A). Hoechst (i and ii) and Bright field images (iii and iv) of WGA-injected (i and iii) and uninjected (ii and iv) eggs are shown 6 hours after fertilisation. Note the lack of any discernable pronuclei in WGA-injected eggs. CDK1-cyclin B (Bi) and MAPK (Bii) activity declines at fertilisation with similar kinetics in WGA-injected (grey columns) and control eggs (black columns). Data are from two experiments, each with two replicates. Fertilisation of WGA-injected eggs leads to persistent  $Ca^{2+}$  oscillations ( $n=16$ ) (Ci) that last significantly longer than controls ( $n=13$ ) (Cii, D). Data show the mean $\pm$ s.d.

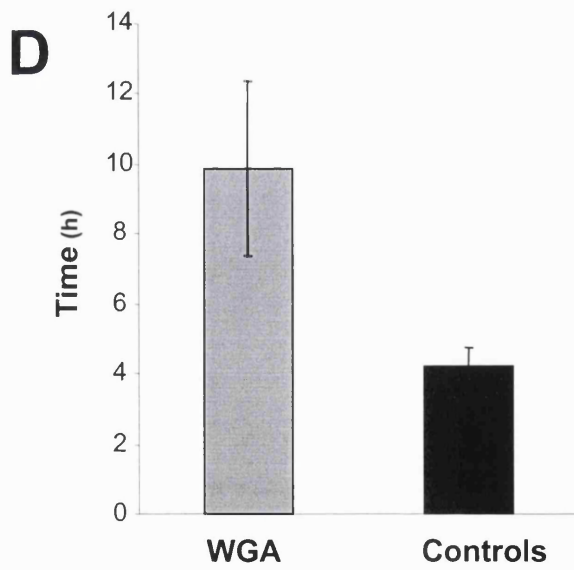
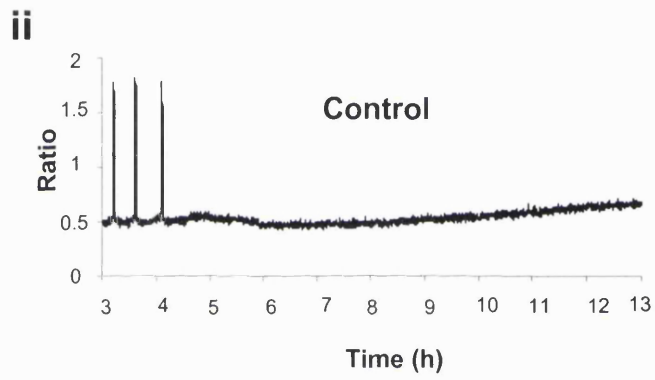
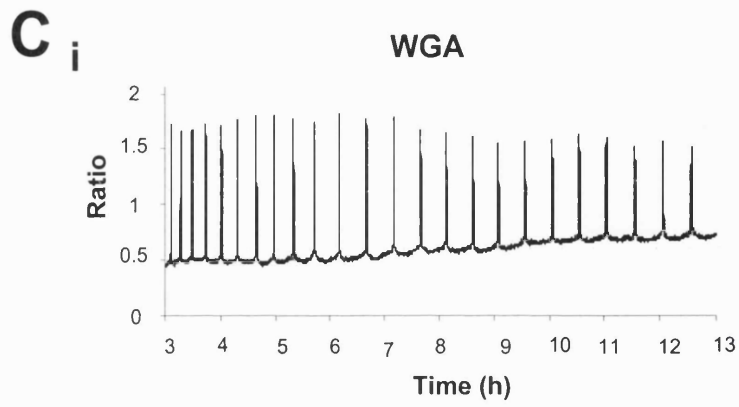


Figure 6.5 continued



are inactive. The oscillations lasted for an average of  $9.9 \pm 2.5$  hours (n=16) compared to  $4 \pm 0.5$  hours in controls (mean  $\pm$  s.d; n=13;  $P < 0.01$ )(Figure 6.5 C,D). The result indicates that Pn formation plays the major role in controlling the cessation of sperm-induced  $\text{Ca}^{2+}$  oscillations.

### **6.2.6 Inhibition of importin $\beta$ -mediated nuclear transport leads to prolonged generation of $\text{Ca}^{2+}$ transients**

The continuation of the  $\text{Ca}^{2+}$  oscillations by Pn formation inhibition supports the hypothesis that during fertilisation, factors necessary for the generation of the oscillations enter the pronuclei during their formation causing the subsequent cessation of the  $\text{Ca}^{2+}$  transients. To further test this hypothesis we used a more specific inhibitor than WGA, importin  $\beta^{45-462}$  (Kutay *et al.*, 1997). This is a mutant form of importin  $\beta$  that competes with the wild type form for binding to the nuclear pore complex, thus inhibiting nuclear import (Kutay *et al.*, 1997). Microinjection of importin  $\beta^{45-462}$  causes either the formation of rudimentary Pns or complete inhibition. This effect leads to persistent oscillations, lasting for a mean duration of  $12.5 \pm 3.5$  hours (n=19) compared to  $3.8 \pm 0.3$  (n=12) for controls ( $P < 0.01$ ; Figure 6.6). These results suggest oscillation-generating factors must enter the pronucleus for the  $\text{Ca}^{2+}$  oscillations to stop.

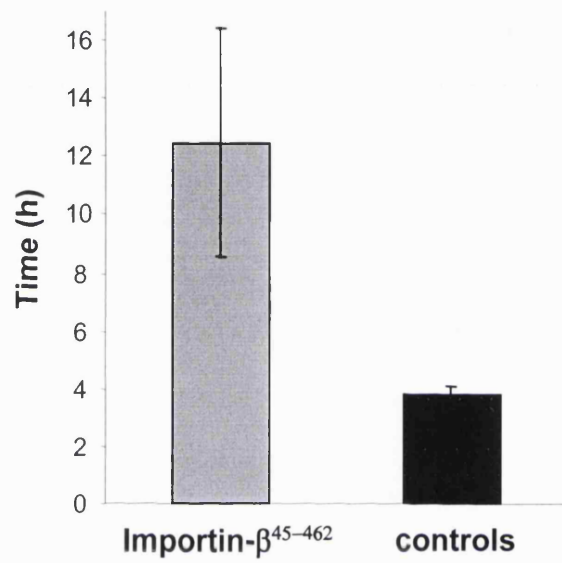


**Figure 6.6 Inhibition of importin  $\beta$ -mediated nuclear transport inhibits pronucleus formation and prolongs  $\text{Ca}^{2+}$  oscillations.** Oocytes were injected with dominant-negative importin  $\beta^{45-462}$  and fertilised to record the effects of inhibition of nuclear transport on  $\text{Ca}^{2+}$  oscillations at fertilisation. Importin  $\beta^{45-462}$ -injected eggs continued oscillating for nearly 12 hours, whereas controls stopped after 4 hours ( $P < 0.01$ ).

### 6.3 Discussion

In mammalian eggs, a possible involvement of M-phase kinases in  $\text{Ca}^{2+}$  oscillations regulation is supported by the effects of microtubule inhibitors (Jones *et al.*, 1995; Day *et al.*, 2000) and the effect of exogenous cyclin B (present study) on fertilisation and the temporal control of the oscillations. However, these treatments also block pronucleus formation. In our work we tried to disassociate the role of M-phase kinases and that of Pn formation. That was achieved by using treatments that may either disrupt M-phase kinase activities without blocking Pn formation, or inhibit Pn formation without affecting the physiological levels of the M-phase kinases. In this way, we managed to correlate the cessation of the  $\text{Ca}^{2+}$  oscillations with the timing of Pn formation, but not with the inactivation with CDK1-cyclin B or MAPK.

Firstly, we correlated the timing of Pn formation and  $\text{Ca}^{2+}$  cessation by using the FITC -NLS-BSA peptide. This molecule accumulates in the nucleus as soon as it is formed giving a more accurate indication of Pn formation than by analysing a bright-field image. We found that the oscillations stop within 30 minutes from Pn formation in 80% of the eggs. 30 minutes can be considered a significantly close timing since the time interval between the two last transients is 30-40 min. In addition, the presence of an abortive spike before the generation of  $\text{Ca}^{2+}$  transients stops completely indicates that the decrease in  $\text{Ca}^{2+}$ -realising activity is not a switch-like mechanism, but rather a gradual one, taking some time before total cessation. The slight variability in the timing of cessation of the oscillations can also be explained by the regenerative process of  $\text{Ca}^{2+}$  signalling,  $\text{IP}_3$  receptor degradation (Jellerette *et al.*, 2000; Brind *et al.*, 2000) and oocyte quality (Cheung *et al.*, 2000). As in the case of

experiments with exogenous cyclin B and spindle depolymerising agents however, in this experiment, it is not possible to disregard the fact that M-phase activities still exist.

Other studies have also tried to dissociate the effects of M-phase kinase activities and Pn formation at fertilisation by using a model system where eggs are bisected into nucleate and anucleate halves (Day *et al.*, 2000). These experiments showed that nucleate and enucleate halves stopped oscillating at about the same time implying that the appearance of Pns does not explain  $\text{Ca}^{2+}$  oscillations cessation. However, the similarity in the decrease in  $\text{Ca}^{2+}$  releasing activities could also be caused by perturbations in intracellular  $\text{Ca}^{2+}$  which are likely to result from embryo bisection, ER reorganisation (FitzHarris *et al.*, 2003), a decrease in the sensitivity of  $\text{IP}_3$ -induced  $\text{Ca}^{2+}$  release (Jones and Whittingham, 1996; Brind *et al.*, 2000; FitzHarris *et al.*, 2003) and the downregulation of  $\text{IP}_3$  receptors (Brind *et al.*, 2000; Jellerette *et al.*, 2000). In addition, since nuclear membranes form a tight membrane network by their association with the ER and mitochondria (Bavister and Squirrell, 2000), it is possible that a proportion of these organelles may remain in the enucleated halves, regulating their  $\text{Ca}^{2+}$ -releasing properties. Thus, we decided to address the possible effect of Pn formation on the timing of  $\text{Ca}^{2+}$  oscillations by using less invasive techniques.

We utilised two separate techniques to block nuclear transport and inhibit Pn formation directly. Based on the finding that WGA sequesters nuclear pore complexes and thus blocks bovine Pn formation (Sutovsky *et al.*, 1998), we microinjected this compound into mouse eggs. The dominant-negative importin- $\beta$  mutant was also used for the same purposes. We confirmed that both these molecules inhibit Pn formation in the mouse without affecting M-phase kinase activities. As in physiological conditions, CDK1-cyclin B was

inactivated by  $Pb2$  extrusion (Verhlaac *et al.*, 1994; Moos *et al.*, 1995; Schultz and Kopf, 1995) and MAPK activity was totally abolished six hours after fertilisation. Nevertheless, the  $Ca^{2+}$  oscillations persisted for much longer. This result demonstrates that Pn formation, and not M-phase kinase activities, is the key factor to determine  $Ca^{2+}$  oscillations cessation at fertilisation.

To support these results, we also investigated a role for the M-phase kinases. We inhibited MAPK activity by using UO126 and found that there were no changes on the  $Ca^{2+}$ -releasing activity of the eggs. These results confirm the conclusions drawn from UO126 treatment of ascidian eggs where MAPK inactivation does not inhibit the  $Ca^{2+}$  oscillations at fertilisation (McDougall and Levasseur, 1998; Levasseur and McDougall, 2000). The other M-phase kinase, CDK1-cyclin B, is inactivated at the time of  $Pb2$  extrusion, but it has been implied that low or oscillating levels of the kinase may still exist for longer (Nixon *et al.*, 2000; Levasseur and McDougall, 2000; Carroll, 2001). We assayed large samples of mouse eggs for CDK1-cyclin B activity but were unable to detect any level of activity. Meanwhile, treatment of fertilised eggs with CHX or UO126 did not result in cessation of  $Ca^{2+}$  oscillations. This means that inhibition of cyclin B synthesis and of MAPK, which stabilises CDK1-cyclin B, can not stop the  $Ca^{2+}$  oscillations independently of Pn formation. Thus, in mammals, Pn formation is the cause for the cessation of the fertilisation-induced  $Ca^{2+}$  oscillations, while the role of the M-phase kinases is limited to determining the time of Pn formation.

These results are contradictory to the observations in ascidian eggs where the oscillations are tightly coupled to CDK1-cyclin B activity (Levasseur and McDougall, 2000).

In addition, in ascidian eggs the first wave of oscillations stops at the MI/MII transition where there are no nuclear membranes present (McDougall and Levasseur, 1998). The differences between mammals and ascidians may lie in species-specific differences in the mechanisms regulating the sperm-derived  $\text{Ca}^{2+}$ -releasing activity. In ascidian fertilisation, since there is no change in the sensitivity of  $\text{IP}_3$ -induced  $\text{Ca}^{2+}$  release during MI/MII, CDK1-cyclin B must control  $\text{IP}_3$  production. However, the cessation of the second wave of  $\text{Ca}^{2+}$  oscillations may be attributed to a desensitisation of  $\text{IP}_3$ -induced  $\text{Ca}^{2+}$  release caused by the loss of CDK1-cyclin B activity (McDougall and Levasseur, 1998; Levasseur and McDougall, 2000). In mammals, this desensitisation occurs at about the time of Pn formation and is probably caused by oocyte ageing (Jones and Whittingham, 1996; Brind *et al.*, 2000). Nevertheless, it has been shown that CDK1-cyclin B controls the oocytes' sensitivity to  $\text{IP}_3$ -induced  $\text{Ca}^{2+}$  release, since loss of the kinase causes desensitisation (FitzHarris *et al.*, 2003). Thus, the kinase may play an indirect role in stopping  $\text{Ca}^{2+}$  oscillations. All these observations lead to the conclusion that the cessation of  $\text{Ca}^{2+}$  oscillations in mammalian fertilisation, is predominantly controlled by Pn formation, but additional factors such as  $\text{IP}_3$  receptor downregulation (Brind *et al.*, 2000) and cell cycle-dependent desensitisation of  $\text{IP}_3$ -induced  $\text{Ca}^{2+}$  release also constitute to the precise time that the oscillations stop in any one egg.

## **7. Conclusions**

The central theme of this work is the understanding the regulation of meiosis during oocyte maturation and fertilisation. We investigated meiosis in living and fixed mouse oocytes by the use of GFP fusion proteins and imaging techniques. This study provides a number of points for discussion:

1. Advantages and limitations from the use of fluorescent probes.
2. Spatial regulations of meiotic events.
3. Differential regulation of MI and MII.
4. Nuclear sequestration of a PLC- a new way of regulating  $Ca^{2+}$ .

### **7.1 Using cyclin B1-GFP to monitor cyclin B levels in oocytes and eggs.**

In this work we have used cyclin B1-GFP protein to address a number of questions. Firstly, the chimeric protein was used for monitoring the level of cyclin B degradation in live grown oocytes undergoing maturation, but also MII arrested eggs at rest and during fertilisation or parthenogenetic activation. Unlike immunofluorescence, the use of the GFP-tagged protein allows the monitoring of the protein in single living oocytes undergoing maturation or fertilisation. This provides a means of studying dynamic events in relation to the developmental processes that the proteins under examination are involved in. In addition, possible artefacts produced by the fixing process during immunofluorescence can be

surpassed by the use of GFP technology. Furthermore, there has not been to be reliable immunofluorescence observations of cyclin B in mouse oocytes. In our laboratory, immunofluorescence experiments using different cyclin B primary antibodies were unsuccessful. During the course of my studies, Ledan and co-workers (2001) monitored cyclin B synthesis and destruction in mouse oocytes undergoing maturation by the use of cyclin B1-GFP mRNA. This study and the ones presented in this thesis (chapters 3 and 4) are complimentary and the use of recombinant protein provides a more quantitative means of determining the effects of cyclin B1-GFP on the cell cycle.

One disadvantage of using cyclin B1-GFP was shown to be its effects on the kinetics of cyclin B destruction since higher levels inhibit the extrusion of both Pb1 (chapter 3) and Pb2 (chapter 6). Apparently, the APC is not capable of degrading all the injected protein causing an inhibition of chromosome segregation in both meiotic divisions. Thus, the presence of an APC substrate at too high a concentration can affect the normal progression of meiosis. To bypass the problems caused by high levels of cyclin B1-GFP when monitoring the progression of oocyte maturation and fertilisation, we microinjected at least 5-fold less of the marker in oocytes or eggs.

The use of limiting levels of GFP revealed another potential problem. Low levels of cyclin B1-GFP allowed normal progression through meiotic events but it became clear that autofluorescence was interfering with the GFP signal (in chapter 4). It is well documented that these signals may overlap (Zernicka-Goetz and Pines, 2001), but as long as the autofluorescence signal remains stable, as it does during meiotic maturation, the GFP signal provides reliable observations. During fertilisation, however, we discovered a series of oscillations in the autofluorescence signal that mirrors the  $\text{Ca}^{2+}$  oscillations. These



oscillations seem to originate from the mitochondria and reflect the changes in FAD<sup>+</sup> metabolism during mouse egg fertilisation (Dumollard *et al.*, 2004, *Development*, In press). Thus, studying the kinetics of cyclin B destruction using low levels of cyclin B1-GFP, at fertilisation, has resulted to the mistaken conclusion that cyclin B destruction is stepwise (Nixon *et al.*, 2002). Revealing that the steps in cyclin B destruction are a result of autofluorescence provides a different view on the mechanisms of cyclin B destruction. In addition, this observation has opened a new area of research on the activation of mitochondrial respiration at fertilisation.

Our work shows that in any cell type, the use of a new fluorescent probe needs extensive characterisation to ensure (1) that the signal is a true reflection of the behaviour of the probe and (2) that the probe does not interfere with the normal progression of the cell cycle.

Dv  
Dv

## 7.2 Spatial regulation of meiosis

Previously, we discussed the changes of cyclin B concentration during meiosis which reflect the temporal regulation of the cell cycle. Our results, however, show that the mammalian meiotic cell cycle is also controlled by the spatial organisation of cell cycle proteins.

### 7.2.1 Spatial control of M-phase entry

In chapter 3 we show that cyclin B enters the GV after release from prophase arrest accumulating in the nucleus prior to GVBD. This result verifies that observed in somatic cells (Pines and Hunter, 1991; Hagting *et al.*, 1998; Huang and Raff, 1999) and implies that

the compartmentalisation of proteins whose activation or inactivation is necessary for the G2/M transition in mitosis like Cdc25, Wee1 and Myt1 also occurs in meiosis.

It is well established by now that CDK1-cyclin B is activated in the cytoplasm in many cell systems (Peter *et al.*, 2002b; Jackman *et al.*, 2003). In the cytoplasm CDK1-cyclin B is thought to be activated at the centrosomes (Jackman *et al.*, 2003) by the cytoplasmic isoform of Cdc25, Cdc25B. The cyclin partner is then both autophosphorylated (Borgne *et al.*, 1999) or phosphorylated by other kinases, like Plk1 (Toyoshima *et al.*, 2001). Cyclin B phosphorylation causes the translocation of the active complex to the nucleus raising the intra-nuclear concentration of CDK1-cyclin B. This eventually leads to the saturation of Wee1 and activation of Cdc25C, the nuclear isoform of Cdc25, through the positive feedback action of CDK1-cyclin B leading to a 'switch-like' (Ferrell, Jr., 1998) activation of CDK1-cyclin B that will induce GVBD.

The big question concerning GVBD is the delay between the time of release from the arresting agent (dbcAMP or IBMX) and the timing of GVBD. In the mouse this delay is 1.5-2 hours. This delay can partly be attributed to the time that is needed for CDK1-cyclin B to saturate the GV and induce GVBD. However, there is also an initial delay between the time of release from arrest and the beginning of cyclin B import in the GV. This was observed after the microinjection of cyclin B1-GFP in GV-stage oocytes. Cyclin B1-GFP entry in the GV is not seen until 20-30 minutes after release from arrest. One possible reason for this delay may be that the disappearance of cAMP in the oocyte does not occur immediately after release, leading to a delayed inactivation of the cAMP/PKA pathway that is thought to be responsible for the prophase arrest (Mehlmann *et al.*, 2002). In addition, there may be a

✓ D  
can't  
be  
spread  
up by  
nuclear

✓

threshold that needs to be overcome in the level of activation of Cdc25 and/or other cell cycle regulators that induce the activation of CDK1-cyclin B.

Our results showing that excess cyclin B induces CDK1-cyclin B activation suggests that cyclin B may be limiting in the initiation of GVBD. However, the resumption of meiosis and progression to GVBD under conditions where protein synthesis is inhibited (Clarke and Masui, 1983; Hashimoto and Kishimoto, 1988) and the finding that cyclin B is 7-fold in excess of CDK1 (Kanatsu-Shinohara *et al.*, 2000) suggests that there is abundant endogenous cyclin B. One explanation for the sensitivity to excess cyclin B may be that the protein is sequestered in the cytoplasm. Evidence for such sequestration has been reported in starfish oocytes where the resumption of meiosis is accompanied by the dispersal of cyclin B aggregates (Terasaki *et al.*, 2003).

### **7.2.2 Spatial control of protein degradation during exit from M-phase**

Unfortunately, immunolocalisation of endogenous cyclin B in mammalian oocytes at metaphase I has not been particularly successful so it is difficult to speculate on its localisation at that stage. From our experiments, however, we find that cyclin B1-GFP remains concentrated on the chromatin after GVBD (chapter 3). This localisation appears to be lost soon after GVBD (data not shown). In addition, we also find that microinjection of cyclin B1-GFP in metaphase I or II causes its localisation on the chromosomes. Although this localisation is transient, it is indicative of the affinity of chromatin to cyclin B binding and, most possibly, of a higher rate of cyclin B destruction at the spindle area. This implies that there is spatial regulation of cyclin B destruction during meiotic metaphase. In somatic

cells, this was shown to be true by Clute and Pines (1999). They found that cyclin B is initially destroyed at the spindle and subsequently at the cytoplasm.

This spatial control of cell cycle protein degradation may imply that there is specific localisation of the cell's destruction machinery, the APC<sup>CDC20</sup> or its regulators during M-phase. It has been shown that the APC activator Cdc20 is predominantly localised at the spindle area (Kallio *et al.*, 1998). This possibly reflects that the initiation of APC activation and cyclin B and securin destruction occurs at the spindle. Thus, it is not surprising that APC regulators that sequester Cdc20, like Mad2, are also localised at the spindle area (Howell *et al.*, 2000). Stronger APC inhibition may be provided by the specific localisation of other APC regulators. In chapter 5 we see that Emi1, an APC regulator, is cytoplasmic with strong localisation at the area surrounding the spindle. Thus, the localisation of APC regulators at the regions where APC components and activators are found, makes certain that the APC remains inactive until the conditions are optimal for activation.

Unlike Mad2, however, Emi1 localisation changes gradually at anaphase from the peri-spindle area to the microtubules of the spindle poles and the midbody (chapter 5). The differential localisation of this APC inhibitor during the cell cycle may provide a means for the spatial regulation of the destruction of different cell cycle proteins during M-phase. Thus, prior to the onset of M-phase, when cyclin B and securin destruction must be inhibited, Emi1 localises around spindle. At entry to M-phase, Emi1 relocates to specific areas like the midbody which may serve to protect other proteins from being destroyed. Plk1, for example, which is important for cytokinesis, is localised at the midbody during telophase in mouse oocytes undergoing maturation (Tong *et al.*, 2002). Since Plks are destroyed in an APC-dependent manner (Shirayama *et al.*, 1998; Charles *et al.*, 1998), it may be necessary that they

are protected from destruction by a localised inhibitor at the midbody region, while APC activity is enabled in other regions of the cell where other cell cycle proteins must be degraded. Thus, the differential localisation of Emi1 may provide the answer to the question of how some proteins are destroyed, while others remain active during M-phase, even if their degradation is controlled by the same destruction pathway. Direct experiments to test this possibility will be an exciting area of research in the future. ← know?

## 7.3 Differential regulation of MI and MII

### 7.3.1 Regulation of MII arrest

There are significant differences between MI and MII of the meiotic cell division. In MI, as we have discussed already, the spindle assembly checkpoint (SAC) does not allow progression to anaphase and degradation of cyclin B and securin until all the chromosomes are aligned at the metaphase plate. When the chromosomes align, the APC binds its activator, Cdc20, which is released from the SAC proteins. APC activation and subsequent proteolytic degradation of its substrates occurs spontaneously after alignment without any exogenous stimulus (Brunet *et al.*, 1999). This is not the case, however, in MII. The egg remains arrested at MII, although all the chromosomes are aligned at the metaphase plate. CSF activity is responsible for this arrest and is only present in MII eggs. The experimental evidence for the specificity of CSF to MII is provided by the finding that CSF activity, as assayed by the ability to arrest blastomeres in metaphase, only appears in mouse oocytes around the time of Pbl formation (Ciemerych and Kubiak, 1998). CSF activity seems to be regulated by the co-operative action of the Mos/MAPK pathway and other pathways that

may involve Mad1, Emi1 or other, yet unidentified factors. A number of factors, like Mos, MAPK, Rsk, CDK2-cyclin E, and Bub1 are able to establish CSF activity and M-phase arrest (Sagata *et al.*, 1989b; Haccard *et al.*, 1993; Gross *et al.*, 1999; Tunquist *et al.*, 2002). The mos/MAPK pathway, however, Mad1 and Emi1 are the only pathways from those examined so far that have the ability to sustain CSF activity since their depletion can cause spontaneous activation in the absence of Ca<sup>2+</sup> release (Phillips *et al.*, 2002; Reimann and Jackson, 2002; Tunquist *et al.*, 2003). These proteins, however, are also present in MI. Nevertheless, MAPK, Emi1 and Mad1 do not cause arrest at MI after chromosome alignment as in MII. MI oocytes undergo cell division and the APC is activated spontaneously after chromosome alignment, while MII eggs remain arrested and the APC inactive until fertilisation. This raises the question of why they do not provide CSF activity in MI. It is possible that in MI oocytes some components of the CSF activity may not be present. These yet unknown components may be synthesised or activated during the transition from MI to MII. Otherwise, the absence of CSF in MI could be attributed to inhibitors of the already existing components of CSF. Furthermore, the activation of the APC<sup>Cdc20</sup> complex may be regulated by a yet unidentified activator, which is released after chromosome alignment in MI, but inactivated during Pbl extrusion. Dv

### 7.3.2 Differential sensitivity to Ca<sup>2+</sup>

The other major difference between the two meiotic metaphases is that although MII is released by intracellular Ca<sup>2+</sup> rises leading to the extrusion of a polar body, MI is not (chapter 4). However, one explanation is that the SAC is active at MI because the spindle is not complete at the time of Ca<sup>2+</sup> release. Otherwise, Ca<sup>2+</sup>-dependent APC regulation is MII-

specific, appearing after Pb1 extrusion around the same time as CSF activity. The fact that CSF appears at the same time as Ca<sup>2+</sup>-dependent APC activation and cyclin B degradation, raises the possibility that the CSF components that appear at Pb1 extrusion may also be responsible for the Ca<sup>2+</sup> sensitivity of the MII arrested state.

In a hypothetical model, a component of the Mos/MAPK pathway or a MAPK pathway-independent factor first appears at the time between anaphase I and metaphase II. This factor/s could have the ability to inhibit the APC through Cdc20 sequestration. This sequestration may then be relieved by the intracellular Ca<sup>2+</sup> rise caused by fertilisation. It is possible that Ca<sup>2+</sup>-induced activation of CaMKII at fertilisation (Lorca *et al.*, 1993; Lorca *et al.*, 1994) inhibits the interaction of the CSF component with Cdc20 thereby allowing APC activation. In our work we were intrigued to see whether Emi1 could be this factor since it is an APC inhibitor that releases Cdc20 at fertilisation after interaction with CaMKII. Reimann and Jackson (2002) have shown that Ca<sup>2+</sup> leads to dephosphorylation of Cdc20 which can explain the dissociation of Cdc20 from Emi1. Alternatively, Emi1 might be a target of CaMKII after Ca<sup>2+</sup>-induced activation since it contains one consensus CaMKII phosphorylation site. However, our work shows that not only is Emi1 present both in MI and MII, but has the same localisation in both meiotic cell cycles.

To conclude, the differences between the two M-phases in meiosis in respect to anaphase entry and polar body extrusion appear to be caused by an APC inhibitor. This protein is absent from MI and only appears in MII. It is either a part of the Mos/MAPK pathway or acts in concert with it to cause CSF arrest at MII. This factor may also provide the Ca<sup>2+</sup> dependence of APC activation at MII. Thus, in its absence, cyclins and securins are

destroyed as soon as the chromosomes are aligned at the metaphase plate. When this factor is present it enhances CSF activity and puts it under the direct control of intracellular  $\text{Ca}^{2+}$  release.

#### **7.4 The nuclear sequestration of a PLC may regulate $\text{Ca}^{2+}$ release in mouse eggs and embryos**

Differential localisation and compartmentalisation is a general phenomenon in meiosis and is not limited to cell cycle regulators. In chapter 6 we showed that sperm-induced  $\text{Ca}^{2+}$  oscillations at fertilisation cease because of pronucleus formation and not by the inactivation of the M-phase kinases, CDK1-cyclin B and MAPK. Work presented in this thesis and addition studies (Marangos *et al.*, 2003a) indicates that the initiation and cessation of the  $\text{Ca}^{2+}$  oscillations observed during the first two embryonic cell cycles (Kono *et al.*, 1996; Day *et al.*, 2000) also depend on the presence or not of a nucleus. In these experiments it was shown that a series of  $\text{Ca}^{2+}$  oscillations begins immediately after NEBD of the first mitosis. These oscillations are regulated similarly to those at fertilisation since they cease just prior to nucleus formation in the two cell embryo, not to reappear after NEBD of the second mitotic cell cycle (Marangos *et al.*, 2003b).

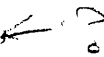
The cessation of the fertilisation-induced  $\text{Ca}^{2+}$  oscillations at pronucleus formation and their reappearance at NEBD of the first mitosis, together with the association of  $\text{Ca}^{2+}$ -releasing activity with pronuclei (Kono *et al.*, 1995; Zernicka-Goetz *et al.*, 1995; Kono *et al.*, 1996) suggest a model for the regulation of  $\text{Ca}^{2+}$  signalling at fertilisation (Figure 7.1). In this model, when the sperm fuses to the plasma membrane of an MII egg it introduces factors



capable of generating  $\text{Ca}^{2+}$  oscillations. These factors are then sequestered by the developing pronuclei leading to the termination of  $\text{Ca}^{2+}$  transients in the egg. At NEBD of the first embryonic cell division these  $\text{Ca}^{2+}$ -releasing factors are released in the cytosol of the embryo causing the generation of  $\text{Ca}^{2+}$  transients. When the factors are again sequestered in the nuclei of the two cell embryo the transients cease. The remaining concentration of the  $\text{Ca}^{2+}$  transient-generating factors is not sufficient to re-initiate a series of oscillations after NEBD in the second mitotic division.

This model is consistent with the findings in our lab and also a number of previous observations like the changes in cell cycle-dependent  $\text{Ca}^{2+}$  release (Kono *et al.*, 1996) or the finding that inhibition of pronucleus formation with nocodazole or colcemid causes long-lasting  $\text{Ca}^{2+}$  oscillations beyond four hours when pronuclei are normally formed (Jones *et al.*, 1995; Day *et al.*, 2000). Furthermore, it is consistent with the observation that MII eggs become activated when fused with fertilised but not parthenogenetically activated eggs (Zernicka-Goetz *et al.*, 1995). In addition, our model can explain the initiation of  $\text{Ca}^{2+}$  oscillations by mammalian sperm extracts after NEBD but not before (Tang *et al.*, 2000) and the fact that only a single  $\text{Ca}^{2+}$  transient is generated in eggs from species in which fertilisation occurs in interphase, after pronucleus formation (Stricker, 1999).

The most support for this model, however, is given by work on the discovery and function of the elusive 'sperm factor'. Recently, a sperm-specific phospholipase C $\zeta$  (PLC $\zeta$ ) has been identified in the mouse and is proposed to be the factor responsible for generating  $\text{Ca}^{2+}$  oscillations at fertilisation (Saunders *et al.*, 2002; Cox *et al.*, 2002). It is not unusual for a PLC to translocate to the nucleus. Other PLC isoforms like PLC $\delta$ 4 and PLC $\beta$ 1 have been

found in the nucleus of somatic cells (Liu *et al.*, 1996; Sun *et al.*, 1997; Faenza *et al.*, 2000) and oocytes (Avazeri *et al.*, 2000). In addition, after our work was published, immunofluorescence experiments showed that PLC $\zeta$  microinjected into MII mouse eggs can be seen in the pronuclei and later on in the nuclei of two cell embryos (Larman *et al.*, 2004,  *In Press*). The translocation of PLC $\zeta$  has also been shown recently by the use of GFP- PLC $\zeta$  (Yoda *et al.*, 2004). Furthermore, this PLC isoform possesses a nuclear localisation signal which when mutated causes the PLC to remain in the cytoplasm and the Ca<sup>2+</sup> oscillations to continue for many hours after pronucleus formation (Larman *et al.*, 2004).

The model described previously which suggested the nuclear compartmentalisation of a sperm-derived Ca<sup>2+</sup> releasing factor (most possibly PLC $\zeta$ ) is the most reasonable explanation of our results. It is also possible, however, that a co-factor or a substrate of the Ca<sup>2+</sup>-releasing activity is sequestered in the nucleus instead of the activity itself. Thus, Ca<sup>2+</sup> oscillations may only be generated when the co-factor or substrate is in the cytoplasm of the egg or embryo. The model indicating that a Ca<sup>2+</sup>-releasing factor or co-factor or substrate may be sequestered and released from nuclei provides a new mechanism for the control of mitotic Ca<sup>2+</sup> oscillations in cells. Since it has been suggested that the duration of Ca<sup>2+</sup> transients in the early embryonic cell cycles may be implicated in the activation of the embryonic genome (Georgi *et al.*, 2002), this mechanism could be necessary for regulating and coordinating complex cell cycle activities. It would be interesting to investigate the effect of prolonged oscillations in the early mitotic cell cycles on DNA recombination, transcription and post-transcriptional events in early embryos.

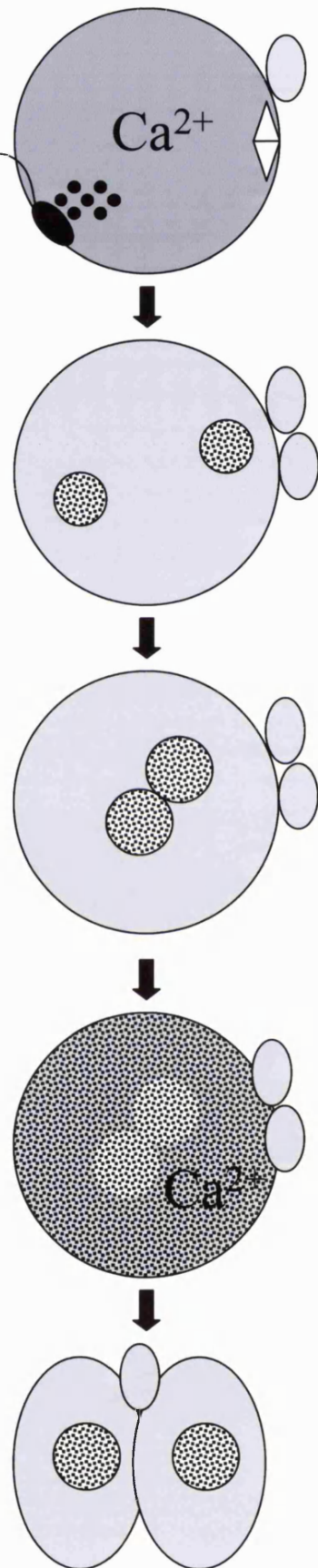


**Figure 7.1 Model depicting the nuclear localisation and release of sperm-derived  $\text{Ca}^{2+}$ -releasing activity.** At fertilisation, the sperm introduces a  $\text{Ca}^{2+}$ -releasing activity. This activity, which may be a PLC or an activator or substrate of PLC (see text), is depicted by black dots or black shading. After fertilisation, the  $\text{Ca}^{2+}$ -releasing activity is proposed to localise to the pronuclei (dark stippling). The nuclear localisation inhibits the ability to generate  $\text{IP}_3$  and so the  $\text{Ca}^{2+}$  oscillations stop. Other factors also appear to be at play to desensitise  $\text{IP}_3$ -induced  $\text{Ca}^{2+}$  release in pronucleate embryos, as depicted by the grey shading of the cytoplasm (see text for more details). The pronuclei migrate to the centre of the embryo and NEBD takes place, marking the start of the first mitotic division. NEBD leads to the factor responsible for  $\text{Ca}^{2+}$ -releasing activity to disperse in the cytoplasm, where it has the capacity to generate  $\text{Ca}^{2+}$  transients. The oscillations stop again at the two-cell stage when the nuclei form. This model of nuclear compartmentalisation of  $\text{Ca}^{2+}$ -releasing activity, including PLCs, may be important for regulating mitotic  $\text{Ca}^{2+}$  transients in a variety of cells (see text).

## Reference list

Abrieu,A., Brassac,T., Galas,S., Fisher,D., Labbe,J.C., Doree,M. (1998). The Polo-like kinase Plx1 is a component of the MPF amplification loop at the G2/M-phase transition of the cell cycle in *Xenopus* eggs. *J.Cell Sci.* *111 ( Pt 12)*, 1751-1757.

Abrieu,A., Doree,M., Fisher,D. (2001). The interplay between cyclin-B-Cdc2 kinase (MPF) and MAP kinase during maturation of oocytes. *J.Cell Sci.* *114*, 257-267.

Aitken,R. (1996). Fertilization and Early Embryogenesis. In: *Scientific Essentials of Reproductive Medicine*, ed. K.H.N.J.Hillier SGLondon: W.B. Saunders Co. Ltd, 219-229.

Aizawa,H., Kawahara,H., Tanaka,K., Yokosawa,H. (1996). Activation of the proteasome during *Xenopus* egg activation implies a link between proteasome activation and intracellular calcium release. *Biochem.Biophys.Res.Comm.* *218*, 224-228.

Anderson,E., Albertini,D.F. (1976). Gap junctions between the oocyte and companion follicle cells in the mammalian ovary. *J.Cell Biol.* *71*, 680-686.

Avazeri,N., Courtot,A.M., Pesty,A., Duquenne,C., Lefevre,B. (2000). Cytoplasmic and nuclear phospholipase C-beta 1 relocation: role in resumption of meiosis in the mouse oocyte. *Mol.Biol.Cell* *11*, 4369-4380.

Bavister,B.D., Squirrell,J.M. (2000). Mitochondrial distribution and function in oocytes and early embryos. *Hum.Reprod.* *15 Suppl 2*, 189-198.

Beach,D., Durkacz,B., Nurse,P. (1982). Functionally homologous cell cycle control genes in budding and fission yeast. *Nature* *300*, 706-709.

Berridge,M.J. (1993). Inositol trisphosphate and calcium signalling. *Nature* *361*, 315-325.

Berridge,M.J. (1997). Elementary and global aspects of calcium signalling. *J.Exp.Biol.* *200 ( Pt 2)*, 315-319.

Berridge,M.J., Irvine,R.F. (1989). Inositol phosphates and cell signalling. *Nature* *341*, 197-205.

Berridge,M.J., Lipp,P., Bootman,M.D. (2000). The versatility and universality of calcium signalling. *Nat.Rev.Mol.Cell Biol.* *1*, 11-21.

Bhatt,R.R., Ferrell,J.E., Jr. (1999). The protein kinase p90 rsk as an essential mediator of cytostatic factor activity. *Science* 286, 1362-1365.

Borgne,A., Ostvold,A.C., Flament,S., Meijer,L. (1999). Intra-M phase-promoting factor phosphorylation of cyclin B at the prophase/metaphase transition. *J.Biol.Chem.* 274, 11977-11986.

Bos-Mikich,A., Swann,K., Whittingham,D.G. (1995). Calcium oscillations and protein synthesis inhibition synergistically activate mouse oocytes. *Mol.Reprod.Dev.* 41, 84-90.

Bos-Mikich,A., Whittingham,D.G., Jones,K.T. (1997). Meiotic and mitotic Ca<sup>2+</sup> oscillations affect cell composition in resulting blastocysts. *Dev.Biol.* 182, 172-179.

Brandeis,M., Rosewell,I., Carrington,M., Crompton,T., Jacobs,M.A., Kirk,J., Gannon,J., Hunt,T. (1998). Cyclin B2-null mice develop normally and are fertile whereas cyclin B1-null mice die in utero. *Proc.Natl.Acad.Sci.U.S.A* 95, 4344-4349.

Brind,S., Swann,K., Carroll,J. (2000). Inositol 1,4,5-trisphosphate receptors are downregulated in mouse oocytes in response to sperm or adenophostin A but not to increases in intracellular Ca(2+) or egg activation. *Dev.Biol.* 223, 251-265.

Brunet,S., Maria,A.S., Guillaud,P., Dujardin,D., Kubiak,J.Z., Maro,B. (1999). Kinetochores are not involved in the formation of the first meiotic spindle in mouse oocytes, but control the exit from the first meiotic M phase. *J.Cell Biol.* 146, 1-12.

Carroll,J. (2001). The initiation and regulation of Ca<sup>2+</sup> signalling at fertilization in mammals. *Semin.Cell Dev.Biol.* 12, 37-43.

Casas,E., Betancourt,M., Bonilla,E., Duculomb,Y., Zayas,H., Trejo,R. (1999). Changes in cyclin B localisation during pig oocyte in vitro maturation. *Zygote.* 7, 21-26.

Charles,J.F., Jaspersen,S.L., Tinker-Kulberg,R.L., Hwang,L., Szidon,A., Morgan,D.O. (1998). The Polo-related kinase Cdc5 activates and is destroyed by the mitotic cyclin destruction machinery in *S. cerevisiae*. *Curr.Biol.* 8, 497-507.

Cheek,T.R., McGuinness,O.M., Vincent,C., Moreton,R.B., Berridge,M.J., Johnson,M.H. (1993). Fertilisation and thimerosal stimulate similar calcium spiking patterns in mouse oocytes but by separate mechanisms. *Development* 119, 179-189.

Chen,Y., Muller,J.D., Ruan,Q., Gratton,E. (2002). Molecular brightness characterization of EGFP in vivo by fluorescence fluctuation spectroscopy. *Biophys.J.* 82, 133-144.

Cheung,A., Swann,K., Carroll,J. (2000). The ability to generate normal Ca(2+) transients in response to spermatozoa develops during the final stages of oocyte growth and maturation. *Hum.Reprod.* 15, 1389-1395.

Cho,W.K., Stern,S., Biggers,J.D. (1974). Inhibitory effect of dibutyryl cAMP on mouse oocyte maturation in vitro. *J.Exp.Zool.* *187*, 383-386.

Choi,T., Aoki,F., Mori,M., Yamashita,M., Nagahama,Y., Kohmoto,K. (1991). Activation of p34cdc2 protein kinase activity in meiotic and mitotic cell cycles in mouse oocytes and embryos. *Development* *113*, 789-795.

Ciemerych,M.A., Kubiak,J.Z. (1998). Cytostatic activity develops during meiosis I in oocytes of LT/Sv mice. *Dev.Biol.* *200*, 198-211.

Clarke,H.J., Masui,Y. (1983). The induction of reversible and irreversible chromosome decondensation by protein synthesis inhibition during meiotic maturation of mouse oocytes. *Dev.Biol.* *97*, 291-301.

Cleveland,D.W., Mao,Y., Sullivan,K.F. (2003). Centromeres and kinetochores: from epigenetics to mitotic checkpoint signaling. *Cell* *112*, 407-421.

Clute,P., Pines,J. (1999). Temporal and spatial control of cyclin B1 destruction in metaphase. *Nat.Cell Biol.* *1*, 82-87.

Collas,P., Chang,T., Long,C., Robl,J.M. (1995). Inactivation of histone H1 kinase by Ca<sup>2+</sup> in rabbit oocytes. *Mol.Reprod.Dev.* *40*, 253-258.

Colledge,W.H., Carlton,M.B., Udy,G.B., Evans,M.J. (1994). Disruption of c-mos causes parthenogenetic development of unfertilized mouse eggs. *Nature* *370*, 65-68.

Cox,L., Larman,M.G., Saunders,C.M., Hashimoto,K., Swann,K., Lai,F.A. (2002). Sperm phospholipase C $\zeta$  from humans and cynomolgus monkeys triggers Ca<sup>2+</sup> oscillations, activation and development of mouse oocytes. *Reproduction.* *124*, 611-623.

Crews,C.M., Erikson,R.L. (1992). Purification of a murine protein-tyrosine/threonine kinase that phosphorylates and activates the Erk-1 gene product: relationship to the fission yeast byr1 gene product. *Proc.Natl.Acad.Sci.U.S.A* *89*, 8205-8209.

Cuthbertson,K.S., Cobbold,P.H. (1985). Phorbol ester and sperm activate mouse oocytes by inducing sustained oscillations in cell Ca<sup>2+</sup>. *Nature* *316*, 541-542.

Day,M.L., McGuinness,O.M., Berridge,M.J., Johnson,M.H. (2000). Regulation of fertilization-induced Ca(2+)spiking in the mouse zygote. *Cell Calcium* *28*, 47-54.

de Vantery,C., Stutz,A., Vassalli,J.D., Schorderet-Slatkine,S. (1997). Acquisition of meiotic competence in growing mouse oocytes is controlled at both translational and posttranslational levels. *Dev.Biol.* *187*, 43-54.

Deguchi,R., Shirakawa,H., Oda,S., Mohri,T., Miyazaki,S. (2000). Spatiotemporal analysis of Ca(2+) waves in relation to the sperm entry site and animal-vegetal axis during Ca(2+) oscillations in fertilized mouse eggs. *Dev.Biol.* *218*, 299-313.

den Elzen,N., Pines,J. (2001). Cyclin A is destroyed in prometaphase and can delay chromosome alignment and anaphase. *J.Cell Biol.* *153*, 121-136.

Deng,M.Q., Shen,S.S. (2000). A specific inhibitor of p34(cdc2)/cyclin B suppresses fertilization-induced calcium oscillations in mouse eggs. *Biol.Reprod.* *62*, 873-878.

Doree,M., Hunt,T. (2002). From Cdc2 to Cdk1: when did the cell cycle kinase join its cyclin partner? *J.Cell Sci.* *115*, 2461-2464.

Doree,M., Peaucellier,G., Picard,A. (1983). Activity of the maturation-promoting factor and the extent of protein phosphorylation oscillate simultaneously during meiotic maturation of starfish oocytes. *Dev.Biol.* *99*, 489-501.

Downs,S.M., Hunzicker-Dunn,M. (1995). Differential regulation of oocyte maturation and cumulus expansion in the mouse oocyte-cumulus cell complex by site-selective analogs of cyclic adenosine monophosphate. *Dev.Biol.* *172*, 72-85.

Draetta,G., Luca,F., Westendorf,J., Brizuela,L., Ruderman,J., Beach,D. (1989). Cdc2 protein kinase is complexed with both cyclin A and B: evidence for proteolytic inactivation of MPF. *Cell* *56*, 829-838.

Draviam,V.M., Orrechia,S., Lowe,M., Pardi,R., Pines,J. (2001). The localization of human cyclins B1 and B2 determines CDK1 substrate specificity and neither enzyme requires MEK to disassemble the Golgi apparatus. *J.Cell Biol.* *152*, 945-958.

Drury,K.C., Schorderet-Slatkine,S. (1975). Effects of cycloheximide on the "autocatalytic" nature of the maturation promoting factor (MPF) in oocytes of *Xenopus laevis*. *Cell* *4*, 269-274.

Duchen,M.R., Surin,A., Jacobson,J. (2003). Imaging mitochondrial function in intact cells. *Methods Enzymol.* *361*, 353-389.

Ducibella,T., Huneau,D., Angelichio,E., Xu,Z., Schultz,R.M., Kopf,G.S., Fissore,R., Madoux,S., Ozil,J.P. (2002). Egg-to-embryo transition is driven by differential responses to Ca(2+) oscillation number. *Dev.Biol.* *250*, 280-291.

Duckworth,B.C., Weaver,J.S., Ruderman,J.V. (2002). G2 arrest in *Xenopus* oocytes depends on phosphorylation of cdc25 by protein kinase A. *Proc.Natl.Acad.Sci.U.S.A* *99*, 16794-16799.

Ducommun,B., Brambilla,P., Felix,M.A., Franza,B.R., Jr., Karsenti,E., Draetta,G. (1991). cdc2 phosphorylation is required for its interaction with cyclin. *EMBO J.* *10*, 3311-3319.

Duncia,J.V., Santella,J.B., III, Higley,C.A., Pitts,W.J., Wityak,J., Fietze,W.E., Rankin,F.W., Sun,J.H., Earl,R.A., Tabaka,A.C., Teleha,C.A., Blom,K.F., Favata,M.F., Manos,E.J., Daulerio,A.J., Stradley,D.A., Horiuchi,K., Copeland,R.A., Scherle,P.A., Trzaskos,J.M., Magolda,R.L., Trainor,G.L., Wexler,R.R., Hobbs,F.W., Olson,R.E. (1998). MEK inhibitors:

the chemistry and biological activity of U0126, its analogs, and cyclization products. *Bioorg.Med.Chem.Lett.* 8, 2839-2844.

Dupre,A., Jessus,C., Ozon,R., Haccard,O. (2002). Mos is not required for the initiation of meiotic maturation in *Xenopus* oocytes. *EMBO J.* 21, 4026-4036.

Edwards,R.G. (1965). Maturation in vitro of mouse, sheep, cow, pig, rhesus monkey and human ovarian oocytes. *Nature* 208, 349-351.

Eisen,A., Reynolds,G.T. (1985). Source and sinks for the calcium released during fertilization of single sea urchin eggs. *J.Cell Biol.* 100, 1522-1527.

Erikson,E., Maller,J.L. (1989). In vivo phosphorylation and activation of ribosomal protein S6 kinases during *Xenopus* oocyte maturation. *J.Biol.Chem.* 264, 13711-13717.

Evans,T., Rosenthal,E.T., Youngblom,J., Distel,D., Hunt,T. (1983). Cyclin: a protein specified by maternal mRNA in sea urchin eggs that is destroyed at each cleavage division. *Cell* 33, 389-396.

Faenza,I., Matteucci,A., Manzoli,L., Billi,A.M., Aluigi,M., Peruzzi,D., Vitale,M., Castorina,S., Suh,P.G., Cocco,L. (2000). A role for nuclear phospholipase Cbeta 1 in cell cycle control. *J.Biol.Chem.* 275, 30520-30524.

Fang,G. (2002). Checkpoint protein BubR1 acts synergistically with Mad2 to inhibit anaphase-promoting complex. *Mol.Biol.Cell* 13, 755-766.

Fang,G., Yu,H., Kirschner,M.W. (1998a). Direct binding of CDC20 protein family members activates the anaphase-promoting complex in mitosis and G1. *Mol.Cell* 2, 163-171.

Fang,G., Yu,H., Kirschner,M.W. (1998b). The checkpoint protein MAD2 and the mitotic regulator CDC20 form a ternary complex with the anaphase-promoting complex to control anaphase initiation. *Genes Dev.* 12, 1871-1883.

Fang,G., Yu,H., Kirschner,M.W. (1999). Control of mitotic transitions by the anaphase-promoting complex. *Philos.Trans.R.Soc.Lond B Biol.Sci.* 354, 1583-1590.

Favata,M.F., Horiuchi,K.Y., Manos,E.J., Daulerio,A.J., Stradley,D.A., Feeser,W.S., Van Dyk,D.E., Pitts,W.J., Earl,R.A., Hobbs,F., Copeland,R.A., Magolda,R.L., Scherle,P.A., Trzaskos,J.M. (1998). Identification of a novel inhibitor of mitogen-activated protein kinase. *J.Biol.Chem.* 273, 18623-18632.

Felix,M.A., Labbe,J.C., Doree,M., Hunt,T., Karsenti,E. (1990). Triggering of cyclin degradation in interphase extracts of amphibian eggs by cdc2 kinase. *Nature* 346, 379-382.

Ferrell,J.E., Jr. (1998). How regulated protein translocation can produce switch-like responses. *Trends Biochem.Sci.* 23, 461-465.



Ferrell, J.E., Jr. (1999). Xenopus oocyte maturation: new lessons from a good egg. *Bioessays* 21, 833-842.

Ferrell, J.E., Jr., Machleder, E.M. (1998). The biochemical basis of an all-or-none cell fate switch in Xenopus oocytes. *Science* 280, 895-898.

Ferrell, J.E., Jr., Wu, M., Gerhart, J.C., Martin, G.S. (1991). Cell cycle tyrosine phosphorylation of p34cdc2 and a microtubule-associated protein kinase homolog in Xenopus oocytes and eggs. *Mol. Cell Biol.* 11, 1965-1971.

FitzHarris, D.G., Marangos, P., Carroll, J. (2003). Cell cycle-dependent regulation of the structure of the endoplasmic reticulum and InsP3-induced Ca<sup>2+</sup> release in mouse oocytes and embryos. *Mol. Biol. Cell* *in press*.

Fornierod, M., Ohno, M., Yoshida, M., Mattaj, I.W. (1997). CRM1 is an export receptor for leucine-rich nuclear export signals. *Cell* 90, 1051-1060.

Fulton, B.P., Whittingham, D.G. (1978). Activation of mammalian oocytes by intracellular injection of calcium. *Nature* 273, 149-151.

Furuno, N., Nishizawa, M., Okazaki, K., Tanaka, H., Iwashita, J., Nakajo, N., Ogawa, Y., Sagata, N. (1994). Suppression of DNA replication via Mos function during meiotic divisions in Xenopus oocytes. *EMBO J.* 13, 2399-2410.

Gabrielli, B.G., Roy, L.M., Maller, J.L. (1993). Requirement for Cdk2 in cytotstatic factor-mediated metaphase II arrest. *Science* 259, 1766-1769.

Gallant, P., Nigg, E.A. (1994). Identification of a novel vertebrate cyclin: cyclin B3 shares properties with both A- and B-type cyclins. *EMBO J.* 13, 595-605.

Gautier, J., Minshull, J., Lohka, M., Glotzer, M., Hunt, T., Maller, J.L. (1990). Cyclin is a component of maturation-promoting factor from Xenopus. *Cell* 60, 487-494.

Gautier, J., Norbury, C., Lohka, M., Nurse, P., Maller, J. (1988). Purified maturation-promoting factor contains the product of a Xenopus homolog of the fission yeast cell cycle control gene cdc2+. *Cell* 54, 433-439.

Geley, S., Kramer, E., Gieffers, C., Gannon, J., Peters, J.M., Hunt, T. (2001). Anaphase-promoting complex/cyclosome-dependent proteolysis of human cyclin A starts at the beginning of mitosis and is not subject to the spindle assembly checkpoint. *J. Cell Biol.* 153, 137-148.

Georgi, A.B., Stukenberg, P.T., Kirschner, M.W. (2002). Timing of events in mitosis. *Curr. Biol.* 12, 105-114.

Gerhart, J., Wu, M., Kirschner, M. (1984). Cell cycle dynamics of an M-phase-specific cytoplasmic factor in Xenopus laevis oocytes and eggs. *J. Cell Biol.* 98, 1247-1255.

Gilkey,J.C., Jaffe,L.F., Ridgway,E.B., Reynolds,G.T. (1978). A free calcium wave traverses the activating egg of the medaka, *Oryzias latipes*. *J.Cell Biol.* 76, 448-466.

Glotzer,M., Murray,A.W., Kirschner,M.W. (1991). Cyclin is degraded by the ubiquitin pathway. *Nature* 349, 132-138.

Goldman,D.S., Kiessling,A.A., Cooper,G.M. (1988). Post-transcriptional processing suggests that c-mos functions as a maternal message in mouse eggs. *Oncogene* 3, 159-162.

Gould,K.L., Nurse,P. (1989). Tyrosine phosphorylation of the fission yeast *cdc2+* protein kinase regulates entry into mitosis. *Nature* 342, 39-45.

Green,D.P. (1997). Three-dimensional structure of the zona pellucida. *Rev.Reprod.* 2, 147-156.

Gross,S.D., Schwab,M.S., Lewellyn,A.L., Maller,J.L. (1999). Induction of metaphase arrest in cleaving *Xenopus* embryos by the protein kinase p90Rsk. *Science* 286, 1365-1367.

Gross,S.D., Schwab,M.S., Taieb,F.E., Lewellyn,A.L., Qian,Y.W., Maller,J.L. (2000). The critical role of the MAP kinase pathway in meiosis II in *Xenopus* oocytes is mediated by p90(Rsk). *Curr.Biol.* 10, 430-438.

Guerrier,P., Moreau,M., Doree,M. (1977). Hormonal control of meiosis in starfish: stimulation of protein phosphorylation induced by 1-methyladenine. *Mol.Cell Endocrinol.* 7, 137-150.

Haccard,O., Sarcevic,B., Lewellyn,A., Hartley,R., Roy,L., Izumi,T., Erikson,E., Maller,J.L. (1993). Induction of metaphase arrest in cleaving *Xenopus* embryos by MAP kinase. *Science* 262, 1262-1265.

Hagting,A., den Elzen,N., Vodermaier,H.C., Waizenegger,I.C., Peters,J.M., Pines,J. (2002). Human securin proteolysis is controlled by the spindle checkpoint and reveals when the APC/C switches from activation by Cdc20 to Cdh1. *J.Cell Biol.* 157, 1125-1137.

Hagting,A., Jackman,M., Simpson,K., Pines,J. (1999). Translocation of cyclin B1 to the nucleus at prophase requires a phosphorylation-dependent nuclear import signal. *Curr.Biol.* 9, 680-689.

Hagting,A., Karlsson,C., Clute,P., Jackman,M., Pines,J. (1998). MPF localization is controlled by nuclear export. *EMBO J.* 17, 4127-4138.

Hajnoczky,G., Robb-Gaspers,L.D., Seitz,M.B., Thomas,A.P. (1995). Decoding of cytosolic calcium oscillations in the mitochondria. *Cell* 82, 415-424.

Hajnoczky,G., Thomas,A.P. (1997). Minimal requirements for calcium oscillations driven by the IP3 receptor. *EMBO J.* 16, 3533-3543.

- Hampl,A., Eppig,J.J. (1995a). Analysis of the mechanism(s) of metaphase I arrest in maturing mouse oocytes. *Development* 121, 925-933.
- Hampl,A., Eppig,J.J. (1995b). Translational regulation of the gradual increase in histone H1 kinase activity in maturing mouse oocytes. *Mol.Reprod.Dev.* 40, 9-15.
- Han,J.K., Nuccitelli,R. (1990). Inositol 1,4,5-trisphosphate-induced calcium release in the organelle layers of the stratified, intact egg of *Xenopus laevis*. *J.Cell Biol.* 110, 1103-1110.
- Harootunian,A.T., Kao,J.P., Paranjape,S., Tsien,R.Y. (1991). Generation of calcium oscillations in fibroblasts by positive feedback between calcium and IP3. *Science* 251, 75-78.
- Hashimoto,N., Kishimoto,T. (1986). Cell cycle dynamics of maturation-promoting factor during mouse oocyte maturation. *Tokai J.Exp.Clin.Med.* 11, 471-477.
- Hashimoto,N., Kishimoto,T. (1988). Regulation of meiotic metaphase by a cytoplasmic maturation-promoting factor during mouse oocyte maturation. *Dev.Biol.* 126, 242-252.
- Hashimoto,N., Watanabe,N., Furuta,Y., Tamemoto,H., Sagata,N., Yokoyama,M., Okazaki,K., Nagayoshi,M., Takeda,N., Ikawa,Y., . (1994). Parthenogenetic activation of oocytes in c-mos-deficient mice. *Nature* 370, 68-71.
- Herbert,M., Levasseur,M., Homer,H., Yallop,K., Murdoch,A., McDougall,A. (2003). Homologue disjunction in mouse oocytes requires proteolysis of securin and cyclin B1. *Nat.Cell Biol.* 5, 1023-1025.
- Herlands,R.L., Schultz,R.M. (1984). Regulation of mouse oocyte growth: probable nutritional role for intercellular communication between follicle cells and oocytes in oocyte growth. *J.Exp.Zool.* 229, 317-325.
- Hershko,A. (1997). Roles of ubiquitin-mediated proteolysis in cell cycle control. *Curr.Opin.Cell Biol.* 9, 788-799.
- Hilioti,Z., Chung,Y.S., Mochizuki,Y., Hardy,C.F., Cohen-Fix,O. (2001). The anaphase inhibitor Pds1 binds to the APC/C-associated protein Cdc20 in a destruction box-dependent manner. *Curr.Biol.* 11, 1347-1352.
- Hirao,Y., Eppig,J.J. (1997). Parthenogenetic development of Mos-deficient mouse oocytes. *Mol.Reprod.Dev.* 48, 391-396.
- Hoeflich,K.P., Ikura,M. (2002). Calmodulin in action: diversity in target recognition and activation mechanisms. *Cell* 108, 739-742.
- Hoffmann,I., Clarke,P.R., Marcote,M.J., Karsenti,E., Draetta,G. (1993). Phosphorylation and activation of human cdc25-C by cdc2--cyclin B and its involvement in the self-amplification of MPF at mitosis. *EMBO J.* 12, 53-63.

Hogan,B., Lacey.E., Costantini,F., Beddington,R. (1994). *Manipulating the Mouse Embryo*. Cold Spring Harbour Laboratory Press.

Howell,B.J., Hoffman,D.B., Fang,G., Murray,A.W., Salmon,E.D. (2000). Visualization of Mad2 dynamics at kinetochores, along spindle fibers, and at spindle poles in living cells. *J.Cell Biol.* 150, 1233-1250.

Hoyt,M.A., Totis,L., Roberts,B.T. (1991). *S. cerevisiae* genes required for cell cycle arrest in response to loss of microtubule function. *Cell* 66, 507-517.

Hsu,J.Y., Reimann,J.D., Sorensen,C.S., Lukas,J., Jackson,P.K. (2002). E2F-dependent accumulation of hEmil regulates S phase entry by inhibiting APC(Cdh1). *Nat.Cell Biol.* 4, 358-366.

Huang,J., Raff,J.W. (1999). The disappearance of cyclin B at the end of mitosis is regulated spatially in *Drosophila* cells. *EMBO J.* 18, 2184-2195.

Huchon,D., Ozon,R., Fischer,E.H., Demaille,J.G. (1981). The pure inhibitor of cAMP-dependent protein kinase initiates *Xenopus laevis* meiotic maturation. A 4-step scheme for meiotic maturation. *Mol.Cell Endocrinol.* 22, 211-222.

Hudmon,A., Schulman,H. (2002). Structure-function of the multifunctional Ca<sup>2+</sup>/calmodulin-dependent protein kinase II. *Biochem.J.* 364, 593-611.

Jackman,M., Firth,M., Pines,J. (1995). Human cyclins B1 and B2 are localized to strikingly different structures: B1 to microtubules, B2 primarily to the Golgi apparatus. *EMBO J.* 14, 1646-1654.

Jackman,M., Lindon,C., Nigg,E.A., Pines,J. (2003). Active cyclin B1-Cdk1 first appears on centrosomes in prophase. *Nat.Cell Biol.* 5, 143-148.

Jaffe,L. (2002). On the conservation of fast calcium wave speeds. *Cell Calcium* 32, 217-229.

Jeffrey,P.D., Russo,A.A., Polyak,K., Gibbs,E., Hurwitz,J., Massague,J., Pavletich,N.P. (1995). Mechanism of CDK activation revealed by the structure of a cyclinA-CDK2 complex. *Nature* 376, 313-320.

Jellerette,T., He,C.L., Wu,H., Parys,J.B., Fissore,R.A. (2000). Down-regulation of the inositol 1,4,5-trisphosphate receptor in mouse eggs following fertilization or parthenogenetic activation. *Dev.Biol.* 223, 238-250.

Jones,K.T., Carroll,J., Merriman,J.A., Whittingham,D.G., Kono,T. (1995). Repetitive sperm-induced Ca<sup>2+</sup> transients in mouse oocytes are cell cycle dependent. *Development* 121, 3259-3266.

Jones,K.T., Whittingham,D.G. (1996). A comparison of sperm- and IP3-induced Ca<sup>2+</sup> release in activated and aging mouse oocytes. *Dev.Biol.* 178, 229-237.

Kalab,P., Kubiak,J.Z., Verlhac,M.H., Colledge,W.H., Maro,B. (1996). Activation of p90rsk during meiotic maturation and first mitosis in mouse oocytes and eggs: MAP kinase-independent and -dependent activation. *Development* 122, 1957-1964.

Kallio,M., Weinstein,J., Daum,J.R., Burke,D.J., Gorbsky,G.J. (1998). Mammalian p53CDC mediates association of the spindle checkpoint protein Mad2 with the cyclosome/anaphase-promoting complex, and is involved in regulating anaphase onset and late mitotic events. *J.Cell Biol.* 141, 1393-1406.

Kanatsu-Shinohara,M., Schultz,R.M., Kopf,G.S. (2000). Acquisition of meiotic competence in mouse oocytes: absolute amounts of p34(cdc2), cyclin B1, cdc25C, and weel in meiotically incompetent and competent oocytes. *Biol.Reprod.* 63, 1610-1616.

Karlsson,C., Katich,S., Hagting,A., Hoffmann,I., Pines,J. (1999). Cdc25B and Cdc25C differ markedly in their properties as initiators of mitosis. *J.Cell Biol.* 146, 573-584.

Kawahara,H., Yokosawa,H. (1994). Intracellular calcium mobilization regulates the activity of 26 S proteasome during the metaphase-anaphase transition in the ascidian meiotic cell cycle. *Dev.Biol.* 166, 623-633.

Kidder,G.M., Mhawi,A.A. (2002). Gap junctions and ovarian folliculogenesis. *Reproduction.* 123, 613-620.

King,R.W., Peters,J.M., Tugendreich,S., Rolfe,M., Hieter,P., Kirschner,M.W. (1995). A 20S complex containing CDC27 and CDC16 catalyzes the mitosis-specific conjugation of ubiquitin to cyclin B. *Cell* 81, 279-288.

Kitajima,T.S., Kawashima,S.A., Watanabe,Y. (2004). The conserved kinetochore protein shugoshin protects centromeric cohesion during meiosis. *Nature* 427, 510-517.

Kline,D., Kline,J.T. (1992). Repetitive calcium transients and the role of calcium in exocytosis and cell cycle activation in the mouse egg. *Dev.Biol.* 149, 80-89.

Kobayashi,H., Minshull,J., Ford,C., Golsteyn,R., Poon,R., Hunt,T. (1991). On the synthesis and destruction of A- and B-type cyclins during oogenesis and meiotic maturation in *Xenopus laevis*. *J.Cell Biol.* 114, 755-765.

Kono,T., Carroll,J., Swann,K., Whittingham,D.G. (1995). Nuclei from fertilized mouse embryos have calcium-releasing activity. *Development* 121, 1123-1128.

Kono,T., Jones,K.T., Bos-Mikich,A., Whittingham,D.G., Carroll,J. (1996). A cell cycle-associated change in Ca<sup>2+</sup> releasing activity leads to the generation of Ca<sup>2+</sup> transients in mouse embryos during the first mitotic division. *J.Cell Biol.* 132, 915-923.

Kosako,H., Gotoh,Y., Nishida,E. (1994). Mitogen-activated protein kinase kinase is required for the mos-induced metaphase arrest. *J.Biol.Chem.* 269, 28354-28358.

Kramer,E.R., Gieffers,C., Holzl,G., Hengstschlager,M., Peters,J.M. (1998). Activation of the human anaphase-promoting complex by proteins of the CDC20/Fizzy family. *Curr.Biol.* 8, 1207-1210.

Kubiak,J.Z., Weber,M., de Pennart,H., Winston,N.J., Maro,B. (1993). The metaphase II arrest in mouse oocytes is controlled through microtubule-dependent destruction of cyclin B in the presence of CSF. *EMBO J.* 12, 3773-3778.

Kutay,U., Izaurralde,E., Bischoff,F.R., Mattaj,I.W., Gorlich,D. (1997). Dominant-negative mutants of importin-beta block multiple pathways of import and export through the nuclear pore complex. *EMBO J.* 16, 1153-1163.

Labbe,J.C., Capony,J.P., Caput,D., Cavadore,J.C., Derancourt,J., Kaghad,M., Lelias,J.M., Picard,A., Doree,M. (1989). MPF from starfish oocytes at first meiotic metaphase is a heterodimer containing one molecule of cdc2 and one molecule of cyclin B. *EMBO J.* 8, 3053-3058.

Labbe,J.C., Lee,M.G., Nurse,P., Picard,A., Doree,M. (1988). Activation at M-phase of a protein kinase encoded by a starfish homologue of the cell cycle control gene *cdc2+*. *Nature* 335, 251-254.

Lawrence,Y., Ozil,J.P., Swann,K. (1998). The effects of a Ca<sup>2+</sup> chelator and heavy-metal-ion chelators upon Ca<sup>2+</sup> oscillations and activation at fertilization in mouse eggs suggest a role for repetitive Ca<sup>2+</sup> increases. *Biochem.J.* 335 ( Pt 2), 335-342.

Ledan,E., Polanski,Z., Terret,M.E., Maro,B. (2001). Meiotic maturation of the mouse oocyte requires an equilibrium between cyclin B synthesis and degradation. *Dev.Biol.* 232, 400-413.

Lee,M.G., Nurse,P. (1987). Complementation used to clone a human homologue of the fission yeast cell cycle control gene *cdc2*. *Nature* 327, 31-35.

Lefebvre,C., Terret,M.E., Djiane,A., Rassinier,P., Maro,B., Verlhac,M.H. (2002). Meiotic spindle stability depends on MAPK-interacting and spindle-stabilizing protein (MISS), a new MAPK substrate. *J.Cell Biol.* 157, 603-613.

Levasseur,M., McDougall,A. (2000). Sperm-induced calcium oscillations at fertilisation in ascidians are controlled by cyclin B1-dependent kinase activity. *Development* 127, 631-641.

Levesque,J.T., Sirard,M.A. (1996). Resumption of meiosis is initiated by the accumulation of cyclin B in bovine oocytes. *Biol.Reprod.* 55, 1427-1436.

Li,J., Meyer,A.N., Donoghue,D.J. (1995). Requirement for phosphorylation of cyclin B1 for *Xenopus* oocyte maturation. *Mol.Biol.Cell* 6, 1111-1124.

Li,J., Meyer,A.N., Donoghue,D.J. (1997). Nuclear localization of cyclin B1 mediates its biological activity and is regulated by phosphorylation. *Proc.Natl.Acad.Sci.U.S.A* 94, 502-507.

- Li,X., Nicklas,R.B. (1995). Mitotic forces control a cell-cycle checkpoint. *Nature* 373, 630-632.
- Lincoln,A.J., Wickramasinghe,D., Stein,P., Schultz,R.M., Palko,M.E., de Miguel,M.P., Tessarollo,L., Donovan,P.J. (2002). Cdc25b phosphatase is required for resumption of meiosis during oocyte maturation. *Nat.Genet.* 30, 446-449.
- Liu,F., Stanton,J.J., Wu,Z., Piwnica-Worms,H. (1997). The human Myt1 kinase preferentially phosphorylates Cdc2 on threonine 14 and localizes to the endoplasmic reticulum and Golgi complex. *Mol.Cell Biol.* 17, 571-583.
- Liu,N., Fukami,K., Yu,H., Takenawa,T. (1996). A new phospholipase C delta 4 is induced at S-phase of the cell cycle and appears in the nucleus. *J.Biol.Chem.* 271, 355-360.
- Lohka,M.J., Hayes,M.K., Maller,J.L. (1988). Purification of maturation-promoting factor, an intracellular regulator of early mitotic events. *Proc.Natl.Acad.Sci.U.S.A* 85, 3009-3013.
- Lorca,T., Abrieu,A., Means,A., Doree,M. (1994). Ca<sup>2+</sup> is involved through type II calmodulin-dependent protein kinase in cyclin degradation and exit from metaphase. *Biochim.Biophys.Acta* 1223, 325-332.
- Lorca,T., Castro,A., Martinez,A.M., Vigneron,S., Morin,N., Sigrist,S., Lehner,C., Doree,M., Labbe,J.C. (1998). Fizzy is required for activation of the APC/cyclosome in *Xenopus* egg extracts. *EMBO J.* 17, 3565-3575.
- Lorca,T., Cruzalegui,F.H., Fesquet,D., Cavadore,J.C., Mery,J., Means,A., Doree,M. (1993). Calmodulin-dependent protein kinase II mediates inactivation of MPF and CSF upon fertilization of *Xenopus* eggs. *Nature* 366, 270-273.
- Lorca,T., Galas,S., Fesquet,D., Devault,A., Cavadore,J.C., Doree,M. (1991). Degradation of the proto-oncogene product p39mos is not necessary for cyclin proteolysis and exit from meiotic metaphase: requirement for a Ca(2+)-calmodulin dependent event. *EMBO J.* 10, 2087-2093.
- Lowe,M., Rabouille,C., Nakamura,N., Watson,R., Jackman,M., Jamsa,E., Rahman,D., Pappin,D.J., Warren,G. (1998). Cdc2 kinase directly phosphorylates the cis-Golgi matrix protein GM130 and is required for Golgi fragmentation in mitosis. *Cell* 94, 783-793.
- Maller,J.L., Krebs,E.G. (1977). Progesterone-stimulated meiotic cell division in *Xenopus* oocytes. Induction by regulatory subunit and inhibition by catalytic subunit of adenosine 3':5'-monophosphate-dependent protein kinase. *J.Biol.Chem.* 252, 1712-1718.
- Marangos,P., Fitzharris,G., Carroll,J. (2003a). Ca<sup>2+</sup> oscillations at fertilization in mammals are regulated by the formation of pronuclei. *Development* 130, 1461-1472.
- Marangos,P., Fitzharris,G., Carroll,J. (2003b). Ca<sup>2+</sup> oscillations at fertilization in mammals are regulated by the formation of pronuclei. *Development* 130, 1461-1472.

- Margottin-Goguet,F., Hsu,J.Y., Loktev,A., Hsieh,H.M., Reimann,J.D., Jackson,P.K. (2003). Prophase Destruction of Emil by the SCF(betaTrCP/Slimb) Ubiquitin Ligase Activates the Anaphase Promoting Complex to Allow Progression beyond Prometaphase. *Dev.Cell* 4, 813-826.
- Masui,Y. (2001). From oocyte maturation to the in vitro cell cycle: the history of discoveries of Maturation-Promoting Factor (MPF) and Cytostatic Factor (CSF). *Differentiation* 69, 1-17.
- Masui,Y., Markert,C.L. (1971). Cytoplasmic control of nuclear behavior during meiotic maturation of frog oocytes. *J.Exp.Zool.* 177, 129-145.
- Matten,W., Daar,I., Vande Woude,G.F. (1994). Protein kinase A acts at multiple points to inhibit *Xenopus* oocyte maturation. *Mol.Cell Biol.* 14, 4419-4426.
- McDougall,A., Levasseur,M. (1998). Sperm-triggered calcium oscillations during meiosis in ascidian oocytes first pause, restart, then stop: correlations with cell cycle kinase activity. *Development* 125, 4451-4459.
- Mehlmann,L.M., Jones,T.L., Jaffe,L.A. (2002). Meiotic arrest in the mouse follicle maintained by a Gs protein in the oocyte. *Science* 297, 1343-1345.
- Miyawaki,A., Llopis,J., Heim,R., McCaffery,J.M., Adams,J.A., Ikura,M., Tsien,R.Y. (1997). Fluorescent indicators for Ca<sup>2+</sup> based on green fluorescent proteins and calmodulin. *Nature* 388, 882-887.
- Moore,J.D., Yang,J., Truant,R., Kornbluth,S. (1999). Nuclear import of Cdk/cyclin complexes: identification of distinct mechanisms for import of Cdk2/cyclin E and Cdc2/cyclin B1. *J.Cell Biol.* 144, 213-224.
- Moos,J., Kopf,G.S., Schultz,R.M. (1996). Cycloheximide-induced activation of mouse eggs: effects on cdc2/cyclin B and MAP kinase activities. *J.Cell Sci.* 109 (Pt 4), 739-748.
- Moos,J., Visconti,P.E., Moore,G.D., Schultz,R.M., Kopf,G.S. (1995). Potential role of mitogen-activated protein kinase in pronuclear envelope assembly and disassembly following fertilization of mouse eggs. *Biol.Reprod.* 53, 692-699.
- Moreno,S., Hayles,J., Nurse,P. (1989). Regulation of p34cdc2 protein kinase during mitosis. *Cell* 58, 361-372.
- Moses,R.M., Kline,D. (1995). Release of mouse eggs from metaphase arrest by protein synthesis inhibition in the absence of a calcium signal or microtubule assembly. *Mol.Reprod.Dev.* 41, 264-273.
- Mueller,P.R., Coleman,T.R., Dunphy,W.G. (1995). Cell cycle regulation of a *Xenopus* Wee1-like kinase. *Mol.Biol.Cell* 6, 119-134.



Murray,A.W., Kirschner,M.W. (1989). Cyclin synthesis drives the early embryonic cell cycle. *Nature* 339, 275-280.

Murray,A.W., Solomon,M.J., Kirschner,M.W. (1989). The role of cyclin synthesis and degradation in the control of maturation promoting factor activity. *Nature* 339, 280-286.

Nebreda,A.R., Hunt,T. (1993). The c-mos proto-oncogene protein kinase turns on and maintains the activity of MAP kinase, but not MPF, in cell-free extracts of *Xenopus* oocytes and eggs. *EMBO J.* 12, 1979-1986.

Newmeyer,D.D., Forbes,D.J. (1988). Nuclear import can be separated into distinct steps in vitro: nuclear pore binding and translocation. *Cell* 52, 641-653.

Nguyen,T.B., Manova,K., Capodiecici,P., Lindon,C., Bottega,S., Wang,X.Y., Refik-Rogers,J., Pines,J., Wolgemuth,D.J., Koff,A. (2002). Characterization and expression of mammalian cyclin b3, a prepachytene meiotic cyclin. *J.Biol.Chem.* 277, 41960-41969.

Nixon,V.L., Levasseur,M., McDougall,A., Jones,K.T. (2002). Ca<sup>2+</sup> oscillations promote APC/C-dependent cyclin B1 degradation during metaphase arrest and completion of meiosis in fertilizing mouse eggs. *Curr.Biol.* 12, 746-750.

Nixon,V.L., McDougall,A., Jones,K.T. (2000). Ca<sup>2+</sup> oscillations and the cell cycle at fertilisation of mammalian and ascidian eggs. *Biol.Cell* 92, 187-196.

Nurse,P. (1975). Genetic control of cell size at cell division in yeast. *Nature* 256, 547-551.

Nurse,P., Thuriaux,P., Nasmyth,K. (1976). Genetic control of the cell division cycle in the fission yeast *Schizosaccharomyces pombe*. *Mol.Gen.Genet.* 146, 167-178.

O W, Baker,T.G. (1976). Initiation and control of meiosis in hamster gonads in vitro. *J.Reprod.Fertil.* 48, 399-401.

O'Keefe,S.J., Wolfes,H., Kiessling,A.A., Cooper,G.M. (1989). Microinjection of antisense c-mos oligonucleotides prevents meiosis II in the maturing mouse egg. *Proc.Natl.Acad.Sci.U.S.A* 86, 7038-7042.

Ookata,K., Hisanaga,S., Okano,T., Tachibana,K., Kishimoto,T. (1992). Relocation and distinct subcellular localization of p34cdc2-cyclin B complex at meiosis reinitiation in starfish oocytes. *EMBO J.* 11, 1763-1772.

Ozil,J.P., Huneau,D. (2001). Activation of rabbit oocytes: the impact of the Ca<sup>2+</sup> signal regime on development. *Development* 128, 917-928.

Palmer,A., Gavin,A.C., Nebreda,A.R. (1998). A link between MAP kinase and p34(cdc2)/cyclin B during oocyte maturation: p90(rsk) phosphorylates and inactivates the p34(cdc2) inhibitory kinase Myt1. *EMBO J.* 17, 5037-5047.

Parrington,J., Lai,F.A., Swann,K. (2000). The soluble mammalian sperm factor protein that triggers Ca<sup>2+</sup> oscillations in eggs: evidence for expression of mRNA(s) coding for sperm factor protein(s) in spermatogenic cells. *Biol.Cell* 92, 267-275.

Parrington,J., Swann,K., Shevchenko,V.I., Sesay,A.K., Lai,F.A. (1996). Calcium oscillations in mammalian eggs triggered by a soluble sperm protein. *Nature* 379, 364-368.

Paules,R.S., Buccione,R., Moschel,R.C., Vande Woude,G.F., Eppig,J.J. (1989). Mouse Mos protooncogene product is present and functions during oogenesis. *Proc.Natl.Acad.Sci.U.S.A* 86, 5395-5399.

Peter,M., Castro,A., Lorca,T., Le Peuch,C., Magnaghi-Jaulin,L., Doree,M., Labbe,J.C. (2001). The APC is dispensable for first meiotic anaphase in *Xenopus* oocytes. *Nat.Cell Biol.* 3, 83-87.

Peter,M., Labbe,J.C., Doree,M., Mandart,E. (2002a). A new role for Mos in *Xenopus* oocyte maturation: targeting Myt1 independently of MAPK. *Development* 129, 2129-2139.

Peter,M., Le Peuch,C., Labbe,J.C., Meyer,A.N., Donoghue,D.J., Doree,M. (2002b). Initial activation of cyclin-B1-cdc2 kinase requires phosphorylation of cyclin B1. *EMBO Rep.* 3, 551-556.

Peter,M., Nakagawa,J., Doree,M., Labbe,J.C., Nigg,E.A. (1990). In vitro disassembly of the nuclear lamina and M phase-specific phosphorylation of lamins by cdc2 kinase. *Cell* 61, 591-602.

Peters,J.M. (2002). The anaphase-promoting complex: proteolysis in mitosis and beyond. *Mol.Cell* 9, 931-943.

Pfleger,C.M., Lee,E., Kirschner,M.W. (2001). Substrate recognition by the Cdc20 and Cdh1 components of the anaphase-promoting complex. *Genes Dev.* 15, 2396-2407.

Phillips,K.P., Petrunewich,M.A., Collins,J.L., Booth,R.A., Liu,X.J., Baltz,J.M. (2002). Inhibition of MEK or cdc2 kinase parthenogenetically activates mouse eggs and yields the same phenotypes as Mos(-/-) parthenogenotes. *Dev.Biol.* 247, 210-223.

Picard,A., Peaucellier,G., Le Bouffant,F., Le Peuch,C., Doree,M. (1985). Role of protein synthesis and proteases in production and inactivation of maturation-promoting activity during meiotic maturation of starfish oocytes. *Dev.Biol.* 109, 311-320.

Pines,J. (1999). Cell cycle. Checkpoint on the nuclear frontier. *Nature* 397, 104-105.

Pines,J., Hunt,T. (1987). Molecular cloning and characterization of the mRNA for cyclin from sea urchin eggs. *EMBO J.* 6, 2987-2995.

Pines,J., Hunter,T. (1990). Human cyclin A is adenovirus E1A-associated protein p60 and behaves differently from cyclin B. *Nature* 346, 760-763.

Pines,J., Hunter,T. (1991). Human cyclins A and B1 are differentially located in the cell and undergo cell cycle-dependent nuclear transport. *J.Cell Biol.* *115*, 1-17.

Pines,J., Hunter,T. (1992). Cyclins A and B1 in the human cell cycle. *Ciba Found.Symp.* *170*, 187-196.

Pines,J., Hunter,T. (1994). The differential localization of human cyclins A and B is due to a cytoplasmic retention signal in cyclin B. *EMBO J.* *13*, 3772-3781.

Polanski,Z., Ledan,E., Brunet,S., Louvet,S., Verlhac,M.H., Kubiak,J.Z., Maro,B. (1998). Cyclin synthesis controls the progression of meiotic maturation in mouse oocytes. *Development* *125*, 4989-4997.

Pomerening,J.R., Sontag,E.D., Ferrell,J.E., Jr. (2003). Building a cell cycle oscillator: hysteresis and bistability in the activation of Cdc2. *Nat.Cell Biol.* *5*, 346-351.

Posada,J., Yew,N., Ahn,N.G., Vande Woude,G.F., Cooper,J.A. (1993). Mos stimulates MAP kinase in *Xenopus* oocytes and activates a MAP kinase kinase in vitro. *Mol.Cell Biol.* *13*, 2546-2553.

Quinn,P., Whittingham,D.G., Stanger,J.D. (1982). Interaction of semen with ova in vitro. *Arch.Androl* *8*, 189-198.

Raff,J.W., Jeffers,K., Huang,J.Y. (2002). The roles of Fzy/Cdc20 and Fzr/Cdh1 in regulating the destruction of cyclin B in space and time. *J.Cell Biol.* *157*, 1139-1149.

Reimann,J.D., Freed,E., Hsu,J.Y., Kramer,E.R., Peters,J.M., Jackson,P.K. (2001a). Emi1 is a mitotic regulator that interacts with Cdc20 and inhibits the anaphase promoting complex. *Cell* *105*, 645-655.

Reimann,J.D., Gardner,B.E., Margottin-Goguet,F., Jackson,P.K. (2001b). Emi1 regulates the anaphase-promoting complex by a different mechanism than Mad2 proteins. *Genes Dev.* *15*, 3278-3285.

Reimann,J.D., Jackson,P.K. (2002). Emi1 is required for cytostatic factor arrest in vertebrate eggs. *Nature* *416*, 850-854.

Richards,J.S. (1980). Maturation of ovarian follicles: actions and interactions of pituitary and ovarian hormones on follicular cell differentiation. *Physiol Rev.* *60*, 51-89.

Rieder,C.L., Cole,R.W., Khodjakov,A., Sluder,G. (1995). The checkpoint delaying anaphase in response to chromosome monoorientation is mediated by an inhibitory signal produced by unattached kinetochores. *J.Cell Biol.* *130*, 941-948.

Robb-Gaspers,L.D., Burnett,P., Rutter,G.A., Denton,R.M., Rizzuto,R., Thomas,A.P. (1998). Integrating cytosolic calcium signals into mitochondrial metabolic responses. *EMBO J.* *17*, 4987-5000.

Rudolf,R., Mongillo,M., Rizzuto,R., Pozzan,T. (2003). Looking forward to seeing calcium. *Nat.Rev.Mol.Cell Biol.* 4, 579-586.

Runft,L.L., Jaffe,L.A., Mehlmann,L.M. (2002). Egg activation at fertilization: where it all begins. *Dev.Biol.* 245, 237-254.

Russell,P., Nurse,P. (1986). *cdc25+* functions as an inducer in the mitotic control of fission yeast. *Cell* 45, 145-153.

Rutter,G.A., Burnett,P., Rizzuto,R., Brini,M., Murgia,M., Pozzan,T., Tavaré,J.M., Denton,R.M. (1996). Subcellular imaging of intramitochondrial  $Ca^{2+}$  with recombinant targeted aequorin: significance for the regulation of pyruvate dehydrogenase activity. *Proc.Natl.Acad.Sci.U.S.A* 93, 5489-5494.

Sagata,N., Daar,I., Oskarsson,M., Showalter,S.D., Vande Woude,G.F. (1989a). The product of the *mos* proto-oncogene as a candidate "initiator" for oocyte maturation. *Science* 245, 643-646.

Sagata,N., Oskarsson,M., Copeland,T., Brumbaugh,J., Vande Woude,G.F. (1988). Function of *c-mos* proto-oncogene product in meiotic maturation in *Xenopus* oocytes. *Nature* 335, 519-525.

Sagata,N., Watanabe,N., Vande Woude,G.F., Ikawa,Y. (1989b). The *c-mos* proto-oncogene product is a cytostatic factor responsible for meiotic arrest in vertebrate eggs. *Nature* 342, 512-518.

Sato,M.S., Yoshitomo,M., Mohri,T., Miyazaki,S. (1999). Spatiotemporal analysis of  $[Ca^{2+}]_i$  rises in mouse eggs after intracytoplasmic sperm injection (ICSI). *Cell Calcium* 26, 49-58.

Saunders,C.M., Larman,M.G., Parrington,J., Cox,L.J., Royse,J., Blayney,L.M., Swann,K., Lai,F.A. (2002). PLC zeta: a sperm-specific trigger of  $Ca^{2+}$  oscillations in eggs and embryo development. *Development* 129, 3533-3544.

Schlatterer,C., Knoll,G., Malchow,D. (1992). Intracellular calcium during chemotaxis of *Dictyostelium discoideum*: a new fura-2 derivative avoids sequestration of the indicator and allows long-term calcium measurements. *Eur.J.Cell Biol.* 58, 172-181.

Schmitt,A., Nebreda,A.R. (2002). Inhibition of *Xenopus* oocyte meiotic maturation by catalytically inactive protein kinase A. *Proc.Natl.Acad.Sci.U.S.A* 99, 4361-4366.

Schultz,R.M., Kopf,G.S. (1995). Molecular basis of mammalian egg activation. *Curr.Top.Dev.Biol.* 30, 21-62.

Schwab,M.S., Roberts,B.T., Gross,S.D., Tunquist,B.J., Taieb,F.E., Lewellyn,A.L., Maller,J.L. (2001). *Bub1* is activated by the protein kinase p90(Rsk) during *Xenopus* oocyte maturation. *Curr.Biol.* 11, 141-150.

Sette,C., Bevilacqua,A., Bianchini,A., Mangia,F., Geremia,R., Rossi,P. (1997). Parthenogenetic activation of mouse eggs by microinjection of a truncated c-kit tyrosine kinase present in spermatozoa. *Development* 124, 2267-2274.

Shirayama,M., Zachariae,W., Ciosk,R., Nasmyth,K. (1998). The Polo-like kinase Cdc5p and the WD-repeat protein Cdc20p/fizzy are regulators and substrates of the anaphase promoting complex in *Saccharomyces cerevisiae*. *EMBO J.* 17, 1336-1349.

Simanis,V., Nurse,P. (1986). The cell cycle control gene *cdc2+* of fission yeast encodes a protein kinase potentially regulated by phosphorylation. *Cell* 45, 261-268.

Siomos,M.F., Badrinath,A., Pasierbek,P., Livingstone,D., White,J., Glotzer,M., Nasmyth,K. (2001). Separase is required for chromosome segregation during meiosis I in *Caenorhabditis elegans*. *Curr.Biol.* 11, 1825-1835.

Steinhardt,R.A., Epel,D., Carroll,E.J., Jr., Yanagimachi,R. (1974). Is calcium ionophore a universal activator for unfertilised eggs? *Nature* 252, 41-43.

Stemmann,O., Zou,H., Gerber,S.A., Gygi,S.P., Kirschner,M.W. (2001). Dual inhibition of sister chromatid separation at metaphase. *Cell* 107, 715-726.

Stricker,S.A. (1999). Comparative biology of calcium signaling during fertilization and egg activation in animals. *Dev.Biol.* 211, 157-176.

Sturgill,T.W., Ray,L.B., Erikson,E., Maller,J.L. (1988). Insulin-stimulated MAP-2 kinase phosphorylates and activates ribosomal protein S6 kinase II. *Nature* 334, 715-718.

Summers,M.C., McGinnis,L.K., Lawitts,J.A., Raffin,M., Biggers,J.D. (2000). IVF of mouse ova in a simplex optimized medium supplemented with amino acids. *Hum.Reprod.* 15, 1791-1801.

Sun,B., Murray,N.R., Fields,A.P. (1997). A role for nuclear phosphatidylinositol-specific phospholipase C in the G2/M phase transition. *J.Biol.Chem.* 272, 26313-26317.

Sutovsky,P., Simerly,C., Hewitson,L., Schatten,G. (1998). Assembly of nuclear pore complexes and annulate lamellae promotes normal pronuclear development in fertilized mammalian oocytes. *J.Cell Sci.* 111 ( Pt 19), 2841-2854.

Svoboda,P., Stein,P., Hayashi,H., Schultz,R.M. (2000). Selective reduction of dormant maternal mRNAs in mouse oocytes by RNA interference. *Development* 127, 4147-4156.

Swann,K. (1990). A cytosolic sperm factor stimulates repetitive calcium increases and mimics fertilization in hamster eggs. *Development* 110, 1295-1302.

Swann,K., Ozil,J.P. (1994). Dynamics of the calcium signal that triggers mammalian egg activation. *Int.Rev.Cytol.* 152, 183-222.

Swann,K., Parrington,J., Jones,K.T. (2001). Potential role of a sperm-derived phospholipase C in triggering the egg-activating Ca<sup>2+</sup> signal at fertilization. *Reproduction*. *122*, 839-846.

Sweeney,C., Murphy,M., Kubelka,M., Ravnik,S.E., Hawkins,C.F., Wolgemuth,D.J., Carrington,M. (1996). A distinct cyclin A is expressed in germ cells in the mouse. *Development* *122*, 53-64.

Swenson,K.I., Farrell,K.M., Ruderman,J.V. (1986). The clam embryo protein cyclin A induces entry into M phase and the resumption of meiosis in *Xenopus* oocytes. *Cell* *47*, 861-870.

Taieb,F.E., Gross,S.D., Lewellyn,A.L., Maller,J.L. (2001). Activation of the anaphase-promoting complex and degradation of cyclin B is not required for progression from Meiosis I to II in *Xenopus* oocytes. *Curr.Biol.* *11*, 508-513.

Takizawa,C.G., Morgan,D.O. (2000). Control of mitosis by changes in the subcellular location of cyclin-B1-Cdk1 and Cdc25C. *Curr.Opin.Cell Biol.* *12*, 658-665.

Tang,T.S., Dong,J.B., Huang,X.Y., Sun,F.Z. (2000). Ca<sup>2+</sup> oscillations induced by a cytosolic sperm protein factor are mediated by a maternal machinery that functions only once in mammalian eggs. *Development* *127*, 1141-1150.

Tay,J., Hodgman,R., Richter,J.D. (2000). The control of cyclin B1 mRNA translation during mouse oocyte maturation. *Dev.Biol.* *221*, 1-9.

Terasaki,M., Okumura,E., Hinkle,B., Kishimoto,T. (2003). Localization and dynamics of Cdc2-cyclin B during meiotic reinitiation in starfish oocytes. *Mol.Biol.Cell* *14*, 4685-4694.

Tombes,R.M., Simerly,C., Borisy,G.G., Schatten,G. (1992). Meiosis, egg activation, and nuclear envelope breakdown are differentially reliant on Ca<sup>2+</sup>, whereas germinal vesicle breakdown is Ca<sup>2+</sup> independent in the mouse oocyte. *J.Cell Biol.* *117*, 799-811.

Tong,C., Fan,H.Y., Lian,L., Li,S.W., Chen,D.Y., Schatten,H., Sun,Q.Y. (2002). Polo-like kinase-1 is a pivotal regulator of microtubule assembly during mouse oocyte meiotic maturation, fertilization, and early embryonic mitosis. *Biol.Reprod.* *67*, 546-554.

Toyoshima,F., Moriguchi,T., Wada,A., Fukuda,M., Nishida,E. (1998). Nuclear export of cyclin B1 and its possible role in the DNA damage-induced G2 checkpoint. *EMBO J.* *17*, 2728-2735.

Toyoshima-Morimoto,F., Taniguchi,E., Shinya,N., Iwamatsu,A., Nishida,E. (2001). Polo-like kinase 1 phosphorylates cyclin B1 and targets it to the nucleus during prophase. *Nature* *410*, 215-220.

Tunquist,B.J., Eyers,P.A., Chen,L.G., Lewellyn,A.L., Maller,J.L. (2003). Spindle checkpoint proteins Mad1 and Mad2 are required for cyostatic factor-mediated metaphase arrest. *J.Cell Biol.* *163*, 1231-1242.

Tunquist,B.J., Maller,J.L. (2003). Under arrest: cytostatic factor (CSF)-mediated metaphase arrest in vertebrate eggs. *Genes Dev.* *17*, 683-710.

Tunquist,B.J., Schwab,M.S., Chen,L.G., Maller,J.L. (2002). The spindle checkpoint kinase *bub1* and cyclin *e/cdk2* both contribute to the establishment of meiotic metaphase arrest by cytostatic factor. *Curr.Biol.* *12*, 1027-1033.

Vautier,D., Chesne,P., Cunha,C., Calado,A., Renard,J.P., Carmo-Fonseca,M. (2001). Transcription-dependent nucleocytoplasmic distribution of hnRNP A1 protein in early mouse embryos. *J.Cell Sci.* *114*, 1521-1531.

Verlhac,M.H., de Pennart,H., Maro,B., Cobb,M.H., Clarke,H.J. (1993). MAP kinase becomes stably activated at metaphase and is associated with microtubule-organizing centers during meiotic maturation of mouse oocytes. *Dev.Biol.* *158*, 330-340.

Verlhac,M.H., Kubiak,J.Z., Clarke,H.J., Maro,B. (1994). Microtubule and chromatin behavior follow MAP kinase activity but not MPF activity during meiosis in mouse oocytes. *Development* *120*, 1017-1025.

Verlhac,M.H., Kubiak,J.Z., Weber,M., Geraud,G., Colledge,W.H., Evans,M.J., Maro,B. (1996). *Mos* is required for MAP kinase activation and is involved in microtubule organization during meiotic maturation in the mouse. *Development* *122*, 815-822.

Verlhac,M.H., Lefebvre,C., Guillaud,P., Rassinier,P., Maro,B. (2000). Asymmetric division in mouse oocytes: with or without *Mos*. *Curr.Biol.* *10*, 1303-1306.

Vitullo,A.D., Ozil,J.P. (1992). Repetitive calcium stimuli drive meiotic resumption and pronuclear development during mouse oocyte activation. *Dev.Biol.* *151*, 128-136.

Wassarman,P.M., Jovine,L., Litscher,E.S. (2001c). A profile of fertilization in mammals. *Nat.Cell Biol.* *3*, E59-E64.

Wassarman,P.M., Jovine,L., Litscher,E.S. (2001a). A profile of fertilization in mammals. *Nat.Cell Biol.* *3*, E59-E64.

Wassarman,P.M., Jovine,L., Litscher,E.S. (2001b). A profile of fertilization in mammals. *Nat.Cell Biol.* *3*, E59-E64.

Wasserman,W.J., Smith,L.D. (1978). The cyclic behavior of a cytoplasmic factor controlling nuclear membrane breakdown. *J.Cell Biol.* *78*, R15-R22.

Watanabe,N., Broome,M., Hunter,T. (1995). Regulation of the human WEE1Hu CDK tyrosine 15-kinase during the cell cycle. *EMBO J.* *14*, 1878-1891.

Watanabe,N., Hunt,T., Ikawa,Y., Sagata,N. (1991). Independent inactivation of MPF and cytostatic factor (*Mos*) upon fertilization of *Xenopus* eggs. *Nature* *352*, 247-248.

Weber,M., Kubiak,J.Z., Arlinghaus,R.B., Pines,J., Maro,B. (1991). c-mos proto-oncogene product is partly degraded after release from meiotic arrest and persists during interphase in mouse zygotes. *Dev.Biol.* 148, 393-397.

Westendorf,J.M., Swenson,K.I., Ruderman,J.V. (1989). The role of cyclin B in meiosis I. *J.Cell Biol.* 108, 1431-1444.

Wianny,F., Zernicka-Goetz,M. (2000). Specific interference with gene function by double-stranded RNA in early mouse development. *Nat.Cell Biol.* 2, 70-75.

Winston,N., Bourgain-Guglielmetti,F., Ciemerych,M.A., Kubiak,J.Z., Senamaud-Beaufort,C., Carrington,M., Brechot,C., Sobczak-Thepot,J. (2000). Early development of mouse embryos null mutant for the cyclin A2 gene occurs in the absence of maternally derived cyclin A2 gene products. *Dev.Biol.* 223, 139-153.

Winston,N.J. (1997). Stability of cyclin B protein during meiotic maturation and the first mitotic cell division in mouse oocytes. *Biol.Cell* 89, 211-219.

Winston,N.J., Maro,B. (1995). Calmodulin-dependent protein kinase II is activated transiently in ethanol-stimulated mouse oocytes. *Dev.Biol.* 170, 350-352.

Winston,N.J., McGuinness,O., Johnson,M.H., Maro,B. (1995). The exit of mouse oocytes from meiotic M-phase requires an intact spindle during intracellular calcium release. *J.Cell Sci.* 108 (Pt 1), 143-151.

Xu,Z., Lefevre,L., Ducibella,T., Schultz,R.M., Kopf,G.S. (1996). Effects of calcium-BAPTA buffers and the calmodulin antagonist W-7 on mouse egg activation. *Dev.Biol.* 180, 594-604.

Yang,J., Bardes,E.S., Moore,J.D., Brennan,J., Powers,M.A., Kornbluth,S. (1998). Control of cyclin B1 localization through regulated binding of the nuclear export factor CRM1. *Genes Dev.* 12, 2131-2143.

Yang,J., Song,H., Walsh,S., Bardes,E.S., Kornbluth,S. (2001). Combinatorial control of cyclin B1 nuclear trafficking through phosphorylation at multiple sites. *J.Biol.Chem.* 276, 3604-3609.

Yang,J., Winkler,K., Yoshida,M., Kornbluth,S. (1999). Maintenance of G2 arrest in the *Xenopus* oocyte: a role for 14-3-3-mediated inhibition of Cdc25 nuclear import. *EMBO J.* 18, 2174-2183.

Yang,T.T., Cheng,L., Kain,S.R. (1996). Optimized codon usage and chromophore mutations provide enhanced sensitivity with the green fluorescent protein. *Nucleic Acids Res.* 24, 4592-4593.

Yding Andersen,C., Byskov,A. (1996). Gonadal Differentiation. In: *Scientific Essentials of Reproductive Medicine*, ed. K.H.N.J.Hillier SGLondon: W.B. Saunders Co. Ltd, 105-119.



Yoda,A., Oda,S., Shikano,T., Kouchi,Z., Awaji,T., Shirakawa,H., Kinoshita,K., Miyazaki,S. (2004). Ca(2+) oscillation-inducing phospholipase C zeta expressed in mouse eggs is accumulated to the pronucleus during egg activation. *Dev.Biol.* 268, 245-257.

Yoneda,Y., Imamoto-Sonobe,N., Yamaizumi,M., Uchida,T. (1987). Reversible inhibition of protein import into the nucleus by wheat germ agglutinin injected into cultured cells. *Exp.Cell Res.* 173, 586-595.

Zachariae,W., Nasmyth,K. (1999). Whose end is destruction: cell division and the anaphase-promoting complex. *Genes Dev.* 13, 2039-2058.

Zernicka-Goetz,M., Ciemerych,M.A., Kubiak,J.Z., Tarkowski,A.K., Maro,B. (1995). Cytostatic factor inactivation is induced by a calcium-dependent mechanism present until the second cell cycle in fertilized but not in parthenogenetically activated mouse eggs. *J.Cell Sci.* 108 ( Pt 2), 469-474.

Zernicka-Goetz,M., Pines,J. (2001). Use of Green Fluorescent Protein in mouse embryos. *Methods* 24, 55-60.

Zernicka-Goetz,M., Pines,J., McLean,H.S., Dixon,J.P., Siemering,K.R., Haseloff,J., Evans,M.J. (1997). Following cell fate in the living mouse embryo. *Development* 124, 1133-1137.

Zernicka-Goetz,M., Pines,J., Ryan,K., Siemering,K.R., Haseloff,J., Evans,M.J., Gurdon,J.B. (1996). An indelible lineage marker for *Xenopus* using a mutated green fluorescent protein. *Development* 122, 3719-3724.

Zur,A., Brandeis,M. (2001). Securin degradation is mediated by fzy and fzr, and is required for complete chromatid separation but not for cytokinesis. *EMBO J.* 20, 792-801.

## Acknowledgements

I would really like to thank my supervisor, John Carroll for maintaining the best possible work environment in the lab, making life very easy and work very pleasant for the past few years. I also thank him for his scientific wisdom and mental support, qualities that made this work, and a number of good publications, possible.

Thanks also to my friends in the lab: Mark, Tasos, Guillaume, Greg, Rachel and Remi for making “scientific” life interesting and enjoyable.

Finally, the biggest thanks to my incredible family, my parents and my brother, for their emotional and occasionally financial support and for coping with us living in different countries all these years. I owe them absolutely everything.

